

Contrails

WADD TECHNICAL REPORT 60-793

DIFFUSION IN REFRACTORY METALS

N. L. Peterson

Advanced Metals Research Corporation

MARCH 1960

Materials Central

Contract No. AF 33(616)-7382

Project No. 7351

USAF WRIGHT AIR DEVELOPMENT DIVISION
AIR RESEARCH AND DEVELOPMENT COMMAND
UNITED STATES AIR FORCE
WRIGHT-PATTERSON AIR FORCE BASE, OHIO

600 -- May 1961 -- 29-1102



FOREWORD

This report was prepared by Advanced Metals Research Corporation under subcontract from Nuclear Metals, Inc. on USAF Contract No. AF33(616)-7382. The contract was initiated under Project No. 7351, "Metallic Materials," Task No. 73512, "Refractory Materials." The work was administered under the direction of Materials Central, Directorate of Advanced Systems Technology, Wright Air Development Division, with Lt. J. Bitzer acting as project engineer.

This report covers work conducted from April 1960 to September 1960.

This work was prepared by N. Peterson, and reviewed by Drs. R. Ogilvie, J. Norton, and E. J. Rapperport.

WADD TR 60-793

Contrails
ABSTRACT

Data available in the open literature on diffusion in tungsten, tantalum, molybdenum, niobium, platinum, hafnium, zirconium, vanadium, chromium, and titanium is reviewed and evaluated. Information on ninety-five binary systems and thirteen ternary or higher order systems is reported.

Care was taken to make this report as complete as possible at this time. For some systems where no diffusion data was available, diffusion coefficients were estimated from existing theories or from data on diffusion controlled processes.

PUBLICATION REVIEW

This report has been reviewed and is approved.

FOR THE COMMANDER

I. Perlmutter

I. Perlmutter
Chief, Physical Metallurgy Branch
Metals and Ceramics Laboratory
Materials Laboratory

Contrails
TABLE OF CONTENTS

	<u>Page No.</u>
I. INTRODUCTION	1
II. GROUP 1	1
A. Diffusion in Tungsten	1
B. Diffusion in Tantalum	18
C. Diffusion in Molybdenum	35
D. Diffusion in Niobium	60
III. GROUP II	76
A. Diffusion in Platinum	76
B. Diffusion in Hafnium	82
C. Diffusion in Zirconium	86
IV. GROUP III	105
A. Diffusion in Vanadium	105
B. Diffusion in Chromium	111
C. Diffusion in Titanium	123
V. REFERENCES	156

Contrails

LIST OF ILLUSTRATIONS

Figure	<u>Page No.</u>
1. Log D vs 1/T for diffusion of molybdenum in polycrystalline and single crystal tungsten.	12
2. Log D vs 1/T is plotted for diffusion in tungsten-nickel alloys of high nickel concentration.	15
3(a). The temperature dependence of the diffusion from a tungsten-nickel alloy into pure nickel.	16
3(b). The temperature dependence of the diffusion from a tungsten layer into pure nickel.	16
4. Relaxation times for stress-induced ordering vs 1/T for several alloys.	25
5. Temperature dependence of the diffusion coefficient for oxygen in tantalum.	29
6. Log K vs 1/T for the reaction of tantalum with oxygen.	31
7. Temperature dependence of diffusion coefficient for tantalum-oxygen system.	32
8. Activation energy for self-diffusion vs melting point for various elements.	36
9. The diffusion coefficient as a function of the atomic percent molybdenum at temperatures, 1 - 1106°C, 2 - 1148°C, and 3 - 1183°C.	41
10. Activation energy vs atomic percent molybdenum for the iron-molybdenum system.	42
11. Log D ₀ vs atomic percent molybdenum for the iron-molybdenum system.	43
12. Log D ₀ vs the activation energy for o - Fe-Mo, Δ -Fe-self-diffusion and \bullet - Fe-Ni.	44
13. Effect of temperature on the coefficient of diffusion of molybdenum in austenite and in ferrite.	46
14. Diffusion coefficient for niobium-molybdenum system at 1100°C.	48
15. Log D vs 1/T for diffusion in molybdenum-nickel alloys of high nickel concentration.	49
16. Variation of the interdiffusion coefficient with composition for the molybdenum-titanium system.	51

Figure		Page No.
17.	D vs composition for uranium-molybdenum system.	54
18.	Dependence of Q on composition for uranium-molybdenum system.	55
19.	Temperature dependence of intrinsic diffusion coefficients for uranium-molybdenum system.	56
20.	Log D vs 1/T for self-diffusion of niobium.	61
21.	Temperature dependence of D for contamination of niobium in oxygen and air.	68
22.	Variation of the diffusion coefficient of Sc^{46} with composition for the niobium-titanium system.	69
23.	Variation of the activation energy for diffusion of Sc^{46} with composition for the niobium-titanium system.	69
24.	D as a function of 1/T for uranium-niobium diffusion.	72
25.	Intrinsic diffusion coefficients as a function of 1/T.	73
26.	Log D vs 1/T for self-diffusion of platinum.	77
27.	The dependence of D on composition. I and II diffused at 1038°C , III diffused at 1002°C	79
28.	Temperature variation of diffusion coefficient for hydrogen in zirconium.	88
29.	Variation of the diffusion coefficient with temperature for diffusion of nitrogen in zirconium.	91
30.	Temperature dependence of the diffusion coefficient of oxygen in zirconium.	94
31.	Variation of the diffusion coefficient with composition for the zirconium-uranium system.	98
32.	Variation of the activation energy for diffusion with composition for the zirconium-uranium system.	99
33.	Variation of the intrinsic diffusion coefficients with temperature for the zirconium-uranium system.	100
34.	Variation of the intrinsic diffusion coefficients with composition for the zirconium-uranium system.	101

Contrails
LIST OF ILLUSTRATIONS (Cont'd.)

Figure		Page No.
35.	Variation of the interdiffusion coefficient with composition for the vanadium-titanium system.	109
36.	Influence of temperature on the interdiffusion coefficient of chromium in iron.	116
37.	Log D vs 1/T for diffusion of Fe ⁵⁹ in Fe - 4% Cr and Fe - 8% Cr alloys.	119
38.	Temperature variation of the diffusion coefficient of nitrogen in alpha and beta-titanium.	129
39.	Temperature variation of the diffusion coefficient of nitrogen in titanium nitride.	130
40.	Temperature variation of the diffusion coefficient of oxygen in beta-titanium.	132
41.	Diffusivity of oxygen in alpha and beta-titanium.	134
42.	Variation of the interdiffusion coefficient with composition for the titanium-aluminum system.	137
43.	Variation of the interdiffusion coefficient with composition for the titanium-manganese system.	140
44.	Log D vs 1/T is plotted for diffusion in titanium-nickel alloys of high nickel concentration.	142
45.	Variation of the interdiffusion coefficient with composition for the titanium-tin system.	143
46.	D vs composition for uranium-titanium system.	146
47.	Dependence of Q on composition for the uranium-titanium system.	147
48.	Temperature dependence of intrinsic diffusion coefficients for uranium-titanium system.	148
49.	Temperature dependence of the diffusion coefficient of Fe ⁵⁹ in alloys of the systems: (1) Ni-Ti, (2) Ni-Ti-Cr, (3) Ni-Ti-Cr-W-Al.	150

Contrails
LIST OF TABLES

Table		Page No.
1.	Tungsten-Boron Diffusion Data Using the Samsonov and Latysheva Technique	4
2.	Tungsten-Carbon Diffusion Data by Samsonov and Latysheva	4
3.	Tungsten-Carbon Diffusion Coefficients for 1700°C	5
4.	Surface Diffusion of Cesium on Tungsten	7
5.	Data on Diffusion of W ¹⁸⁵ into Iron	8
6.	Experimental Data of Grube and Schneider for Diffusion in Tungsten-Iron System at Low Tungsten Compositions	9
7.	Surface Diffusion of Potassium on Tungsten	10
8.	Diffusion of Molybdenum into Single Crystal and Polycrystalline Tungsten	11
9.	Surface Diffusion of Sodium on Tungsten	13
10.	Tungsten-Nickel Diffusion at Low Tungsten Compositions	13
11.	Grain Boundary Diffusion in Tungsten-Thorium System	17
12.	Summary of Diffusion Data for Tungsten	19
13.	Self-diffusion Data for Tantalum	22
14.	Tantalum-Boron Diffusion Data Using the Analytical Method of Samsonov and Latysheva	23
15.	Diffusion Data for Tantalum-Carbon System	23
16.	Tantalum-Carbon Diffusion Coefficients as Determined by Internal Friction Methods	24
17.	Tantalum Diffusion Data of Powers and Doyle	27
18.	Diffusion Data for the Tantalum-Oxygen System as Determined from Internal Friction Measurements	28
19.	Tantalum-Nitrogen Diffusion Coefficients	30
20.	Summary of Diffusion Data for Tantalum	34
21.	Data on the Diffusion of Boron in Molybdenum	37

Continued
LIST OF TABLES (Cont'd.)

Table	<u>Page No.</u>
22. Data Obtained by Samsonov and Latysheva on Diffusion of Carbon in Molybdenum	37
23. Data on the Diffusion of Nitrogen in Molybdenum	38
24. Molybdenum-Cobalt Diffusion at High Molybdenum Concentrations .	39
25. Molybdenum-Iron Diffusion at Low Molybdenum Concentrations . . .	45
26. Data for Nickel-Molybdenum Diffusion	47
27. Kirkendall Marker Movements in Molybdenum-Titanium Diffusion Couples	50
28. Diffusion Coefficients for Diffusion of Molybdenum in Titanium .	52
29. Molybdenum-Uranium Diffusion Coefficients at Various Concentrations of Uranium	53
30. Intrinsic Diffusion Coefficients in Uranium-Molybdenum System .	53
31. Summary of Diffusion Data for Molybdenum	57
32. Niobium-Boron Diffusion Data Using the Analytical Method of Samsonov and Latysheva	60
33. Data on the Diffusion of Carbon in Niobium	62
34. Diffusion Coefficients for the Diffusion of Carbon in Niobium as Determined by Internal Friction Measurements	63
35. Niobium-Nitrogen Diffusion Data of Powers and Doyle	64
36. Niobium-Oxygen Diffusion Data by Powers and Doyle	66
37. Niobium-Oxygen Diffusion Data of Jaffee, Klopp and Sims	67
38. Diffusion of Sc ⁴⁶ into Various Titanium-Niobium Alloys	70
39. Phases Found in Niobium-Chromium, Niobium-Iron and Niobium-Nickel Diffusion Couples	70
40. Summary of Diffusion Data for Niobium	74
41. Diffusion Data for the Self-diffusion of Platinum	76
42. Intrinsic Diffusion Coefficients in Platinum-Gold System	78



LIST OF TABLES (Cont'd.)

Table		Page No.
43.	Platinum-Gold Diffusion Data at High Gold Concentrations	78
44.	Platinum-Copper Diffusion Data at High Copper Concentra- tions	80
45.	Platinum-Copper Diffusion at High Platinum Concentrations . . .	81
46.	Diffusion Data for the Platinum-Nickel System at High Platinum Concentrations	82
47.	Summary of Diffusion Data for Platinum	83
48.	Zirconium-Carbon Diffusion Data Using the Samsonov and Latysheva Technique	86
49.	Diffusion of Hydrogen in Alpha-Zirconium at Low Hafnium Content.	87
50.	Diffusion of Hydrogen in Alpha-Zirconium Containing 1% Hafnium .	87
51.	Diffusion Data for Hydrogen Diffusion in Zircaloy-2	89
52.	Zirconium-Nitrogen Diffusion Data for Beta-Zirconium of Low Hafnium Content	90
53.	Zirconium-Nitrogen Diffusion Data for Beta-Zirconium Contain- ing 1.8 - 2.2% Hafnium	92
54.	Diffusion of Oxygen in Alpha-Zirconium	93
55.	Zirconium-Uranium Diffusion Coefficients for Various Zirconium Concentrations	97
56.	Intrinsic Diffusion Coefficients for the Zirconium-Uranium System	97
57.	Summary of Diffusion Data for Zirconium	102
58.	Vanadium-Nitrogen Diffusion Data of Powers and Doyle	106
59.	Diffusion Coefficients for the Diffusion of Oxygen in Vanadium as Determined by Internal Friction Measurements	107
60.	Summary of Diffusion Data for Vanadium	110
61.	Chromium Concentration of Chromium-Cobalt Diffusion Specimens .	112
62.	Diffusion of Co ⁶⁰ in Cobalt-Chromium and Cobalt-Nickel-Chromium Alloys	113

Contrails
LIST OF TABLES (Cont'd.)

Table	Page No.
63. Frequency Factor and Activation Energy for Diffusion of Co ⁶⁰ in Cobalt-Chromium and Cobalt-Nickel-Chromium Alloys	113
64. Grain-Boundary Diffusion of Co ⁶⁰ in Cobalt-Chromium and Cobalt-Nickel-Chromium Alloys	114
65. Chromium-Iron Diffusion Data for 1150 and 1350°C	115
66. Diffusion in the Chromium-Iron System	117
67. Data on the Diffusion of Cr ⁵¹ into Iron and Steel	117
68. Data on the Diffusion of Fe ⁵⁹ into Chromium-Iron Alloys of 4% and 8% Chromium	118
69. Frequency Factor and Activation Energy for Diffusion of Fe ⁵⁹ in Several Iron-Chromium Alloys	120
70. Diffusion Data for the Diffusion of Cr ⁵¹ into an Alloys of Ti - 15% Cr	121
71. Data on the Diffusion of Cr ⁵¹ into Pure Titanium	121
72. Frequency Factor and Activation Energy for Diffusion of Cr ⁵¹ into Pure Titanium and Several Chromium-Titanium Alloys	122
73. Data on the Diffusion of Chromium in Uranium at Low Chromium Concentrations	122
74. Summary of Diffusion Data for Chromium	124
75. Titanium-Boron Diffusion Data Using the Samsonov and Latysheva Technique	126
76. Titanium-Carbon Diffusion Data	127
77. Data on the Diffusion of Carbon in Alpha and Beta-Titanium	127
78. Data on Oxygen Diffusion in Titanium Containing Small Amounts of a Third Element	136
79. Titanium-Iron Diffusion Data for Alloys of Low Titanium Concentrations	138
80. Data on Diffusion in the Titanium-Nickel System at Low Titanium Concentrations	141
81. Titanium-Uranium Diffusion Coefficients for Various Titanium-Concentrations	145

Contrails
LIST OF TABLES (Cont'd.)

Table		<u>Page No.</u>
82.	Intrinsic Diffusion Coefficients in the Titanium-Uranium System	149
83.	Data on the Diffusion of Co ⁶⁰ in an Alloy of 81% Cobalt, 15% Iron and 4% Titanium	149
84.	Frequency Factor and Activation Energy for Diffusion of Fe ⁵⁹ in Ni-Ti, Ni-Cr-Ti, and Ni-Cr-W-Al-Ti Alloys	151
85.	Diffusion Data for Iron-Nickel Base Alloys	152
86.	Summary of Diffusion Data for Titanium	153

I. INTRODUCTION

In the past few years, the importance of diffusion in refractory metals has become increasingly emphasized due to the application of these metals to high temperature uses such as space vehicles, jet engines, and nuclear processes.

For practical as well as for fundamental reasons, the rates of diffusion in alloys of these metals are of considerable consequence. Most reactions which occur in the solid state are greatly dependent upon the diffusion of atoms through the lattice structure and along grain boundaries. Thus, diffusion is frequently rate-controlling in such processes as grain growth, homogenization, oxidation, age hardening, sintering, creep, and elastic after effects. In addition to the substitutional alloying elements used in the refractory metal alloys, the interstitial alloying elements such as carbon, oxygen, nitrogen, and hydrogen also are often present in sufficient quantities to influence the alloy properties significantly.

In the processes of determining which elements should fall under the term refractory metals, three groups of elements were categorized with respect to their general importance:

- Group I - Diffusion of niobium (columbium), molybdenum, tantalum, and tungsten with any other element.
- Group II - Diffusion of zirconium, hafnium, platinum, iridium, osmium, rhenium, rhodium, and ruthenium with any other element. Data was found only on zirconium, hafnium, and platinum.
- Group III - Diffusion of titanium, chromium, and vanadium with any other element.

II. GROUP I

A. Diffusion in Tungsten

1. Self-diffusion

Self-diffusion of tungsten was reported in 1956 by two Russian investigators, Vasiler and Chernomorchenko.⁽¹⁾ The radioactive isotope W^{185} was oxidized to WO_3 and applied as a uniform coat 40 to 50 microns thick, onto the surface of tungsten discs. The activity was measured at the surface of the discs as a function of time at temperatures in the range of 1287 to 1453°C. The data fits the equation

$$D = 6.3 \times 10^7 \exp (-135,000/RT).$$

Manuscript released by the author December 1, 1960, for publication as a WADD Technical Report.

Contrails

The data appears to be quite good, but at temperatures as low as the ones used in this investigation, one would expect a fair amount of grain boundary diffusion. The activation energy is of the right order of magnitude for lattice diffusion, but the D_0 is excessively large for self-diffusion by a vacancy or ring mechanism. The authors estimate their error in D as being 25 to 30 percent.

Using the field emission microscope, Muller⁽²⁾ measured the surface migration of tungsten atoms on tungsten in the temperature range 927 to 1227°C. He obtained a value for the activation energy of surface diffusion of

$$Q = 106,500 \pm 800 \text{ cal/mole.}$$

This value appears to be quite large, and there was some doubt expressed in the literature as to whether Muller was measuring surface diffusion or volume diffusion. By applying the theory of Herring⁽³⁾ to the rate of blunting of tungsten needles which were heated and observed in the electron microscope, Boling and Dolan⁽⁴⁾ concluded that surface diffusion was the controlling mechanism in Muller's experiments.

In a more recent investigation by Sokolovskaia,⁽⁵⁾ the activation energy for surface diffusion was found to be $Q = 73,200 \pm 4,500 \text{ cal/mole}$. The measurements utilized the field emission microscope and were carried out over the temperature range of 927 to 1327°C.

Barbour, Charbonnier, Dolan, Dyke, Martin and Trolan⁽⁶⁾ reported surface diffusion data for tungsten over the temperature range of 1527 to 2427°C. A pulse field emission microscope was used to measure the rounding of the points of tungsten needles. From a least squares line through 43 experimental points, the equation

$$D = 4 \exp [-(72,000 \pm 1800)/RT]$$

was arrived at. This appears to be the most complete and probably the most reliable data on surface diffusion in tungsten.

Sokolovskaia⁽⁵⁾ and Bettler and Charbonnier⁽⁷⁾ showed that the activation energy is considerably smaller if a large continuously applied electric field is used. The high electrostatic field at the crystal surface, present through induced polarization of the surface atoms, produces a reduction of the potential hill which an atom must surmount in order to migrate from one stable site to another.

2. Interstitial Diffusion

a. Tungsten-Boron

Two Russian investigators, Samsonov and Latysheva^(8,9) studied the diffusion of boron and carbon into a number of transition elements.

Contrails

Since their "diffusion constants" are not the standard diffusion coefficients encountered in physical metallurgy, their technique and results will be reported in detail here, but will be referred to only briefly under the other system that they have investigated. In systems where there is other data available, their data is greatly in error. Nevertheless, the data is interesting and possibly of value.

Specimens, 3 to 4 mm diameter cylinders, were charged with carbon by placing the specimens in a suitable holder and were surrounded with lamp black. For saturation with boron, a charge of 99.1% purified amorphous boron was used in a mixture of 3% NH_4Cl as a diffusion activator. The time at temperature for each temperature was two hours. On the basis of weight changes, hardness data, metallographic observations, and x-ray analyses, the compounds formed on the surface were determined.

Diffusion constants (which appear to really be constants associated with the rate of growth of the compound layer) were calculated from the relation

$$D (C - C_2) = C_0 K$$

where D is the diffusion coefficient, $C - C_2$ is the difference in concentration of the metalloid on the boundaries of the layers, and K is defined as

$$K = \frac{1 - x^2 + 2x^2 \ln x}{4t} \cdot R^2$$

where x is the radius of the specimen (R) minus the thickness of the diffusion zone and t is the time.

The activation energy, Q , was calculated from the relation

$$D (C - C_2) = D_0 \exp (-Q/RT).$$

The data for tungsten-boron diffusion is shown in Table 1 and may be given by

$$D = 3.72 \times 10^3 \exp [(-20,400 \pm 6400)/RT].$$

Samsonov⁽¹⁰⁾ in an earlier report, stated that $Q = 17,200$ cal/mole. The growth of the W_2B phase was measured and the same analysis as outlined above was used to calculate the activation energy.

Table 1

Tungsten-Boron Diffusion Data Using the Samsonov and Latysheva Technique (8,9)

Temp. (°C)	D (C - C ₂)	Q (cal/mole)	D ₀ (cm ² /sec)	C - C ₂ (g/cm ³)	D (cm ² /sec)
1000	0	20,400 ± 6400	860 ± 170	0.231	3.72 x 10 ³ exp ($\frac{-20,400}{RT}$)
1100	0.6220				
1300	3.0688				
1400	8.6520				
1700	18.0432				
1800	21.6496				
1900	56.7896				

b. Tungsten-Carbon

There is very little agreement between the different investigators on diffusion of carbon into tungsten, even though several of them used the same technique. Samsonov and Latysheva, (8,9) employing the method described previously under the tungsten-boron system, gave a value of

$$D = 1.82 \times 10^6 \exp [-(39,500 \pm 13,400)/RT].$$

The data is given in Table 2. The growth of the W₂C phase was used for determining the diffusion coefficient over the temperature range of 1400 to 2000°C.

Table 2

Tungsten-Carbon Diffusion Data by Samsonov
and Latysheva (8,9)

Temp. (°C)	D (C - C ₂)	Q (cal/mole)	D ₀ (cm ² /sec)	C - C ₂ (g/cm ³)	D (cm ² /sec)
1400	0	39,500 ± 13,400	96,500 ± 9300	0.033	1.82 x 10 ⁶ exp ($\frac{-39,500}{RT}$)
1600	4.4330				
1700	9.5976				
1800	15.5372				
1900	20.6088				
2000	27.7140				

Kreimer, Efron, and Uaranova,⁽¹¹⁾ utilizing the same analytical system described by Samsonov and Latysheva, obtained

$$D(C - C_2) = 2750 \exp [-(112,000 \pm 3,000)/RT]$$

$$D = 25,000 \exp [-(112,000 \pm 3,000)/RT]$$

over the temperature range of 1500 to 1800°C. The data appears to have much less scatter than that of Ref. 8, but the activation energy still may be too large.

Pirani and Sandor⁽¹²⁾ placed large grained tungsten beads in a carbon bed and heated them to temperatures of 1535 to 1805°C. The depth of the tungsten-carbon phase was measured at various times at each temperature. The activation energy for the growth of the tungsten-carbon phase (assumed to be diffusion controlled) was found to be

$$Q = 59,000 \pm 5,000 \text{ cal/mole.}$$

D_0 was calculated from the Dushman-Langmuir equation, $[D = \frac{Qd^2}{Nh} \exp (-Q/RT)]$ where d = the jump distance in cm, Q is in cal/mole, h is in cal/sec, and D is in cm^2/sec , to be $D_0 = 0.31 \text{ cm}^2/\text{sec}$.

Zwikker⁽¹³⁾ measured diffusion of carbon in tungsten at 1700°C by means of thermionic emission. He obtained the values listed in Table 3.

Table 3

Tungsten-Carbon Diffusion Coefficients for 1700°C⁽¹³⁾

Type of Wire	D (cm^2/sec)
Single crystal wire	0.12×10^{-12}
Drawn wire	0.52×10^{-12}
Drawn wire with 0.75% ThO_2	0.63×10^{-12}
Pintsch wire	2.55×10^{-12}

Large voids observed in the Pintsch wire was given as the reason for the higher diffusion coefficient. Taking $D = 5 \times 10^{-13} \text{ cm}^2/\text{sec}$, $Q = 125,000 \text{ cal/mole}$ is calculated from the Dushman-Langmuir equation.

It is clear that more accurate data is needed on diffusion of carbon in tungsten.

Surface migration of carbon on tungsten was followed with the field emission microscope by Klein.⁽¹⁴⁾ A tungsten point was shadowed with carbon, heated to various temperatures, and observed in the field emission microscope at room temperature at given time intervals. A sharp moving interface was followed which gave a linear relationship between distance moved and the square root of time. Measurements were made at 850, 975, and 1100°K. This data yields an activation energy of $Q = 55,000 \pm 7,000$ cal/mole, indicating that Q for lattice diffusion of carbon in tungsten is probably of the order of 100,000 cal/mole.

c. Tungsten-Argon

Surface diffusion of argon on tungsten was measured by Gomer⁽¹⁵⁾ with the field emission microscope. A value of the activation energy for this process is given as

$$Q = 600 \pm 200 \text{ cal/mole.}$$

The very low value of Q signifies an extremely small binding energy between argon and tungsten atoms at the surface, as might be expected from the inertness of argon.

d. Tungsten-Hydrogen

Surface migration of hydrogen on tungsten was followed with the field emission microscope by Wortman, Gomer, and Lundy.⁽¹⁶⁾ A monolayer of hydrogen on tungsten gives an activation energy for surface diffusion of $Q = 9,000$ cal/mole. An earlier paper by Gomer and Hulm⁽¹⁷⁾ gave $Q = 16,000$ cal/mole for 0.1 monolayer of hydrogen. However, this corresponds to movement from higher energy sites only, since there are not sufficient hydrogen atoms to completely fill all sites.

e. Tungsten-Oxygen

Wortman, Gomer, and Lundy⁽¹⁶⁾ measured surface migration of oxygen on tungsten. They found that a monolayer of oxygen on tungsten gives $Q = 19,000$ cal/mole, while a 0.1 monolayer gives $Q = 30,000$ cal/mole.⁽¹⁴⁾

Muller,⁽¹⁸⁾ also using the field emission microscope, found $Q = 16,000$ cal/mole for the surface diffusion of oxygen on tungsten, which is in good agreement with Wortman's⁽¹⁶⁾ value of $Q = 19,000$ cal/mole.

3. Substitutional Diffusion

a. Tungsten-Barium

Muller⁽¹⁹⁾ and Becker⁽²⁰⁾ have observed surface migration of barium on tungsten with the field emission microscope but neither of them

calculated diffusion coefficients from their data. Becker gives data for several different crystallographic planes and for different voltages, temperatures and thicknesses of barium.

b. Tungsten-Cerium

Dushman, Dennison, and Reynolds⁽²¹⁾ have measured the lattice diffusion of cerium in tungsten by observing the thermionic emission as a function of time.² The samples were 4-mil diameter filaments. At 2000°K (1727°C), $D = 95 \times 10^{-11}$ cm²/sec and $D = 1.15 \exp (-83,000/RT)$. Measurements were not mentioned for temperatures other than 2000°K. Hence, the D_0 and Q values were probably determined with the Dushman-Langmuir equation. Diffusion coefficients calculated for temperatures other than 2000°K are probably not on firm ground. No mention was made as to the cerium content of the filaments, but from the relatively large value of Q , the cerium content must be small.

c. Tungsten-Cesium

The surface diffusion of cesium on tungsten was measured by Langmuir and Taylor⁽²²⁾ using the thermionic emission technique. These investigators made measurements for both the first adsorbed layer and the second adsorbed layer of cesium on the tungsten surface.

Table 4

Surface Diffusion of Cesium on Tungsten⁽²²⁾

First Adsorbed Layer			
Temp. (°C)	D (cm ² /sec)	D_0 (cm ² /sec)	Q (cal/mole)
27	1.2×10^{-11}	0.2	14,000
227	1.5×10^{-7}		
427	8.0×10^{-6}		
540	4.0×10^{-5}		
Second Adsorbed Layer			
27	3.4×10^{-4}	0.0164	2,300
227	2.2×10^{-3}		
427	3.2×10^{-3}		

The considerably lower activation energy for the second adsorbed layer is due to the movement from higher energy sites for the first adsorbed layer. The

movement of the second adsorbed layer probably comes closer to surface diffusion of cesium on cesium, which would be expected to have a smaller activation energy than surface diffusion of cesium on tungsten.

d. Tungsten-Iron

Vasiler, Kamardin, Skatskii, Chernomorchenko, and Shuppe⁽²³⁾ studied the diffusion of Fe^{59} into tungsten. The tracer was applied by electrolysis of FeCl_3 onto a slab of tungsten, 150 mm² by 0.4 mm thick. Diffusion samples were run at 1210, 1313, 1409, and 1513°K. The data fits the equation

$$D = 1.4 \times 10^{-2} \exp (-66,000/RT)$$

with an error in D estimated by the authors as being 30%. Gruzin⁽²⁴⁾ diffused W^{185} into αFe , γFe , and a 0.82% carbon steel. The diffusion anneals were carried out in the temperature range of 700 to 1250°C. The data is given in Table 5.

Table 5
Data on Diffusion of W^{185} into Iron⁽²⁴⁾

Temp. (°C)	$D \times 10^{12}$ (cm ² /sec)	
	Iron	0.82% C Steel
700	0.7	0.4
750	2.0	0.9
775	---	2.0
800	7.8	3.8
850	34	6.0
875	16	---
900	10	13.0
950	19	7.5
1000	14	15
1050	12	17
1100	18	44
1150	69	190
1200	210	230
1250	460	560

This data was found to fit the following equations:

$$D_{\alpha\text{Fe}} = 3.8 \times 10^2 \exp (-70,000/RT)$$

$$D_{\gamma\text{Fe}} = 1 \times 10^3 \exp (-90,000/RT)$$

$$D_{\gamma\text{steel}} = 13 \exp (-75,000/RT).$$

Van Liempt⁽²⁵⁾ determined the rate of diffusion of iron in tungsten by measuring the rate of evaporation of iron from a W - 0.04% Fe alloy. He stated that $D = 11.5 \exp (-143,000/RT)$. This value for the activation energy is greater by a factor of two than that observed by Vasiler et al.⁽²³⁾ Possibly the rate determining step in Van Liempt's evaporation experiments was not diffusion, but rather a phase boundary controlled reaction. This data has also been interpreted as representing self-diffusion in tungsten. Certainly, the tracer technique of Vasiler's is much preferred over the rate of evaporation measurements of Van Liempt as far as determining diffusion coefficients is concerned.

Grube and Schneider⁽²⁶⁾ bonded pure iron to an iron-tungsten alloy and diffused them at 1280, 1330, and 1400°C. The samples were sectioned and chemically analyzed by conventional methods. The diffusion coefficients are definitely a function of composition. However, the concentration gradients were analyzed by the Grube analysis,⁽²⁷⁾ since the Matano analysis⁽²⁸⁾ had not yet been published when this work was done. Their data is listed in Table 6.

Table 6
Experimental Data of Grube and Schneider⁽²⁶⁾ for Diffusion in
Tungsten-Iron System at Low Tungsten Compositions

x (cm)	Treatment 1 Temp., 1280°C Time, 24 hr C ₀ , 4.2% W		Treatment 2 Temp., 1330°C Time, 18 hr C ₀ , 3.85% W		Treatment 3 Temp., 1400°C Time, 7 hr C ₀ , 11% W	
	C (% W)	D x 10 ¹⁰ (cm ² /sec)	C (% W)	D x 10 ¹⁰ (cm ² /sec)	C (% W)	D x 10 ¹⁰ (cm ² /sec)
0.0025	3.2	3.95	3.42	24.1	9.12	24.6
0.0075	1.43	3.59	2.59	24.2	5.05	19.1
0.0125	0.57	4.07	1.87	24.8	2.41	19.2
0.0175	0.10	3.46	1.20	23.2	1.08	20.8
0.0225			0.79	24.3	0.97	32.2
0.0275			0.51	25.7	0.69	40.0
0.0325					0.39	43.4
0.0375					0.10	38.4

This data does not lend itself to a determination of the activation energy, because the temperature range is too narrow and there is too much scatter in an Arrhenius plot.

e. Tungsten-Potassium

Bosworth⁽²⁹⁾ measured the surface diffusion of potassium on tungsten by the photoelectric emission method. The values he obtained are tabulated in Table 7.

Table 7

Surface Diffusion of Potassium on Tungsten⁽²⁹⁾

Temp. (°C)	D (cm ² /sec)
480	0.57×10^{-5}
590	10.0×10^{-5}
780	280×10^{-5}

The equation

$$D = 0.43 \exp (-15,200/RT)$$

is a good representation of this data. It should be noted that these values are for low potassium concentration. As the potassium concentration increased, the diffusion coefficient was observed to decrease. This is the opposite behavior from what was observed for tungsten-cesium,⁽²²⁾ tungsten-hydrogen,^(16,19) and tungsten-oxygen.^(16,17)

f. Tungsten-Molybdenum

Diffusion of molybdenum into polycrystalline tungsten and tungsten single crystals was carried out by Van Liempt.⁽³⁰⁾ The molybdenum was in the form of gaseous MoCl₅ mixed with hydrogen. Layers of the metal were machined off and chemically analyzed by standard procedures. The molybdenum concentration varied between 0 and 20 weight percent molybdenum.

Table 8

Diffusion of Molybdenum into Single Crystal
and Polycrystalline Tungsten⁽³⁰⁾

Polycrystalline Tungsten		Tungsten Single Crystals	
Temp. (°C)	$D \times 10^{12}$ (cm ² /sec)	Temp. (°C)	$D \times 10^{12}$ (cm ² /sec)
1533	1.3	1533	0.26
1770	11.0	1770	1.12
2010	106.0	2010	22.0
2260	640.0	2260	78.0

This data fits the equations:

$$D_{\text{single crystal}} = 6.3 \times 10^{-4} \exp (-80,500/RT)$$

$$D_{\text{poly crystal}} = 5 \times 10^{-3} \exp (-80,500/RT).$$

The diffusion coefficient for tungsten-molybdenum diffusion may be quite dependent on concentration due to the differences in melting points but no such dependence was reported. (This data was published before the publication of the Matano analysis.) A plot of log D vs 1/T is shown in Fig. 1.

Another value was published for 2400°C at a later date by Van Liempt:⁽³¹⁾

$$D = 1 \times 10^{-8} \text{ cm}^2/\text{sec (polycrystalline tungsten at 2400°C)}.$$

g. Tungsten-Sodium

The surface diffusion of sodium on tungsten has been determined by Bosworth⁽²⁹⁾ using the method of photo-electric emission. A small patch of sodium was placed on the center of a tungsten strip filament and heated for various times at pre-determined temperatures. The strip was then traversed with a well defined spot of light and the photo-electric properties measured along the strip. By this method the following data in Table 9 was obtained.

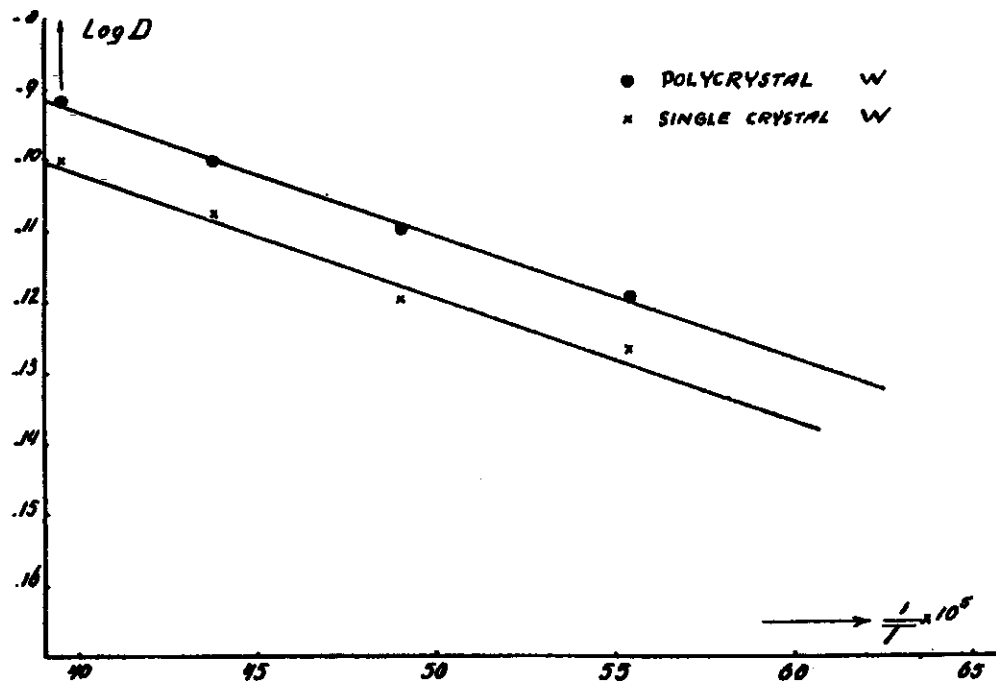


Fig. 1 - Log D vs $1/T$ for diffusion of molybdenum in polycrystalline and single crystal tungsten. (30)

Table 9

Surface Diffusion of Sodium on Tungsten⁽²⁹⁾

Temp. (°K)	D x 10 ⁵ (cm ² /sec)	Temp. (°K)	D x 10 ⁵ (cm ² /sec)
293	0.8	500	50.0
350	3.2	520	77.0
375	6.0	555	128
410	13.0	620	200
420	20.0	690	270
430	30.0	740	310
450	34.0	800	330

These values were found to fit the equation

$$D = 0.1 \exp (-5560/RT).$$

The data looks quite good and very complete. It would correspond to the second adsorbed layer of the tungsten-cesium system. That is, there was sufficient sodium present so that Bosworth was not measuring diffusion from the higher energy sites, but was measuring true surface diffusion.

h. Tungsten-Nickel

Swalin and Martin⁽³²⁾ prepared pressure welded diffusion couples of pure nickel and a Ni 1.5% W alloy. Spectrophotometric analysis on lathe turning was used to determine the concentration gradient.

Table 10

Tungsten-Nickel Diffusion at Low Tungsten Compositions⁽³²⁾

Temp. (°C)	D (cm ² /sec)
1153	1.78 x 10 ⁻¹¹
1187	3.40 x 10 ⁻¹¹
1220	4.17 x 10 ⁻¹¹
1252	1.07 x 10 ⁻¹⁰
1289	1.85 x 10 ⁻¹⁰

The variation of the diffusion coefficient with temperature may be expressed by

$$D = 11.1 \exp (-76,800/RT).$$

Although the temperature range used in this investigation is rather small, the data is sufficiently good to limit the error in the activation energy to ± 1000 cal/mole. A plot of $\log D$ vs $1/T$ is shown in Fig. 2.

Allison and Moore⁽³³⁾ evaporated W^{185} onto the surface of nickel single crystals and large grained polycrystals in the temperature range of 1100 to 1275°C. The usual sectioning and counting procedures were used. Both single crystal and polycrystalline data obey the equation

$$D = 1.13 \exp (-71,000/RT).$$

The scatter in their results is quite small.

Specimens were also diffused between pure nickel and a Ni - 4.9% W alloy. This data fits the same equation as above. A plot of $\log D$ vs $1/T$ is shown in Figs. 3(a) and (b).

i. Tungsten-Silicon

The growth of the WSi_2 phase was observed as a function of temperature by Samsonov and Solonnikova⁽³⁴⁾ for tungsten cylinders packed in silicon powder. Using the analysis outlined under the tungsten-boron system,^(8,9) these investigators determined the activation energy for the process. No data points were given and no Arrhenius plot was shown. The activation energy was given as $Q = 5,780$ cal/mole which is excessively low. Their results are probably worthless for use as diffusion data, but might have some practical value in other applications.

j. Tungsten-Thorium

Dushman and Langmuir⁽³⁵⁾ measured the diffusion of thorium in tungsten at 2300°K using the field emission microscope. They obtained $D = 1.1 \times 10^{-9}$ cm²/sec at 2300°K. The activation energy was calculated by means of the Dushman-Langmuir equation as $Q = 94,000 \pm 3,000$ cal/mole.

Langmuir⁽³⁶⁾ obtained the data in Table 11 by the same technique. These values yield an activation energy of $Q = 94,000$ cal/mole and $D_0 = 1.13$ cm²/sec which agrees with the value of Ref. 35.

Langmuir⁽³⁷⁾ interpreted this data as being representative of grain boundary diffusion.

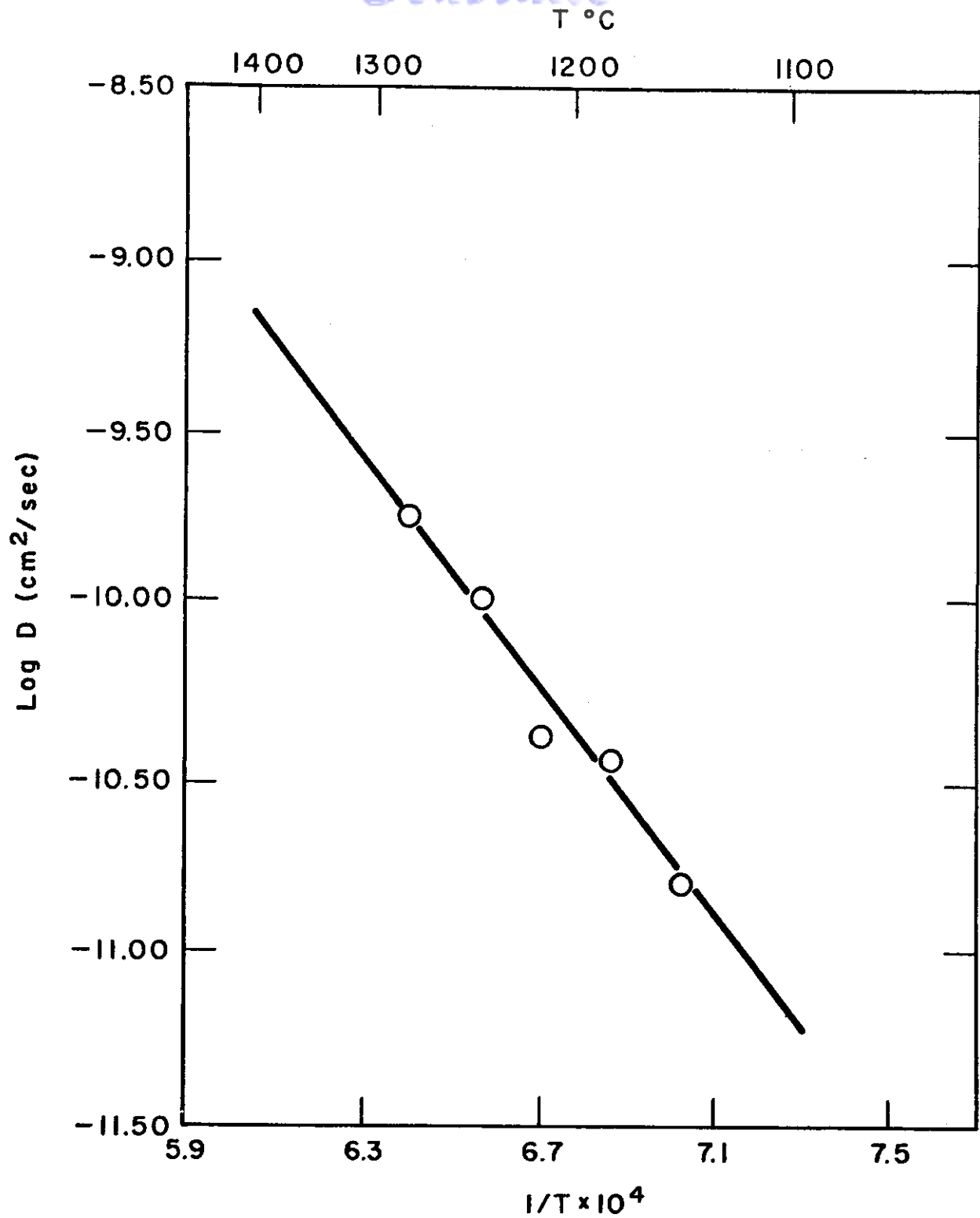


Fig. 2 - $\text{Log } D$ vs $1/T$ is plotted for diffusion in tungsten-nickel alloys of high nickel concentration.(32)

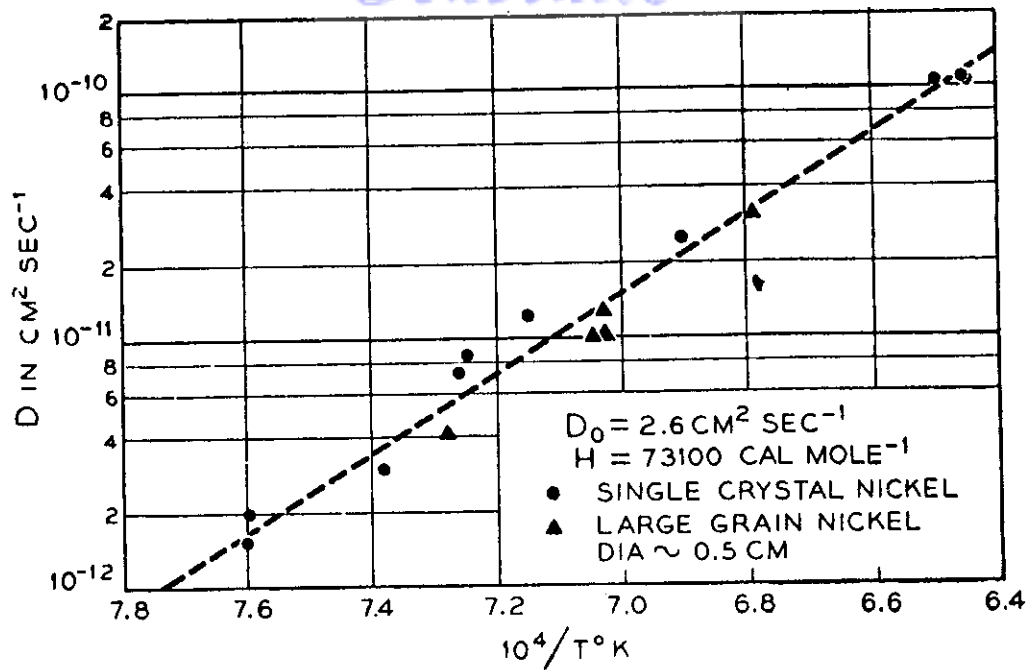


Fig. 3(a) - The temperature dependence of the diffusion from a tungsten-nickel alloy into pure nickel.(33)

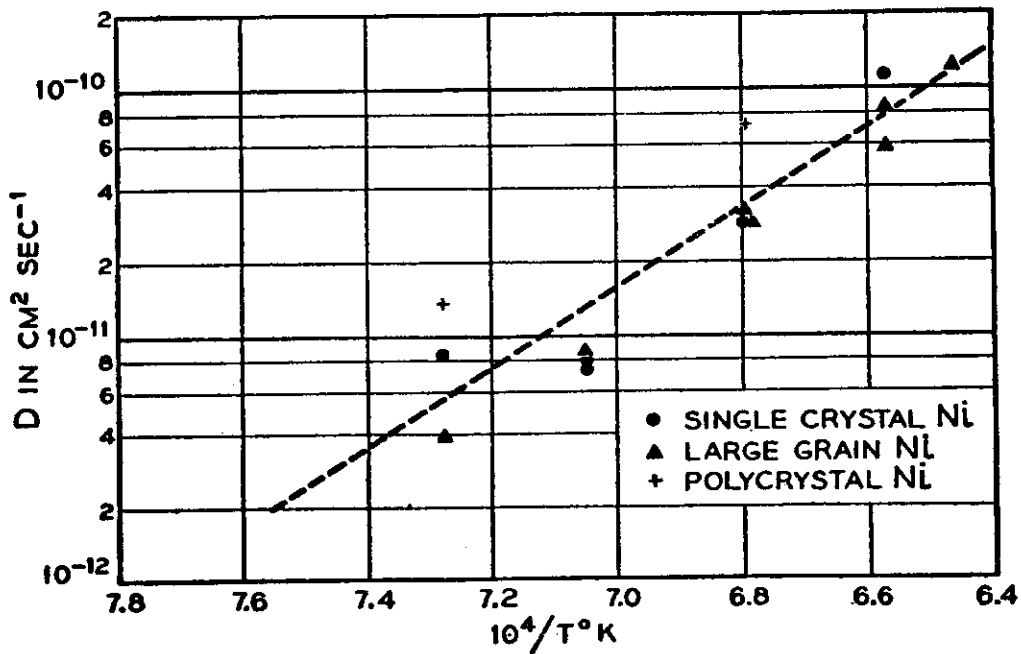


Fig. 3(b) - The temperature dependence of the diffusion from a tungsten layer into pure nickel.(33)

Table 11

Grain Boundary Diffusion in Tungsten-
Thorium System⁽³⁶⁾

Temp. (°K)	D (cm ² /sec)
2055	1.1×10^{-10}
2300	1.12×10^{-9}
2400	3.57×10^{-9}
2500	6.8×10^{-9}

Fonda, Young, and Walker⁽³⁸⁾ found $D = (1 \pm 0.2) \times 10^{-11}$ cm²/sec at 2400°K. Langmuir⁽³⁷⁾ interpreted this data as lattice diffusion data and calculated $Q = 120,000$ cal/mole and $D_0 = 1$ from the Dushman-Langmuir equation.

From data obtained by Brattain and Becker,⁽³⁹⁾ using an electron emission technique, Langmuir⁽³⁷⁾ calculated $Q = 66,400$ cal/mole and $D_0 = 0.47$. This was interpreted as surface diffusion.

In summary, the values stated by Langmuir⁽³⁷⁾ are:

$$D_{\text{surface}} = 0.47 \exp (-66,400/RT)$$

$$D_{\text{grain boundary}} = 1.13 \exp (-94,000/RT)$$

$$D_{\text{lattice}} = 1.0 \exp (-120,000/RT).$$

With the exception of the data of Ref. 36, all values of the activation energy were calculated by means of the Dushman-Langmuir equation from data at one temperature. This leaves some doubt as to the accuracy of the values given for D_0 and Q . Unfortunately, there is no data available that was obtained by the more accurate sectioning or electron probe methods for comparison.

k. Tungsten-Uranium, Tungsten-Yttrium, and
Tungsten-Zirconium

The measurement of the lattice diffusion of uranium, yttrium, and zirconium in tungsten was done by Dushman, Dennison, and Reynolds⁽¹¹⁾ by observing the thermionic emission as a function of time. The samples used were 4-mil diameter filaments. The following diffusion data was obtained at 2000°K:

for uranium:

$$D = 1.3 \times 10^{-11} \text{ cm}^2/\text{sec}$$

$$D = 1.14 \exp (-100,000/RT)$$

for yttrium:

$$D = 1.82 \times 10^{-8} \text{ cm}^2/\text{sec}$$

$$D = 0.11 \exp (-62,000/RT)$$

for zirconium:

$$D = 3.24 \times 10^{-9} \text{ cm}^2/\text{sec}$$

$$D = 1.1 \exp (-78,000/RT).$$

Measurements were not mentioned for temperatures other than 2000°K (1727°C). Hence, the D_0 and Q values were probably determined with the Dushman-Langmuir equation, hence diffusion coefficients calculated for temperatures other than 2000°K are probably not on firm ground.

The data for diffusion in tungsten is summarized in Table 12.

B. Diffusion in Tantalum

1. Self-diffusion

Self-diffusion in tantalum has been measured by several investigators. Eager and Langmuir⁽⁴⁰⁾ activated a small volume of a tantalum strip in the thermal column of the NRX pile and then heated these strips in vacuum in the temperature range of 2100 to 2800°K. The radioactivity after diffusion was measured along the length of the strip. This data fitted the equation:

$$D = 2 \exp (-110,000/RT).$$

A great deal of grain boundary diffusion was observed by autoradiographic techniques in samples diffused at temperatures near 1800°K. An attempt at measuring surface diffusion by evaporating a surface deposit of radioactive tantalum on a clean tantalum strip yielded D_{surface} as being approximately 10^7 times larger than D_{lattice} at 1800°K.

Gruzin and Meshkov⁽¹⁴⁾ deposited Ta¹⁸² onto tantalum discs. Two discs were then clamped together with their active faces in contact and diffused between 1200 and 1300°C for times up to 320 hours. Their data is given in Table 13.

Table 12
Summary of Diffusion Data for Tungsten

Diffusing Element	Composition Range (wt. %)	Temp. (°C)	D (cm^2/sec)	D (cm^2/sec)	D (cm^2/sec)	Q (cal/mole)	Reference
W	Surface diffusion	927-1227 927-1327 1527-2427			4	106,500 73,200 72,000	2 5 6
W (self)		1287-1453			6.3×10^7	135,800	1
B	4.5	1000-1900 900-1300			3.72×10^3 1.37×10^{-5}	20,400 17,200	8,9 10
C	Surface diffusion 6 6 6	577-827 1400-2000 1500-1800 1535-1805 1700		$(0.52-2.55) \times 10^{-12}$	1.82×10^6 2.5×10^4 0.31	55,000 39,500 112,000 59,000	14 8,9 11 12 13
A	Surface diffusion					600	15
H	Surface diffusion					9,000	16
O	Surface diffusion					19,000	16
Ce		1727		95×10^{-11}	1.15	83,000	21
Cs	1st adsorbed layer	27 227 427 540		1.2×10^{-11} 1.5×10^{-7} 8.0×10^{-6} 4.0×10^{-5}	0.2	14,000	22
	2nd adsorbed layer	27 227 427		3.4×10^{-4} 2.2×10^{-3} 3.2×10^{-3}	0.0164	2,300	22
Fe	Fe tracer (0% Fe)	937-1240			1.4×10^{-2}	66,000	23
CoFe	W tracer (100% Fe)	700-900			3.8×10^2	70,000	24

(Cont'd. on next page.)

Table 12 (Cont'd.)

Diffusing Element	Composition Range (wt. %)	Temp. (°C)	D (cm ² /sec)	D_0 (cm ² /sec)	Q (cal/mole)	Reference
γ Fe	W tracer (100% Fe)	950-1250		1×10^3	90,000	24
γ Fe + 0.82% C	W tracer (99.18% Fe)	950-1250		13	75,000	24
Fe	0.04	1927-2527		11.5	143,300	25
Fe	89-100	1280 1330 1400	$(3.4-4.0) \times 10^{-10}$ $(2.3-2.6) \times 10^{-9}$ $(1.9-4.3) \times 10^{-9}$			26
K	Surface	207 317 507	0.57×10^{-5} 10.0×10^{-5} 280×10^{-5}	0.43	15,200	29
Mo (W single crystal)	0-20	1533 1770 2010 2260	0.26×10^{-12} 1.12×10^{-12} 22.0×10^{-12} 78.0×10^{-12}	6.3×10^{-4}	80,500	30
Mo (W polycrystal)	0-20	1533 1770 2010 2260	1.3×10^{-12} 11.0×10^{-12} 106×10^{-12} 640×10^{-12}	5×10^{-3}	80,500	30
Na	Surface	20 137 177 227 282 347 527	0.8×10^{-5} 13.0×10^{-5} 34.0×10^{-5} 50.0×10^{-5} 128×10^{-5} 200×10^{-5} 330×10^{-5}	0.1	5,560	29
Ni	98.5-100	1153 1187 1220 1252 1289	1.78×10^{-11} 3.40×10^{-11} 4.17×10^{-11} 1.07×10^{-10} 1.85×10^{-10}	11.1	76,800	32

(Cont'd. on next page.)

Table 12 (Cont'd.)

Diffusing Element	Composition Range (wt. %)	Temp. (°C)	D (cm^2/sec)	D (cm^2/sec)	Q (cal/mole)	Reference
Ni	W tracer (100% Ni) 95.1-100	1100-1275		1.13	71,000	33
Si	20				5,780	8,9
Th	Grain boundary diffusion	1782	1.1×10^{-10}	1.13	94,000	36
		2027	1.12×10^{-9}			
		2127	3.57×10^{-9}			
		2227	6.8×10^{-9}			
	Surface			0.47	66,400	37,39
	Lattice	2127	1×10^{-11}	1.0	120,000	37,38
U		1727	1.3×10^{-11}	1.14	100,000	11
Y		1727	1.82×10^{-8}	0.11	62,000	11
Zr		1727	3.24×10^{-9}	1.1	78,000	11

Self-diffusion Data for Tantalum⁽¹⁴⁾

Temp. (°C)	D x 10 ¹³ (cm ² /sec)
1200	1
1250	2.5
1300	7.6

Gruzin and Meshkov⁽⁴²⁾ at a later date stated that self diffusion in tantalum may be represented by the equation:

$$D = 1.3 \times 10^3 \exp (-110,000/RT).$$

This shows excellent agreement in the activation energy with the data of Eager,⁽⁴⁰⁾ but a considerable discrepancy exists between the two values of D_0 . Since the value of D_0 is normally expected to be in the range of 0.1 to 10 for self diffusion, Eager's value of 2 is probably the better value to use.

2. Interstitial Diffusion

a. Tantalum-Boron

Samsonov and Latysheva^(8,9) using the technique described previously under the tungsten-boron system gave a value of

$$D = 5.92 \times 10^3 \exp [-(16,900 \pm 6,100)/RT].$$

The data is given in Table 14. The growth of the TaB₂ phase was used for determining the diffusion coefficient over the temperature range of 1200 to 2000°C. As previously mentioned the validity of these values as diffusion data is very questionable.

b. Tantalum-Carbon

Samsonov and Latysheva,^(8,9) employing the analytical method found on page 3, found that the diffusion coefficient may be represented by the equation:

$$D = 1.98 \times 10^4 \exp [-(19,300 \pm 6,500)/RT].$$

Table 14

Tantalum-Boron Diffusion Data Using the Analytical
Method of Samsonov and Latysheva^(8,9)

Temp. (°C)	D (C - C ₂)	Q (cal/mole)	D ₀ (cm ² /sec)	C - C ₂ (g/cm ³)	(cm ² /sec)
1200	11.8206	16,900 ± 6100	1280 ± 240	0.216	5.92 x 10 ³ exp ($\frac{-16,900}{RT}$)
1300	27.3438				
1400	44.1540				
1500	65.9340				
1600	86.3874				
1800	99.6530				
2000	125.5320				

The data is given in Table 15. The diffusion coefficient over the temperature range of 1000 to 1800°C was evaluated by considering the growth of the Ta₂C phase. A comparison of this data with the much more accurate data of Powers and Doyle and others which will be presented further on, shows that the activation energy given by Ref. 8 is too small by a factor of two and the D₀ value is too large by a factor of 10⁶. This serves as a measure of the caution that one should use when considering the application of the data presented in Refs. 8, 9, and 34.

Table 15

Diffusion Data for Tantalum-Carbon System^(8,9)

Temp. (°C)	D (C - C ₂)	Q (cal/mole)	D ₀ (cm ² /sec)	C - C ₂ (g/cm ³)	(cm ² /sec)
1000	0	19,300 ± 6500	3300 ± 600	0.166	1.98 x 10 ⁴ exp ($\frac{-19,300}{RT}$)
1300	4.4715				
1400	7.7440				
1500	9.2400				
1600	13.1450				
1800	20.9385				

In 1948, Ke⁽⁴³⁾ applied the measurements of internal friction to the diffusion of carbon in tantalum. A torsion pendulum was used to measure the damping in tantalum wire specimens which had been heat treated in a carbon containing atmosphere. The application of stress causes the interstitial solution in tantalum to distribute preferentially in the lattice. This redistribution of atoms produces a damping peak in the curve of internal friction as a function of temperature. Ke⁽⁴³⁾ and later Wert⁽⁴⁴⁾ located a peak at 140 to 150°C which they attributed to the diffusion of carbon in tantalum. (Actually, the peak was shown by Powers and Doyle^(45,46) to be a result of the diffusion of small amounts of oxygen rather than of carbon.) Ke obtained an activation energy of $Q = 25,000$ cal/mole, and Wert found that this data fitted the equation:

$$D = 0.015 \exp (-27,000/RT).$$

Powers and Doyle⁽⁴⁷⁾ found the internal friction peak for carbon diffusion in tantalum to be at 324.9, 337.7, and 354.9°C for frequencies of 0.270, 0.538, and 1.330 cps, respectively. From these data, the activation energy was found to be 39,600 cal/mole.

The most complete information on diffusion of interstitials was recently published by Powers and Doyle.⁽⁴⁸⁾ Data was obtained by both internal friction and elastic after-effects measurements. This is summarized in Table 16.

Table 16

Tantalum-Carbon Diffusion Coefficients as Determined
by Internal Friction Methods⁽⁴⁸⁾

Method of Measurement	D_0 (cm ² /sec)	Q (cal/mole)
Internal friction	0.014 ± 0.003	$39,500 \pm 200$
Elastic after-effects	0.0054 ± 0.001	$38,400 \pm 200$
Combined	0.0061 ± 0.0012	$38,510 \pm 260$

A plot of the log of the relaxation time vs $1/T^\circ K$ for these values is illustrated in Fig. 4. This data is of exceptionally good quality, and the absence in the literature of more of this caliber work is most noticeable.

A theory has been presented by Ferro⁽⁴⁹⁾ for calculating the diffusion of interstitials into body-centered cubic metals. A theoretical value is evaluated by using the elastic constants of the matrix metal and the interstitial atom diameter. The values arrived at for diffusion of carbon in tantalum are:

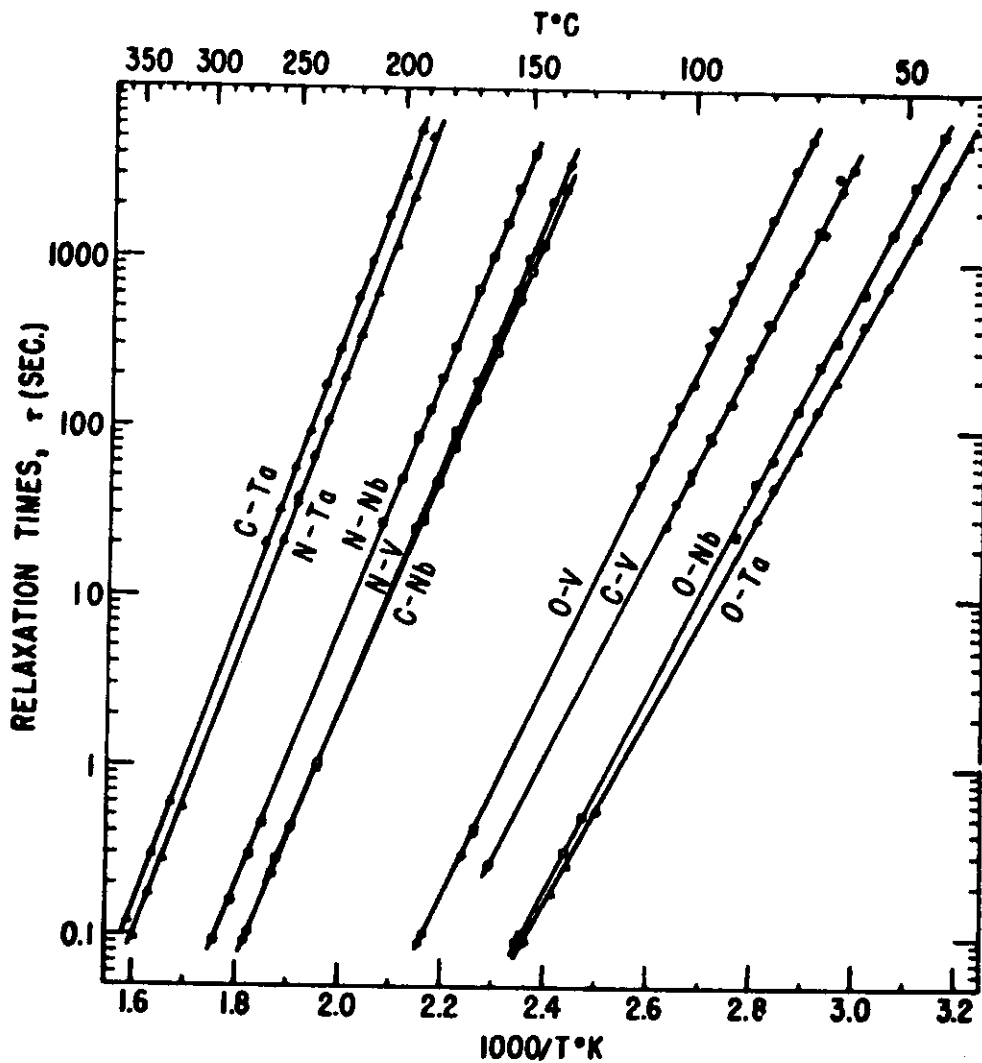


Fig. 4 - Relaxation times for stress-induced ordering vs $1/T$ for several alloys. (48)

Contrails

$$Q = 42,000 \text{ cal/mole,}$$

$$D_o = 0.009 \text{ cm}^2/\text{sec.}$$

These compare quite favorably with the values obtained by Powers and Doyle.

c. Tantalum-Hydrogen

The weight gain of tantalum heated in hydrogen was measured by Gulbransen and Andrews⁽⁵⁰⁾ as a function of time and temperature. At least two different rate laws were found to be operating. However, between 700 and 900°C a parabolic rate law appeared to exist. The authors felt that the sensitivity of the hydride reaction to surface films and the impurities and inhomogeneities in the metal made an evaluation of a diffusion coefficient, difficult. The data may be of interest for reaction rates, but no diffusion data is presented.

Using the theory of Ferro,⁽⁴⁹⁾ D_o and Q may be calculated as:

$$Q = 6,800 \text{ cal/mole,}$$

$$D_o = 0.0009 \text{ cm}^2/\text{sec.}$$

In the absence of good experimental values, these may serve as an order of magnitude answer.

d. Tantalum-Oxygen

Diffusion of oxygen in tantalum has been measured by three different techniques over three different temperature ranges. Internal friction measurements have been made in the temperature interval of 50 to 350°C, weight gain measurements from 250 to 350°C, and microhardness measurements on concentration gradients from 700 to 1400°C. Agreement is quite good over the entire temperature range.

Ke,⁽⁴³⁾ using the internal friction method, found the activation energy to be 29,000 cal/mole in the temperature range of 152 to 170°C. He found that the relaxation process had no single relaxation time as in the other diffusion processes measured by this method. This was interpreted by the author to mean that the atoms are at both the octahedral and tetrahedral positions, while in the other cases the atoms are at only the octahedral sites.

Since Ke's value of Q is slightly larger than that obtained by the other investigators, he might have had a large amount of oxygen or some amount of nitrogen in his sample. A large oxygen content or nitrogen content can raise the

observed activation energy for oxygen diffusion [Powers and Doyle⁽⁴⁶⁾]. This may also explain why Ke observed no single relaxation time.

Powers and Doyle^(45,46) observed that the internal friction in tantalum arising from the diffusion of interstitially dissolved oxygen at low concentrations could be described with a single relaxation time, but at higher oxygen concentrations the experimentally determined internal friction curve became broadened and skewed, with the internal friction considerably higher on the high temperature side of the peak. The same behavior in the oxygen peak was produced by small additions of nitrogen. A summary of their data is given in Table 17.

Table 17
Tantalum Diffusion Data of Powers and Doyle⁽⁴⁶⁾

System	Frequency of Applied Stress (cps)	Reciprocal Peak Temp. ($1/T \times 10^3$)	Activation Energy (cal/mole)	t_0 ($10^{14}/\text{sec}$)	Comments
O in Ta (low conc. 0.015 wt. %)	0.285	2.494	25,800	0.5	Q = 25,900 from peak breadth measurement.
	0.612	2.438			
	1.673	2.358			
O in Ta (high conc. 0.12 wt. %)	0.266	2.431	27,800	0.1	Q = 27,800 is some average of that for normal Ta-O peak and the O-O interaction peak.
	0.559	2.381			
	1.541	2.305			
Low O conc. High N conc. (0.0225 wt. % O 0.08 wt. % N)	0.293	2.492	26,100	0.3	Normal oxygen peak.
	0.891	2.408			
	1.722	2.357			
	0.293	2.275	27,300	1.0	Oxygen-nitrogen interaction peak.
	0.891	2.191			
	1.722	2.147			
N in Ta (low conc. 0.02 wt. %)	0.285	1.689	37,500	0.8	Q = 37,000 from peak breadth measurement.
	0.570	1.652			
	0.927	1.625			
	1.662	1.596			

Thus, small concentration differences and small amounts of a third element may significantly change the diffusion coefficients obtained by this technique. This may serve as part of the reason for the relatively small disagreement between the diffusion coefficients obtained by the different investigators using the internal friction method.

Ang⁽⁵¹⁾ used both the torsion pendulum and a high frequency method for his internal friction measurements. This allowed him to take data over a large temperature range, 155 to 355°C. He obtained $D_0 = 0.0190 \text{ cm}^2/\text{sec}$ and $Q = 27,300 \text{ cal/mole}$. Marx, Baker, and Silvertsen⁽⁵²⁾ using only the high frequency method reported the same values as Ang.

The most recent work of Powers and Doyle,⁽⁴⁸⁾ listed in Table 18, gave diffusion coefficients for oxygen diffusion in tantalum obtained by internal friction, elastic after-effects, and peak breadth measurements over the temperature range of 50 to 150°C.

Table 18

Diffusion Data for the Tantalum-Oxygen System as
Determined from Internal Friction Measurements⁽⁴⁸⁾

Method of Measurement	D_0 (cm^2/sec)	Q (cal/mole)
Internal friction	0.006 ± 0.002	$25,700 \pm 300$
Elastic after-effects	0.0038 ± 0.0007	$25,400 \pm 100$
Combined	0.0044 ± 0.0008	$25,450 \pm 130$
Peak breadth		$25,000 \pm 300$

The log of the relaxation time vs $1/T^\circ\text{K}$ for this data is also plotted in Fig. 4.

Ferro⁽⁴⁹⁾ obtained theoretical values of $D_0 = 0.004 \text{ cm}^2/\text{sec}$ and $Q = 29,000 \text{ cal/mole}$ which are in good agreement with the experimental data.

The diffusion of oxygen in tantalum in the temperature range of 700 to 1400°C was measured by Gebhardt, Seghezzi, and Stegherr⁽⁵³⁾ by loading band shaped specimens with gas at one end and then allowing diffusion to occur. Microhardness measurements were used to determine the concentration of oxygen as a function of distance along the band. Their data fitted the equation:

$$D = 0.015 \exp (-26,700/RT).$$

which is in superb agreement with the internal friction data at much lower temperatures. These results are plotted in Fig. 5.

Gulbransen and Andrew⁽⁵⁰⁾ measured the weight gain of tantalum heated in oxygen as a function of time and temperature. The rate law for the rate controlling step was found to be parabolic (probably diffusion). Over the temperature range of 250 to 450°C the relationship followed was:

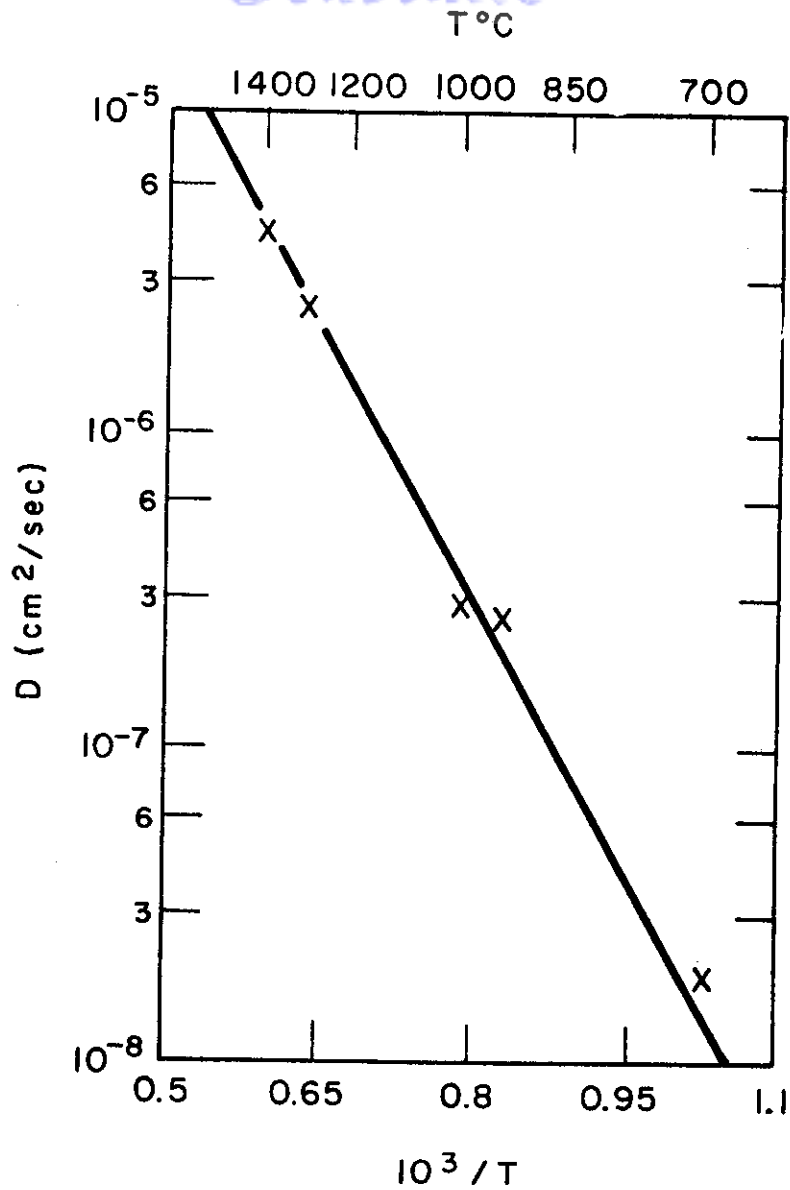


Fig. 5 - Temperature dependence of the diffusion coefficient for oxygen in tantalum. (53)

$$D = 8 \times 10^{-5} \exp (-27,400/RT).$$

Figure 6 shows a plot of $\log D$ vs $1/T^{\circ}K$ for this data.

The diffusion of oxygen in tantalum over twelve orders of magnitude is seen in Fig. 7. The data of Gulbransen and Andrew⁽⁵⁰⁾ was obtained by the least reliable technique of the three methods, so not as much weight has been applied to this data in drawing the curve in Fig. 7. Such good agreement over a wide range of temperatures is most remarkable

e. Tantalum-Nitrogen

By using internal friction measurements, Ke⁽⁴³⁾ found that activation energy, $Q = 44,000$ cal/mole, for diffusion of nitrogen in tantalum. This value is somewhat larger than that found in the more precise work of Powers and Doyle.

Powers and Doyle⁽⁴⁶⁾ obtained a value of $Q = 37,500$ cal/mole over the temperature range of 320 to $350^{\circ}C$. This was for samples containing 0.02 weight percent nitrogen. For samples containing 0.0225 weight percent oxygen and 0.08 weight percent nitrogen, they found that the oxygen peak was moved such that Q was 26,100 cal/mole instead of 25,800 cal/mole. Also a peak was found with an activation energy of $Q = 27,300$ cal/mole, due to the oxygen-nitrogen interactions. This data is summarized in Table 17.

Ang,⁽⁵¹⁾ utilizing both the torsion pendulum and high frequency methods for internal friction measurements, found that $D_0 = 0.0123$ cm²/sec and $Q = 39,800$ cal/mole over the rather large temperature range of 360 to $662^{\circ}C$. Good agreement with Ang's work is given by the data of Marx, Baker, and Silvertsen⁽⁵²⁾ which was obtained with the high-frequency method.

The most recent work of Powers and Doyle,⁽⁴⁸⁾ given in Table 19, reported the diffusion coefficients for nitrogen diffusing in tantalum obtained by internal friction, elastic after-effects, and peak breadth measurements over the temperature range of 190 to $350^{\circ}C$.

Table 19
Tantalum-Nitrogen Diffusion Coefficients

Method of Measurement	D_0 (cm ² /sec)	Q (cal/mole)
Internal friction	0.0042 ± 0.0020	$37,500 \pm 500$
Elastic after-effects	0.0060 ± 0.0010	$37,900 \pm 200$
Combined	0.0056 ± 0.0010	$37,840 \pm 200$
Peak breadth		$37,100 \pm 400$

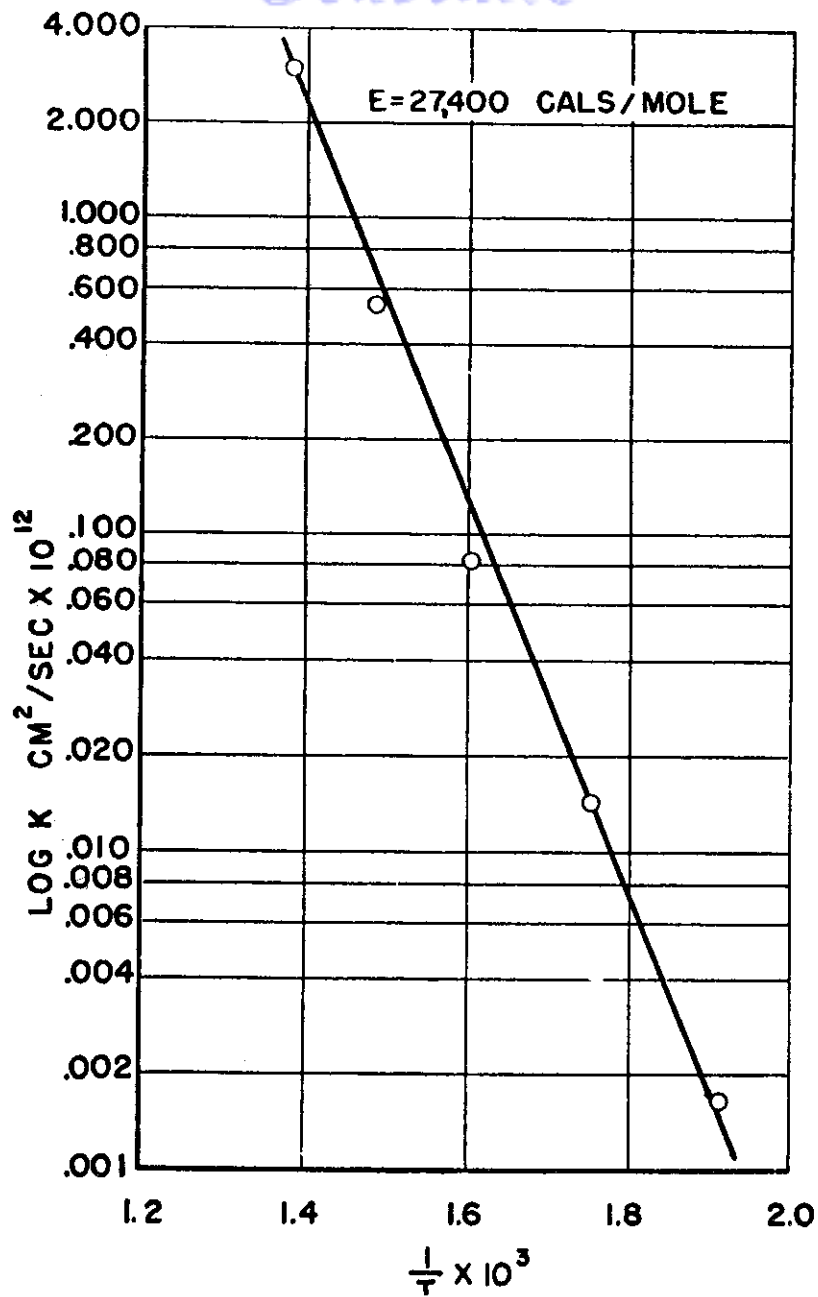


Fig. 6 - Log K vs $1/T$ for the reaction of tantalum with oxygen.(50)

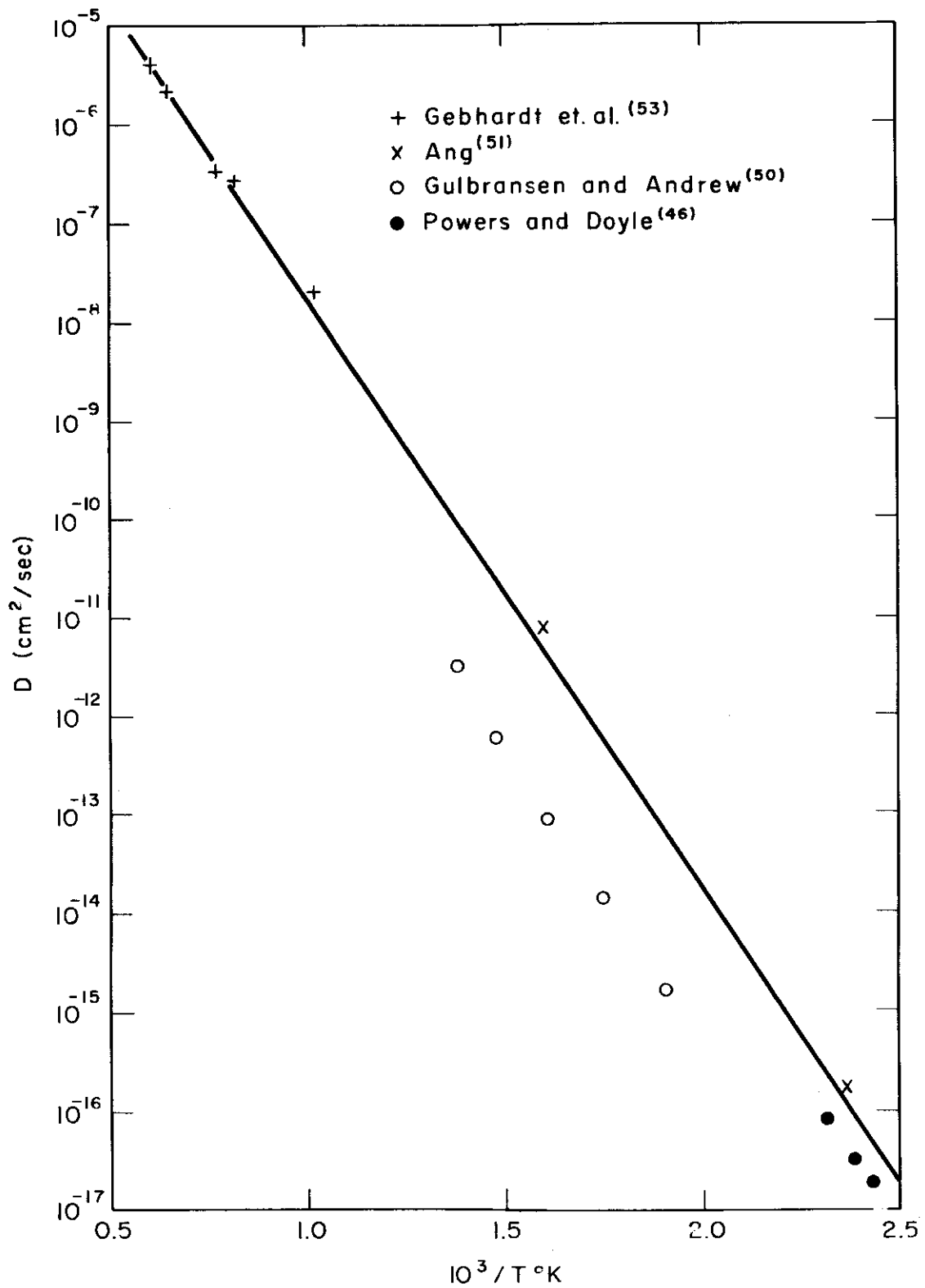


Fig. 7 - Temperature dependence of diffusion coefficient for tantalum-oxygen system.

The log of the relaxation time vs $1/T^{\circ}\text{K}$ plot for this data is given in Fig. 4.

Ferro⁽⁴⁹⁾ calculated a theoretical value of D_0 and Q for diffusion of nitrogen in tantalum using the elastic constants of the matrix metal and the interstitial atom diameter. He obtained $Q = 35,000$ cal/mole and $D_0 = 0.008$ cm^2/sec . These results are in quite fine agreement with the better experimental values.

Gulbransen and Andrew⁽⁵⁰⁾ measured the weight gained by a tantalum strip heated in nitrogen as a function of time and temperature. The activation energy of the rate limiting step (assumed to be diffusion) was found to be $Q = 39,400$ cal/mole. Measurements were made over the temperature range of 500 to 850°C. The log D vs $1/T$ curve is linear from 600 to 850°C, but at 500°C diffusion may not be the controlling mechanism.

3. Substitutional Diffusion

a. Tantalum-Iron

The diffusion of the iron isotope Fe^{59} into tantalum, was measured by Vasiler, Karmardin, Skalskii, Chernomorchenko, and Shuppe.⁽²³⁾ Fe^{59} was added by electrolysis of FeCl_3 onto slabs of tantalum 150 mm^2 in area and 0.4 mm thick. Data from the four temperatures investigated (1514, 1313, 1254, and 1203°K) may be represented by the equation:

$$D = 5.05 \times 10^{-1} \exp (-71,400/RT).$$

The authors estimate their error in D as being 30%.

b. Tantalum-Silicon

Samsonov and Solonnikova⁽³⁴⁾ applied the analytical method described under tungsten-boron diffusion (page 3) to the rate of growth of the TaSi_2 phase. An "activation energy" is given as $Q = 6,040$ cal/mole. This value is exceptionally low and, as previously stated, the value of this data is questionable.

c. Tantalum-Niobium

Preliminary data of this author gives $D = 5 \times 10^{-15}$ cm^2/sec at 1100°C. This value was obtained by diffusing a sandwich couple composed of the pure metals for 16 days at 1100°C. The concentration vs penetration curve was measured with the electron probe. Because of the very steep concentration gradient obtained under these conditions of time and temperature, the data is somewhat questionable, but is given solely due to the lack of other data in this system.

Tantalum diffusion data is summarized in Table 20.

Table 20
Summary of Diffusion Data for Tantalum

Diffusing Element	Composition Range (wt. %)	Temp. (°C)	D (cm^2/sec)	D_0 (cm^2/sec)	Q (cal/mole)	References
Ta (self)		1827-2527	1×10^{-13} 2.5×10^{-13} 7.6×10^{-13}	2	110,000	40
		1200				41
		1250				41
		1300				41
				1.3×10^3	110,000	42
B	20	1200-2000		5.92×10^3	16,900	8,9
C	3	1000-1800		1.98×10^4	19,300	8,9
						43
						44
						47
		325-355		0.015	27,000	48
		200-350		0.006	39,600	
					38,510	
H				0.0009	6,800	54
O	0.015 0.12	152-170			29,000	43
		128-150				46
		138-160				46
		155-355				51,52
		50-150				48
		250-450				50
		700-1400		0.015	26,700	53
N	0.02	320-350			44,000	43
		360-662				46
		190-350				51
		600-850				48
				0.0123	39,800	50
				0.0056	37,840	
					39,400	
Fe	Fe tracer (100% Ta)	930-1240		5.05×10^{-1}	71,400	23
Si	25				6,040	34
Nb		1100	5×10^{-15}			55

C. Diffusion in Molybdenum

1. Self-diffusion

The self-diffusion of molybdenum has not been measured, but may be estimated from high temperature creep data and melting point relations.

The high temperature creep data of Parke⁽⁵⁶⁾ has been analyzed by Orr, Sherby, and Dorn.⁽⁵⁷⁾ They found the activation energy for high temperature creep of molybdenum to be $\Delta H = 120,000$ cal/mole.

From the plot of activation energy for self-diffusion vs melting point shown in Fig. 8, Q may be estimated for molybdenum as $Q = 105,000$ cal/mole. LeClaire⁽⁵⁸⁾ suggested the empirical formula, $Q = 38 T_m$, where T_m is the melting point in $^{\circ}K$. This agrees quite well with the curve in Fig. 8. From this relation, the activation energy for self diffusion in molybdenum is given by $Q = 110,000$ cal/mole.

Nachtrieb and Handler⁽⁵⁹⁾ stated the empirical formula $Q = 16.5 \Delta H_f$ where ΔH_f is the heat of fusion. Kelley⁽⁶⁰⁾ estimated $\Delta H_f = 6,660$ from vapor pressure measurements which gives $Q = 110,000$ cal/mole for self diffusion in molybdenum.

LeClaire⁽¹⁹⁰⁾ developed a rather complete theoretical treatment of self-diffusion from which he calculated the equation

$$D = 16 \exp (-120,000/RT)$$

for the self diffusion of molybdenum. This value of the activation energy agrees well with the activation energy for high temperature creep and with the estimates from the empirical formulas of LeClaire⁽⁵⁸⁾ and Nachtrieb and Handler⁽⁵⁹⁾ stated above.

2. Interstitial Diffusion

a. Molybdenum-Boron

The diffusion coefficient of boron in molybdenum was determined by Samsonov and Latysheva^(8,9) (using their method described on page 3) from the recorded rates of growth of the Mo_2B phase. Their values fit the equation

$$D = 4.74 \times 10^3 \exp [-(14,300 \pm 5,400)/RT]$$

over the temperature range of 1100 to 1800 $^{\circ}C$. The data is shown in Table 21.

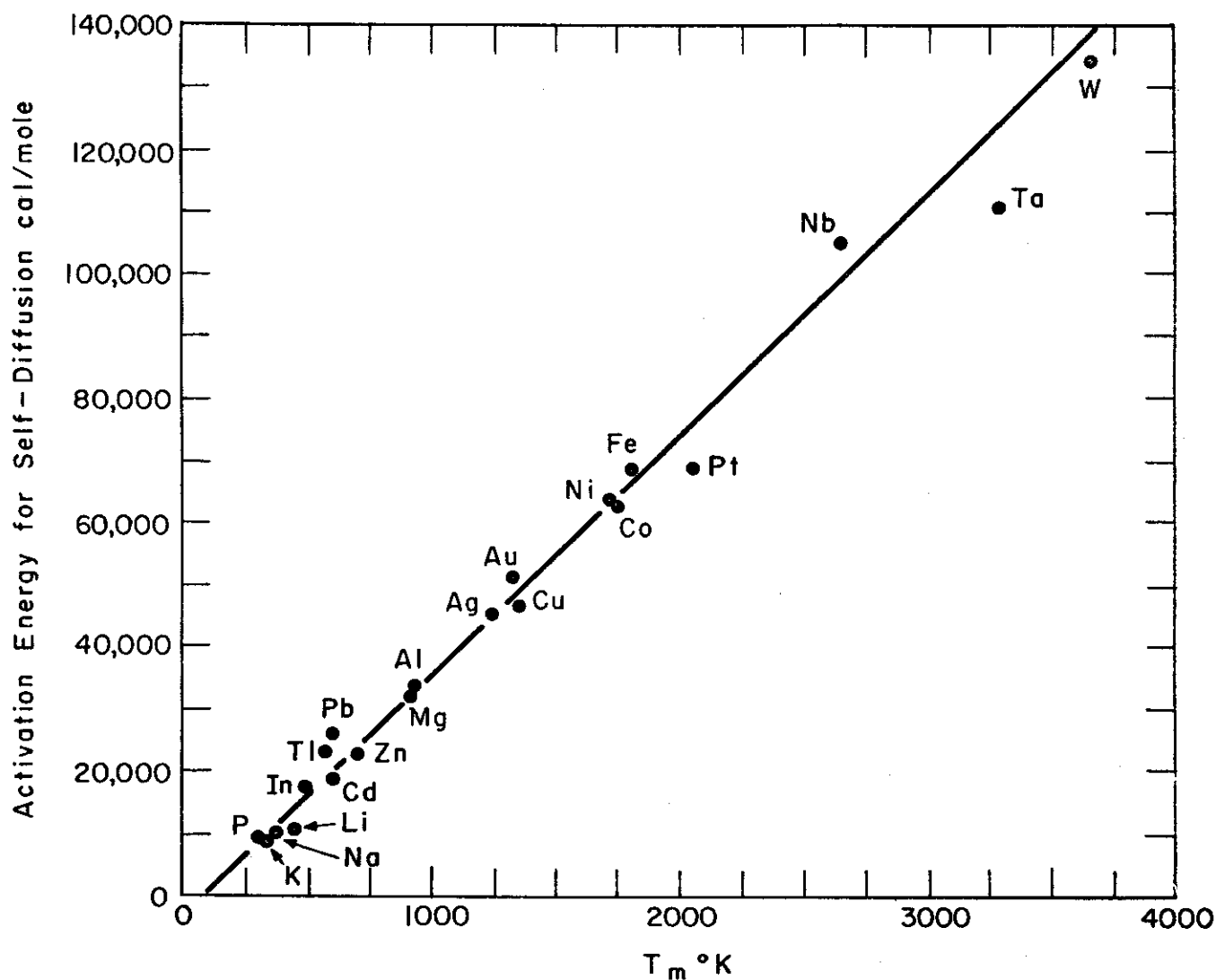


Fig. 8 - Activation energy for self-diffusion vs melting point for various elements.

References: P(62); K(63); Na(63,64,65); Li(63,69); In(67); Cd(68); Ti(69); Zn(70,71,72); Pb(73,74,75); Mg(73,74); Al(75); Cu(75,76,77); Ag(78,79,80,81); Au(82,83,84); Co(85,86); Ni(87,88); Fe(89,90,91,92); Pt(93); Nb(94); Ta(40,41,42); W(1)

Table 21

Data on the Diffusion of Boron in Molybdenum^(8,9)

Temp. (°C)	D (C - C ₂)	Q (cal/mole)	D ₀ (cm ² /sec)	C - C ₂ (g/cm ³)	D (cm ² /sec)
1100	0.2910	14,300 ± 5400	1300 ± 260	0.281	$4.74 \times 10^3 \exp \left(\frac{-14,300}{RT} \right)$
1300	6.0340				
1400	7.2567				
1500	9.6940				
1600	10.7184				
1800	18.6644				

Samsonov⁽¹⁰⁾ in an earlier paper gave the activation energy as Q = 12,200 cal/mole. The dependability of the data of these investigators has previously been discussed and shown to be questionable.

b. Molybdenum-Carbon

Samsonov and Latysheva^(8,9) measured the growth of the Mo₂C phase over the temperature range of 1200 to 2000°C. By applying the previously described analysis, they obtained

$$D = 2.26 \times 10^6 \exp [-(33,400 \pm 10,300)/RT].$$

The data is tabulated in Table 22.

Table 22

Data Obtained by Samsonov and Latysheva on
Diffusion of Carbon in Molybdenum^(8,9)

Temp. (°C)	D (C - C ₂)	Q (cal/mole)	D ₀ (cm ² /sec)	C - C ₂ (g/cm ³)	D (cm ² /sec)
1200	0	33,400 ± 10,300	7,700 ± 7400	0.033	$2.26 \times 10^6 \exp \left(\frac{-33,400}{RT} \right)$
1500	3.9712				
1600	9.7920				
1700	16.2560				
1800	21.4400				
2000	36.6080				

c. Molybdenum-Hydrogen

By heating a closed end evacuated molybdenum tube in hydrogen, Smithells and Ransley⁽⁶¹⁾ calculated the diffusion of hydrogen in molybdenum. The amount of hydrogen passing through the tube wall was measured very accurately. Varying the pressure from 1.68 mm to 126 mm changed the diffusion coefficient from 2.3×10^{-5} to 23.9×10^{-5} at 1673°K; however, the activation energy stayed constant. The units of D are the volume of gas in cm³ at N.P.T. diffusing per second through 1 cm² of surface and 1 mm thickness. Although the units of D are somewhat different, the activation energy (Q = 20,200 cal/mole) should be consistent with more conventional measurements.

More recently, Hill⁽¹⁸⁵⁾ determined the rate of diffusivity of hydrogen in molybdenum from measurements of the rate of gas evolution from hydrogen doped specimens. The molybdenum samples were heated in hydrogen at 1 atmosphere pressure at temperatures from 1280 to 1700°C and then quenched in water. These samples were then heated in vacuum over the temperature range 575 to 980°C during which the amount of evolved hydrogen was measured. Their data may be described by the equation:

$$D = 0.059 \exp (-14,700/RT).$$

This data appears to be more reliable as diffusion data than that of Ref. 61.

d. Molybdenum-Nitrogen

Smithells and Ransley⁽⁶¹⁾ measured the diffusion of nitrogen in molybdenum using the techniques described under molybdenum-hydrogen diffusion. They found that varying the nitrogen pressure gave different values of D, but the activation energy remained constant. Changing the pressure from 4.4 mm to 130 mm caused D to vary from 0.39×10^{-6} to 2.1×10^{-6} at 1773°K. Their data for P = 130 mm is given in Table 23.

Table 23

Data on the Diffusion of Nitrogen in Molybdenum⁽⁶¹⁾

Temp. (°K)	D x 10 ⁷	Temp. (°K)	D x 10 ⁷
1373	0.78	1723	16.5
1423	1.08	1773	20.6
1473	2.12	1823	44.2
1573	6.10	1873	51.8
1673	10.80		

The units of D are the volume of gas in cm^3 at N.P.T. diffusing per second through 1 cm^2 of surface and 1 mm thickness. The activation energy obtained from this data is $Q = 45,000 \text{ cal/mole}$.

Utilizing the data of Maringer and Muehlenkamp,⁽⁹⁵⁾ the activation energy for diffusion of nitrogen in molybdenum can be calculated by the method of Wert and Marx⁽⁹⁶⁾ from the temperature of the internal friction peak. This gives $Q = 53,000 \text{ cal/mole}$, a somewhat less reliable value than that of Smithells and Ramsley, but the agreement is not bad.

Ferro's⁽⁴⁹⁾ calculations for the diffusion of interstitial into body-centered cubic metals using the elastic constants of the metal of the matrix and the interstitial atom diameter, gives the activation energy for diffusion of nitrogen in molybdenum as $Q = 55,000 \text{ cal/mole}$. This compares favorably with the value for Maringer's⁽⁹⁵⁾ data but somewhat less favorably with the data of Smithells et al.⁽⁶¹⁾

3. Substitutional Diffusion

a. Molybdenum Cobalt

Byron and Lambert⁽⁹⁷⁾ prepared diffusion couples composed of concentric cylinders with a pure cobalt rod in the middle and a pure molybdenum cylinder bonded around it. These were annealed at 900 , 1100 , and 1275°C and the diffusion coefficient determined from the rate of growth of the diffusion zone. Samples were also prepared between pure molybdenum and $\text{Mo} - 3.42\% \text{ Co}$ alloy. These were diffused at 1500 and 1700°C . The diffusion gradient was determined by machining off layers and chemical analysis. By applying the Matano analysis, D was shown to be constant between 0 and $3.4\% \text{ Co}$ in molybdenum. There results are given in Table 24.

Table 24

Molybdenum-Cobalt Diffusion at High Molybdenum Concentrations⁽⁹⁷⁾

Temp. ($^\circ\text{C}$)	D (cm^2/sec)
900	70.7×10^{-14}
1100	14.8×10^{-12}
1275	23.1×10^{-12}
1500	4.18×10^{-10}
1700	1.93×10^{-10}

These values may be expressed as the relation:

$$D = 2.82 \times 10^{-6} \exp (-34,800/RT).$$

The data in general is rather poor. The concentration gradients, when determined, had insufficient points to draw a curve for a Matano analysis, and the log D vs 1/T plot has much more scatter than normal.

b. Molybdenum-Iron

Neiman and Shinyaev⁽⁹⁸⁾ measured the diffusion of radioactive iron (Fe^{59}) into iron-molybdenum alloys (24, 33, 40, and 48 atomic percent molybdenum) at temperatures of 1106, 1148, and 1183°C. Layers were removed by electrolytic polishing from the samples after annealing, and the radioactivity was counted. Log D vs atomic percent molybdenum, Q vs atomic percent molybdenum, log D_0 vs atomic percent molybdenum, and log D_0 vs Q are plotted in Figs. 9, 10, 11, and 12 respectively. They showed that

$$\ln D_0 = aQ + b$$

where $a = 0.32 \times 10^{-3}$ and $b = 22$ for the systems iron-molybdenum and iron-nickel.⁽⁹⁹⁾

The existence of the Fe_3Mo_2 phase is strongly reflected in the Q and D_0 values.

The data on first appearance looks very good. However, except for the 40 atomic percent molybdenum point, all their data points are taken in a two-phased region, which is not mentioned in the article. This makes the data of little value, since all they are showing is the change in the percent of the alpha and epsilon phases in their samples which could be obtained from the phase diagram.

Grube and Lieberwirth⁽¹⁰⁰⁾ prepared diffusion couples between iron-molybdenum alloys (6 - 12% Mo) and pure iron for diffusion at 1200°C. Slices were machined off and chemically analyzed. The diffusion coefficient was determined from the concentration gradient by the Grube method. No composition dependence is reported. The diffusion coefficient was reported as

$$D = 2.3 - 3 \times 10^{-9} \text{ cm}^2/\text{sec at } 1200^\circ\text{C}.$$

Ham⁽¹⁰¹⁾ carried out diffusion measurements on samples of pure iron bonded to iron-molybdenum alloys of 0 - 6% Mo. The samples were diffused at temperatures of 931 to 1265°C, sectioned, and chemically analyzed. The data is given in Table 25. The log D vs 1/T plot can be seen in Fig. 13. In general, the data is quite good, but there were only two temperatures used in the molybdenum-alpha iron investigation.

The following relationships were found to hold:

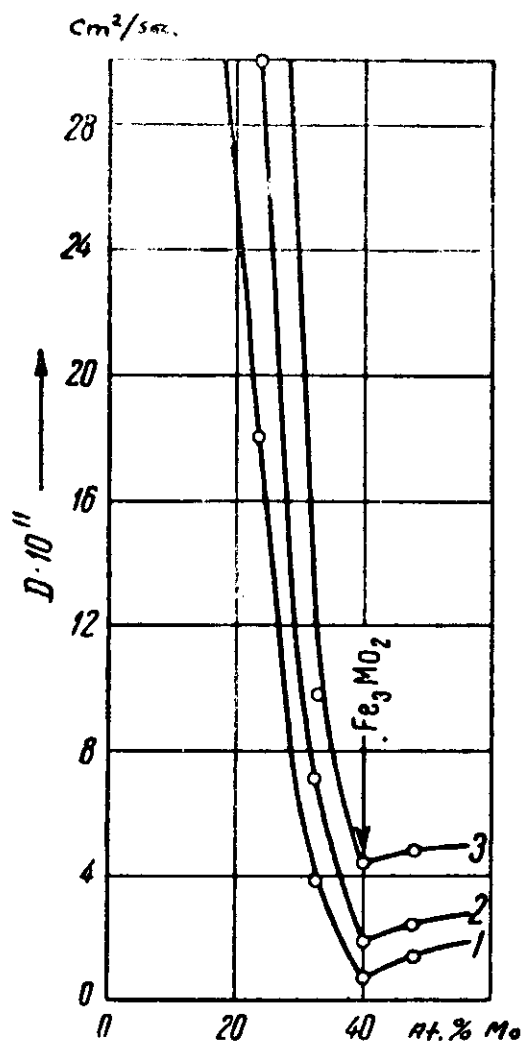


Fig. 9 - The diffusion coefficient as a function of the atomic percent molybdenum at temperatures, 1 - 1106°C, 2 - 1148°C, and 3 - 1183°C. (98)

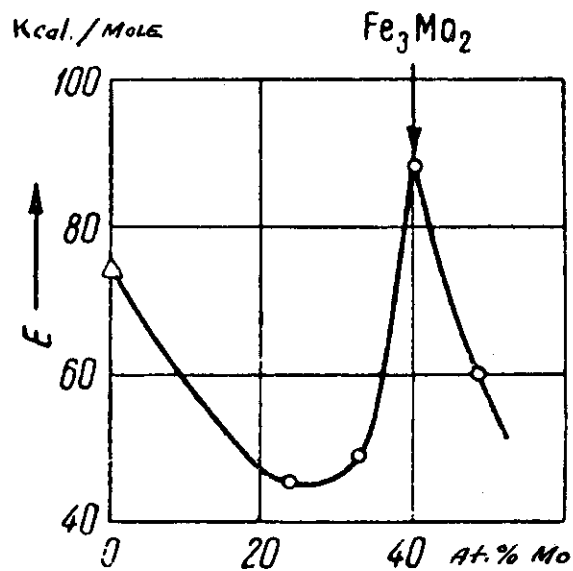


Fig. 10 - Activation energy vs atomic percent molybdenum for the iron-molybdenum system. (98)

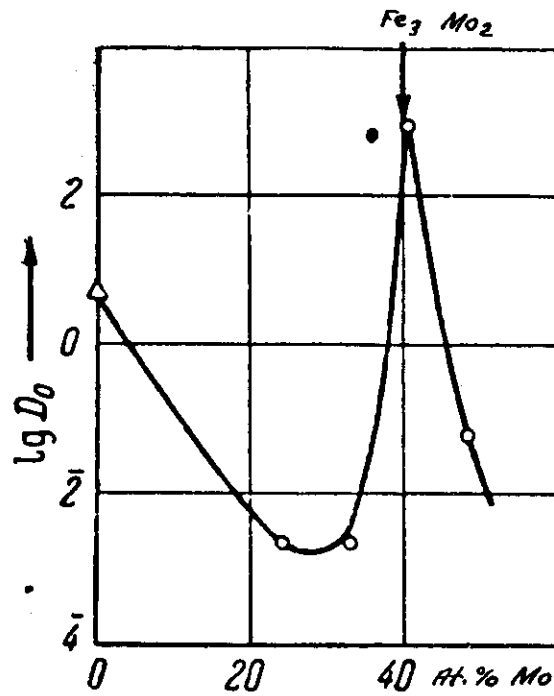


Fig. 11 - $\log D_0$ vs atomic percent molybdenum for the iron-molybdenum system. (98)

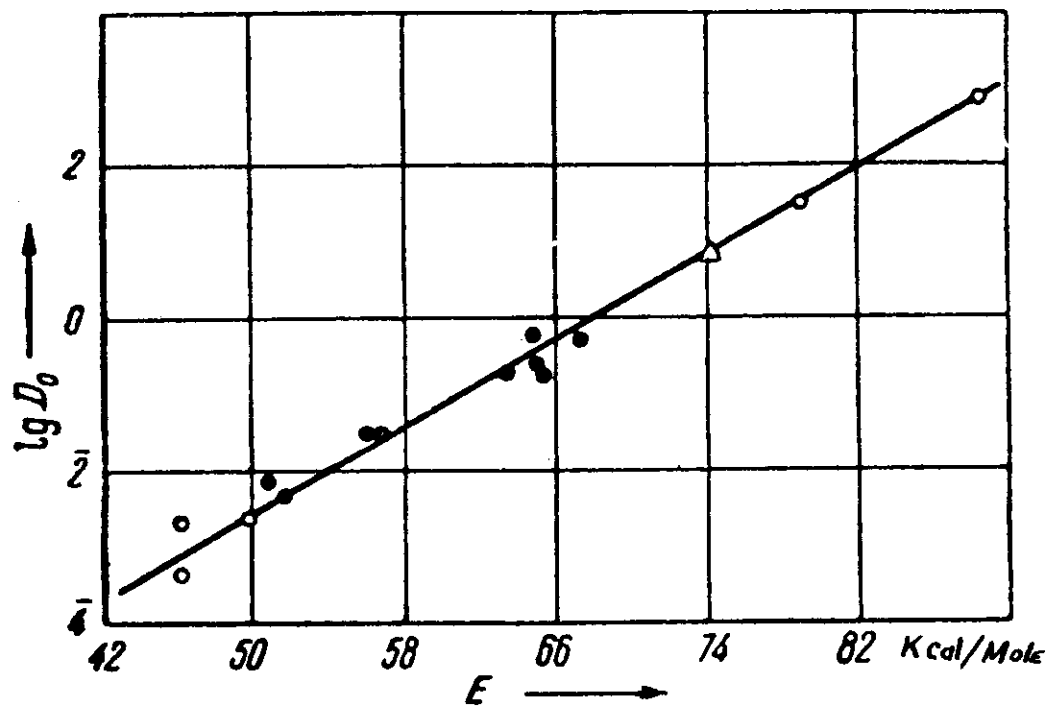


Fig. 12 - Log D_0 vs the activation energy for
 ○ - Fe-Mo, (98) △ - Fe-self-diffusion (89)
 and ● - Fe-Ni. (99)

Mo-Fe_γ

$$D = 0.068 \exp (-59,000/RT)$$

Mo-Fe_γ with 0.4 wt. % C

$$D = 0.091 \exp (-59,000/RT)$$

Mo-Fe_α

$$D = 3.467 \exp (-57,700/RT).$$

Table 25

Molybdenum-Iron Diffusion at Low Molybdenum Concentration⁽¹⁰¹⁾

Initial Concentration (at. % Mo)		Wt. % Carbon	Temp. (°F)	Phase	D x 10 ¹⁰ (cm ² /sec)
C	C ₂				
0.532	<0.005	<0.03	2305	γ	3.12
0.540	<0.005	<0.03	2204	γ	1.42
0.550	<0.005	<0.03	2104	γ	0.613
0.540	0.145	0.38	2305	γ	3.62
0.520	0.145	0.44	2204	γ	1.68
0.530	0.145	0.47	2104	γ	0.73
1.470	0.000	0.25	2301	γ	4.11
3.607	1.928	<0.03	1708	α	1.23
0.585	0.004	<0.03	2300	γ	2.40
1.475	<0.005	0.35	1708	γ	0.0189
3.629	1.958	<0.03	2301	α	216.0

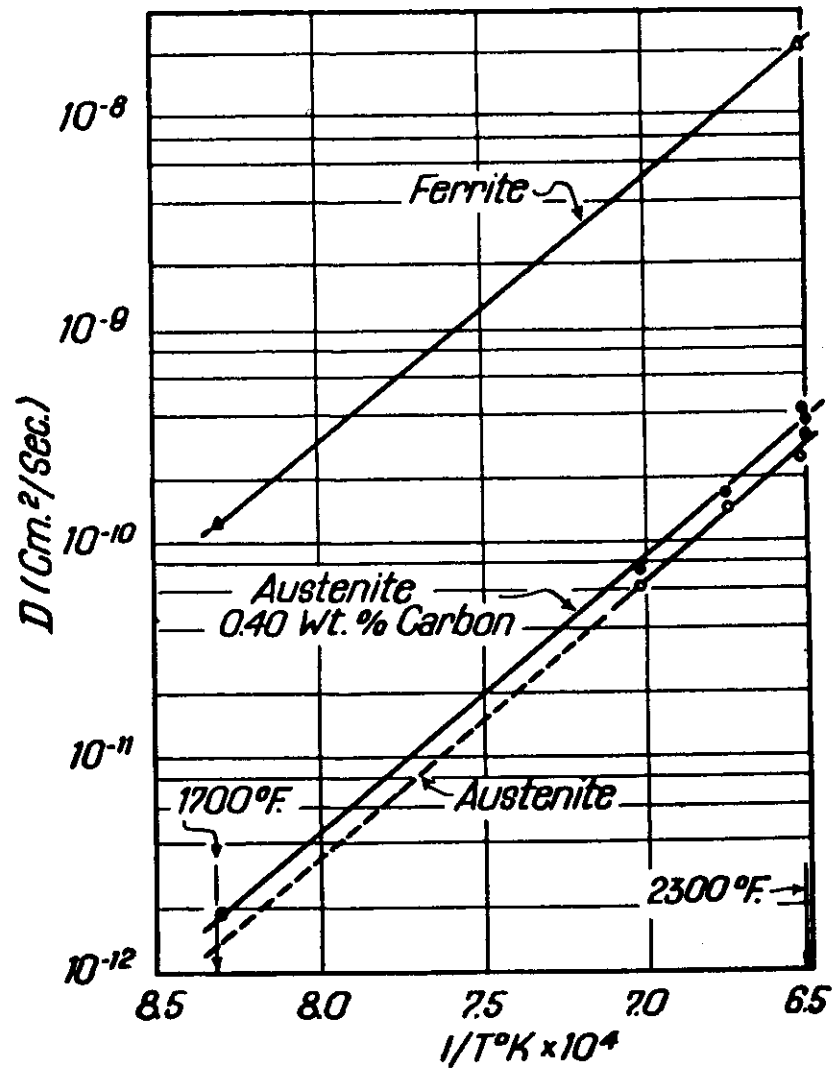


Fig. 13 - Effect of temperature on the coefficient of diffusion of molybdenum in austenite and in ferrite.(101)

c. Molybdenum-Niobium

Birks and Seebold⁽¹⁰²⁾ ran a diffusion couple of pure niobium-pure molybdenum at 1100°C for 48 hours. The penetration curve was measured with the electron probe microanalyzer. The concentration gradient extended over a distance of 6 microns which is considerably too small to get sufficient data to analyze by the Matano method. However, the diffusion coefficient, as a function of composition, was determined by the Matano method. These values are shown in Fig. 14. A re-evaluation of this data demonstrates that the D values given are a factor of 10³ too small. This correction has been made in Fig. 14. D varies between 3 to 7 x 10⁻¹⁴ at 1100°C over the composition range of 0 to 100% molybdenum.

d. Molybdenum-Nickel

Budde⁽¹⁰³⁾ measured the diffusion between pure nickel and nickel-molybdenum alloys up to 20.8 atomic percent molybdenum. His data is listed in Table 26

Table 26

Data for Nickel-Molybdenum Diffusion⁽¹⁰³⁾

Temp. (°C)	D (cm ² /sec)
1120	1.43 x 10 ⁻¹⁰
1290	1.03 x 10 ⁻⁹

and may be represented by the equation:

$$D = 0.0134 \exp (-50,800/RT).$$

Since this investigation was carried out at only two temperatures, the D₀ and Q values are quite uncertain.

Swalin, Martin, and Olsen⁽¹⁰⁴⁾ carried out diffusion between pure nickel and Ni - 0.93 at. % Mo alloy at temperatures ranging from 1150 to 1400°C. The samples were sectioned and chemically analyzed. A plot of log D vs 1/T for this data is shown in Fig. 15. The diffusion-temperature relation for this system may be given by

$$D = 3.0 \exp [-68,900 \pm 1,000/RT].$$

Good precision has been obtained by careful experimentation.

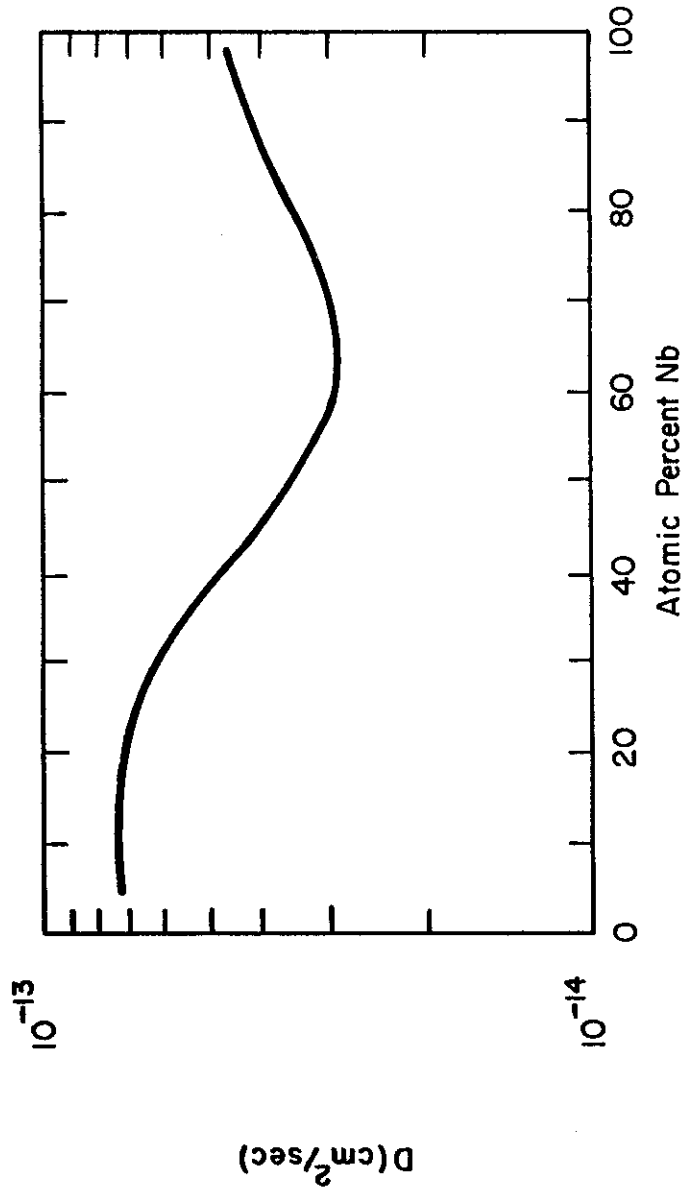


Fig. 14 - Diffusion coefficient for niobium-molybdenum system at 1100°C. (102)

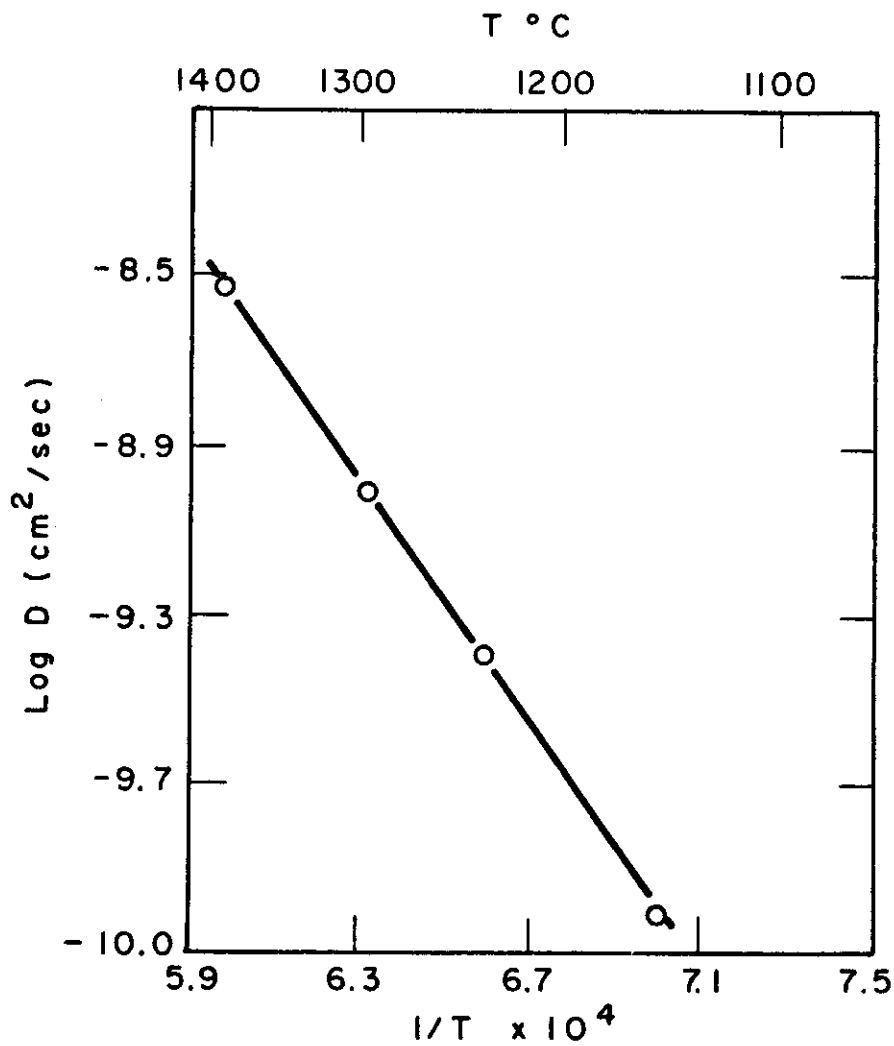


Fig. 15 - Log D vs 1/T for diffusion in molybdenum-nickel alloys of high nickel concentration. (104)

e. Molybdenum-Titanium

Shewmon and Bechtold⁽¹⁰⁵⁾ measured the magnitude of the Kirkendall effect in molybdenum-titanium diffusion couples. Couples were prepared with the pure metals and ThO₂ was included as the markers. No diffusion coefficients were measured. Their data is tabulated in Table 27.

Table 27

Kirkendall Marker Movements in Molybdenum-Titanium Diffusion Couples⁽¹⁰⁵⁾

Temp. (°C)	Time (min)	x (in.)
1470	4135	10.7×10^{-3}
1605	380	8.9×10^{-3}
1640	120	6.8×10^{-3}
1400	3228	4.9×10^{-3}

If the markers are assumed to be at the same concentration for each sample, and since $x = 2\gamma \sqrt{Dt}$ for any composition, then a plot of $\log \frac{x^2}{t}$ vs $\frac{1}{T}$ should give the activation energy. This treatment yields a very good straight line with $Q = 101,500$ cal/mole, a value which should apply for a composition somewhat greater than 50% titanium since the markers moved into the titanium. Such a value is not unrealistic but may be somewhat large.

Diffusion has been carried out by Goold⁽¹⁰⁶⁾ between pure titanium and a Ti - 8.1 at. % (15 wt. %) Mo alloy at 938 to 1248°C. Samples were sectioned and chemically analyzed. The diffusion coefficient was determined as a function of concentration by means of the Matano analysis. ThO₂ markers were included in some samples in order to determine the intrinsic diffusion coefficients. D as a function of atomic percent molybdenum is shown in Fig. 16. For 1 at. % Mo, D may be given by the formula

$$D = 1.0 \times 10^{-5} \exp [-(24,000 \pm 3,400)/RT].$$

At 1250°C, the intrinsic diffusion coefficients for 96 at. % Ti are:

$$D_{Ti} = 6.72 \times 10^{-9} \text{ cm}^2/\text{sec}$$

$$D_{Mo} = 3.95 \times 10^{-9} \text{ cm}^2/\text{sec}$$

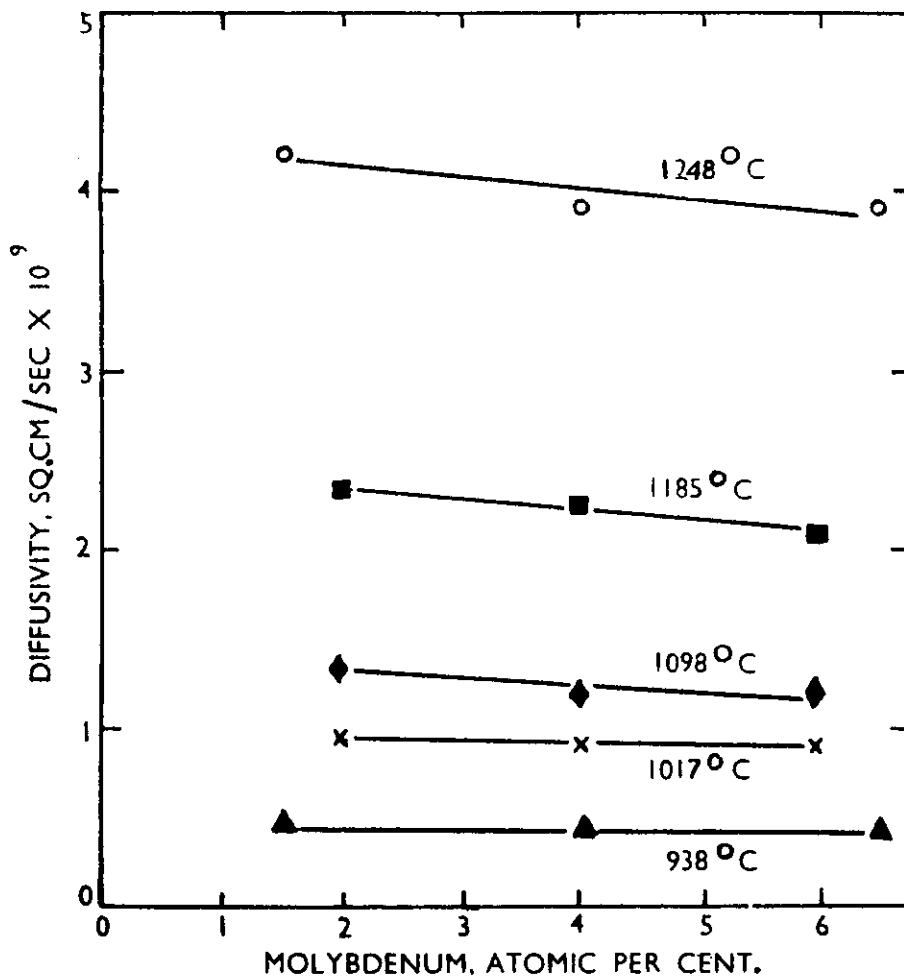


Fig. 16 - Variation of the interdiffusion coefficient with composition for the molybdenum-titanium system. (106)

Although the data was taken with great care, the activation energy is quite small compared to other diffusion data with molybdenum or titanium. A full description of other titanium data is given later in this report.

f. Molybdenum-Thorium

Nelting⁽¹⁰⁷⁾ using the thermionic emission method, obtained the values for diffusion of molybdenum in thorium listed in Table 28.

Table 28

Diffusion Coefficients for Diffusion of Molybdenum in Thorium⁽¹⁰⁷⁾

D (cm ² /sec)	Temp. (°C)
3.6×10^{-10}	1615
2.3×10^{-9}	1700
1×10^{-6}	2000

If log D vs 1/T is plotted for this data, one finds that Q = 176,000 cal/mole. This is exceptionally large which leads one to doubt this data.

g. Molybdenum-Silicon

Samsonov and Solonnikova⁽³⁴⁾ applied the analysis described under tungsten-boron diffusion (page 3) to the rate of growth of the MoSi₂ phase. An activation energy was given as Q = 9,470 cal/mole. The doubtful validity of the work of these authors has been discussed earlier in this paper.

h. Molybdenum-Uranium

A very complete investigation of the diffusion in the molybdenum-uranium system has been carried out by Adda and Philibert.⁽¹⁰⁸⁾ Pressure bonded diffusion couples were prepared between pure uranium and an alloy of U - 30 at. % Mo. Diffusion anneals were carried out between 850 and 1050°C, and the concentration gradients were determined with the electron microbeam probe. The diffusion coefficients and the activation energies were determined as a function of the concentration. This data is given in Table 29 and may be seen in Figs. 17 and 18.

Intrinsic diffusion coefficients were also measured. This data is summarized in Table 30 and is shown graphically in Fig. 19. The care with which these experiments were performed is reflected in the high quality of the data.

A summary of diffusion in molybdenum is given in Table 31.

Table 29

Molybdenum-Uranium Diffusion Coefficients at Various Concentrations of Uranium (108)

Concentration (at. % U)	D (cm ² /sec)				Q (cal/mole)	D ₀ (cm ² /sec)
	850°C	950°C	1000°C	1050°C		
74	8.9×10^{-11}	2.6×10^{-10}	5.5×10^{-10}	8.6×10^{-10}	34,000	2.1×10^{-4}
76	8.3×10^{-11}	2.6×10^{-10}	6.0×10^{-10}	1.1×10^{-9}	38,500	4.5×10^{-4}
80	9.9×10^{-11}	3.0×10^{-10}	1.1×10^{-9}	1.4×10^{-9}	39,400	3.0×10^{-3}
84	1.3×10^{-10}	4.8×10^{-10}	1.3×10^{-9}	2.9×10^{-9}	45,700	9.6×10^{-2}
88	2.0×10^{-10}	8.9×10^{-10}	2.3×10^{-9}	7.1×10^{-9}	52,200	3.2
90	2.6×10^{-10}	1.3×10^{-9}	3.2×10^{-9}	1.5×10^{-8}	56,800	28
92	4.0×10^{-10}	2.0×10^{-9}	5.7×10^{-9}	1.7×10^{-8}	55,000	16
94	6.9×10^{-10}	2.8×10^{-9}	6.9×10^{-9}	1.7×10^{-8}	53,000	20
96	6.2×10^{-10}	4.0×10^{-9}	7.4×10^{-9}	1.5×10^{-8}	45,800	5.8×10^{-1}
98	8.3×10^{-10}	4.8×10^{-9}	1.2×10^{-8}	1.7×10^{-8}	47,500	2.2

Table 30
Intrinsic Diffusion Coefficients in Uranium-Molybdenum System (108)

Temp. (°C)	850	950	1000	1050
At. % U	94	94	92	90
Intrinsic D _U	3.4×10^{-9}	1.4×10^{-8}	1.6×10^{-8}	3.4×10^{-8}
Intrinsic D _{Mo}	5.2×10^{-10}	2.1×10^{-9}	5×10^{-9}	1.3×10^{-8}

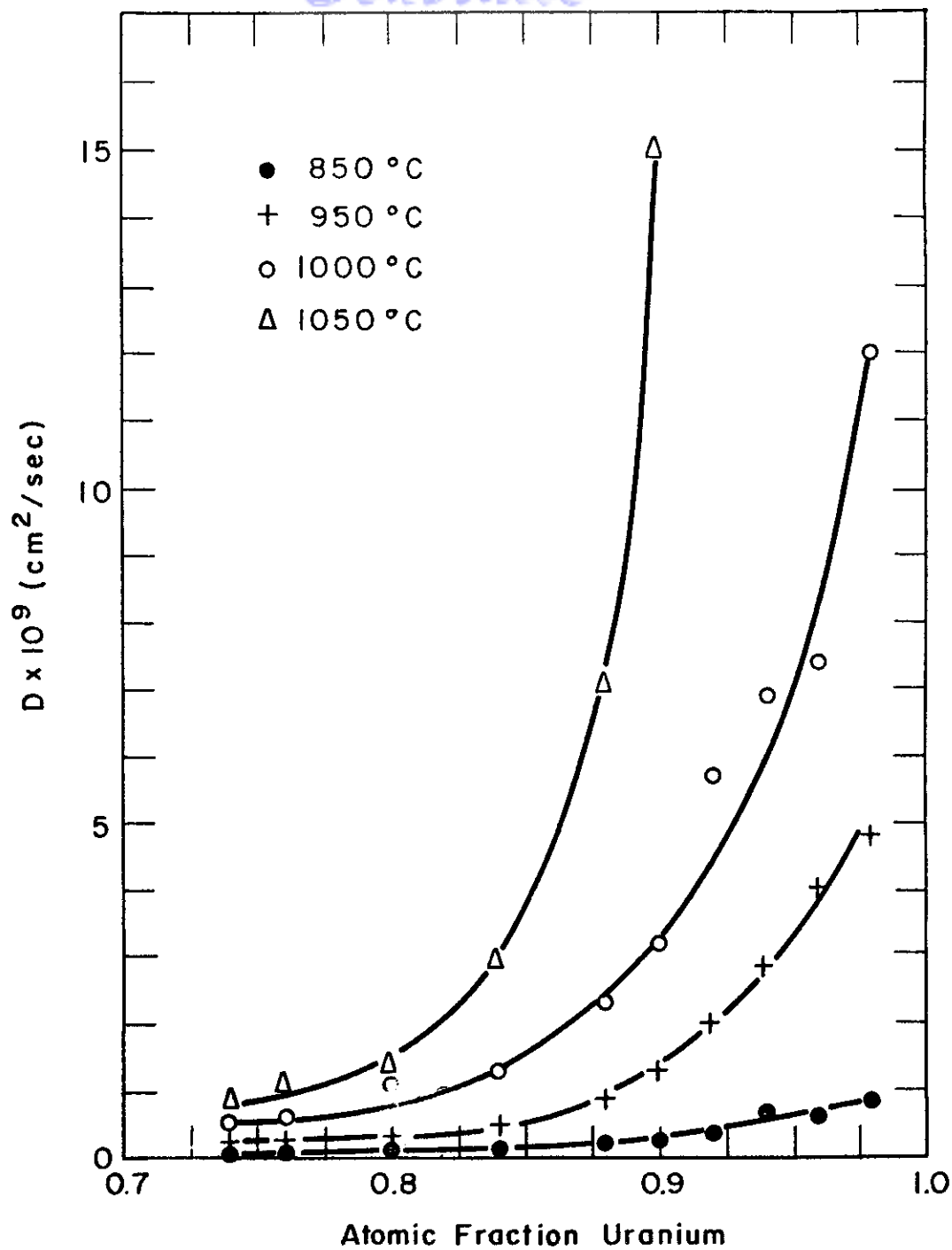


Fig. 17 - D vs composition for uranium-molybdenum system. (108)

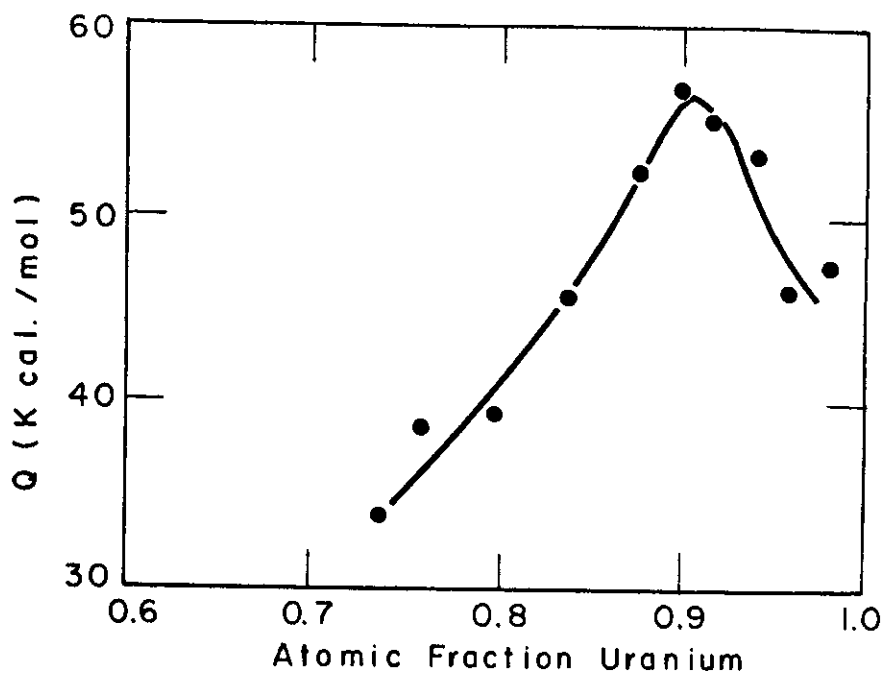


Fig. 18 - Dependence of Q on composition for uranium-molybdenum system.(108)

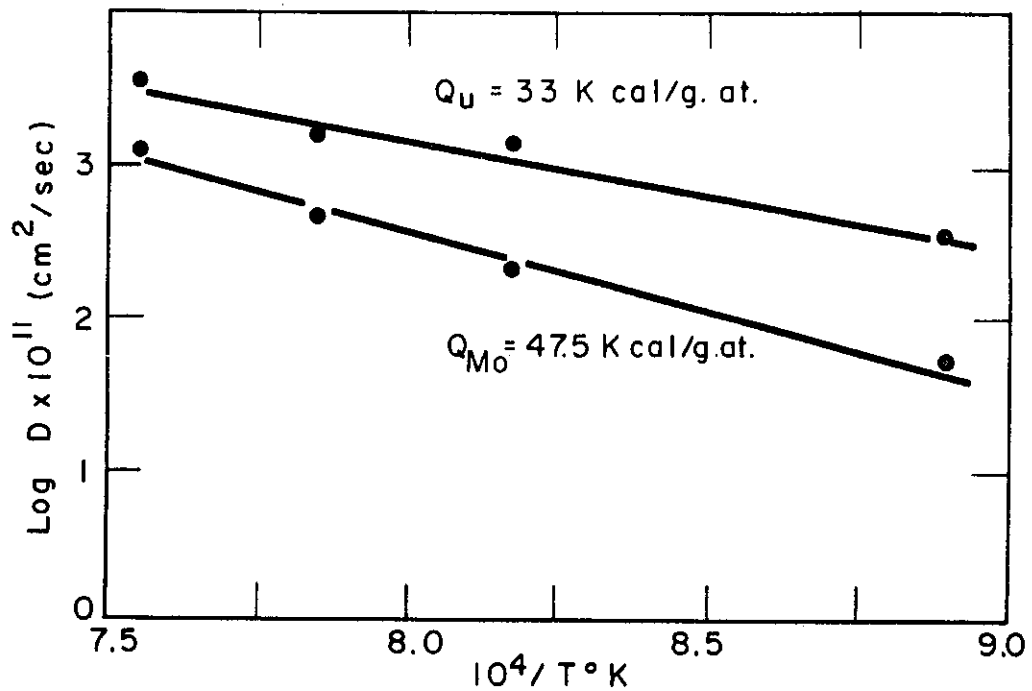


Fig. 19 - Temperature dependence of intrinsic diffusion coefficients for uranium-molybdenum system.(108)

Table 31

Summary of Diffusion Data for Molybdenum

Diffusing Element	Composition Range (wt. %)	Temp. (°C)	D (cm ² /sec)	D ₀ (cm ² /sec)	Q (cal/mole)	References
Mo (self)	Estimate from creep data				120,000	55,56
	Estimate from melting point				110,000	
	Theoretical estimate			16	120,000	190
B	5.5	1100-1800		4.74×10^3	14,300 12,200	8,9 10
C	6	1200-2000		2.26×10^6	33,400	8,9
H		1000-1500 575-980		0.059	20,200 14,700	61 185
N		1100-1600			45,000 53,000	61 95
Co						
	0-100	900 1100 1275	70.7×10^{-14} 14.8×10^{-12} 23.1×10^{-12}	2.82×10^{-6}	34,800	97
	0-3.4	1500 1700	4.18×10^{-10} 1.53×10^{-10}	2.82×10^{-6}	34,800	97
γFe						
	52-76	1106 1148 1183	1.18×10^{-11} 2.30×10^{-11} $4.5-50 \times 10^{-11}$	$3 \times 10^{-3}-10^3$	47,000-87,000	98
	88-100	1200	$2.3-3 \times 10^{-9}$			100
	94-100	1152-1265		0.068	59,000	101

(Cont'd. on next page)

Table 31 (Cont'd.)

Diffusing Element	Composition Range (wt. %)	Temp. (°C)	D (cm ² /sec)	D (cm ² /sec)	Q (cal/mole)	References
γFe with 0.4 wt. % C	94-100	931-1265		0.091	59,000	101
αFe	94-100	931-1265		3.467	57,700	101
Nb	0-100	1100	$3-7 \times 10^{-14}$			102
Ni	70	1120 1290	1.43×10^{-10} 1.03×10^{-9}	0.0134	50,800	103
	100-99.07	1150-1400		3.0	68,900	104
Ti (intrinsic)	92-100 96	938-1248 1250	$T_i = 6.72 \times 10^{-9}$ $M_o = 3.95 \times 10^{-9}$	1.0×10^{-5}	24,000	106
Th		1615 1700 2000	3.6×10^{-10} 2.3×10^{-9} 1×10^{-6}			107
Si	30				9,470	34
U	70-100	850 950 1000 1050	8.9×10^{-11} 8.3×10^{-9} 2.6×10^{-10} 4.8×10^{-8} 5.5×10^{-10} 1.2×10^{-8} 8.6×10^{-10} 1.7×10^{-8}	2.1×10^{-4} - 28	34,000-56,800	108
(intrinsic)	94-90	850-1050	$D_u = 3.4 \times 10^{-9}$ to 3.4×10^{-8} $D_{M_o} = 5.2 \times 10^{-10}$ to 1.3×10^{-8}		33,000 47,500	108

(Cont'd. on next page)

Table 31 (Cont'd.)

Diffusing Element	Composition Range (wt. %)	Temp. (°C)	D (cm^2/sec)	D_0 (cm^2/sec)	Q (cal/mole)	References
Mo (single crystals)	80-100	1533	0.26×10^{-12}	6.3×10^{-4}	80,500	30
		1770	1.12×10^{-12}			
		2010	22.0×10^{-12}			
		2260	78.0×10^{-12}			
Mo (W polycrystal)	80-100	1533	1.3×10^{-12}	5×10^{-3}	80,500	30
		1770	11.0×10^{-12}			
		2010	106.0×10^{-12}			
		2260	640.0×10^{-12}			

D. Diffusion in Niobium

1. Self-diffusion

Resnick and Castleman⁽⁹⁴⁾ vapor-plated Nb⁹⁵ onto niobium sheet by hydrogen reduction of NbCl₅. The specimens were annealed in pairs with the active surfaces facing each other in the temperature range of 1585 to 2120°C. A log D vs 1/T plot of this data is shown in Fig. 20. Although there is a fair amount of scatter in this data, a sufficient number of data points have been taken to give a good average value. The data fits the equation:

$$D = 12.4 \pm 0.8 \exp [-(105,000 \pm 3,000)/RT].$$

This activation energy is in excellent agreement with the values predicted from the melting point⁽⁵⁸⁾ and from the heat of fusion⁽⁵⁹⁾ of niobium.

2. Interstitial Diffusion

a. Niobium-Boron

Samsonov and Latysheva's^(8,9) technique (page 3) was used by them to determine the "diffusion coefficient" of boron in niobium from the measured rates of growth of the NbB₂ phase. The relationship found was:

$$D = 4.74 \times 10^3 \exp [-(14,300 \pm 5,400)/RT]$$

over the temperature range of 1400 to 2000°C. The data is given in Table 32. The validity of the data of these investigators has previously been discussed and shown to be questionable.

Table 32

Niobium-Boron Diffusion Data Using the Analytical
Method of Samsonov and Latysheva^(8,9)

Temp. (°C)	D (C - C ₂)	Q (cal/mole)	D (cm ² /sec)	C - C ₂ (g/cm ³)	D (cm ² /sec)
1400	5.4550	14,130 ± 4900	1420 ± 280	0.254	5.62 x 10 ³ exp ($\frac{-14,130}{RT}$)
1600	9.5490				
1800	12.1980				
2000	14.0580				

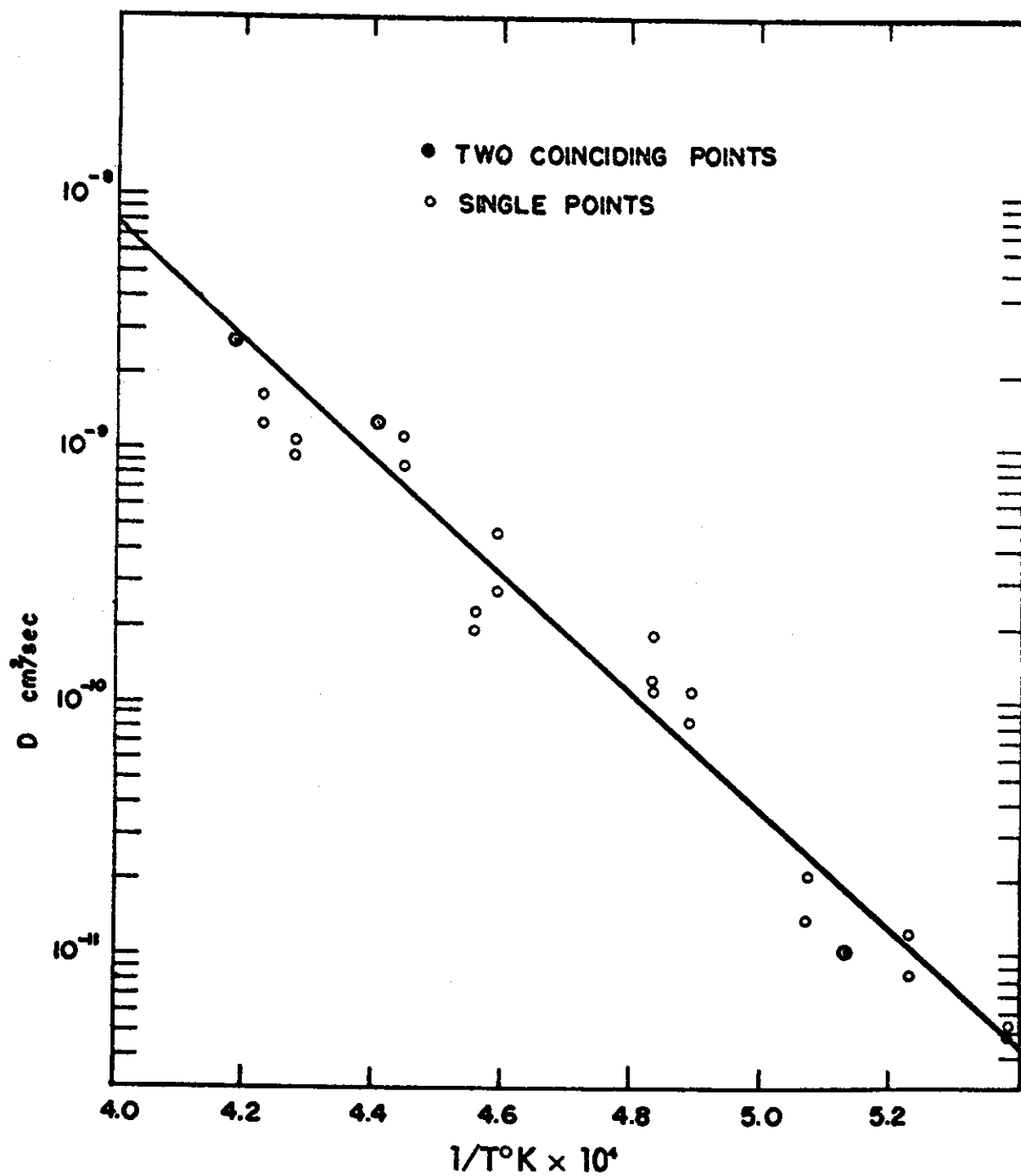


Fig. 20 - Log D vs $1/T$ for self-diffusion of niobium. (94)

b. Niobium-Carbon

Samsonov and Latysheva^(8,9) measured the growth of the Nb₂C phase over the temperature range of 1000 to 2000°C and by applying their analysis, they obtained:

$$D = 3.14 \times 10^4 \exp [-(18,900 \pm 5,700)/RT].$$

The data is shown in Table 33.

Table 33

Data on the Diffusion of Carbon in Niobium^(8,9)

Temp. (°C)	D (C - C ₂)	Q (cal/mole)	D ₀ (cm ² /sec)	C - C ₂ (g/cm ³)	(cm ² /sec)
1000	0	18,900 ± 5700	2120 ± 400	0.067	3.14 x 10 ⁴ exp ($\frac{-18,900}{RT}$)
1300	4.8950				
1400	6.7650				
1500	9.5590				
1600	13.2000				
1800	16.7200				
1900	19.6900				
2000	21.9450				

Wert⁽⁴⁴⁾ measuring internal friction with the torsion pendulum, found that diffusion of carbon in niobium fitted the equation:

$$D = 0.015 \exp (-27,000/RT).$$

This activation energy is somewhat lower than the more accurate data of Powers and Doyle⁽⁴⁸⁾ and may be due to oxygen contamination of the sample. Oxygen diffusion has an activation energy around 27,000 cal/mole.

Internal friction measurements with the torsion pendulum were carried out by Powers and Doyle⁽¹⁰⁹⁾ on niobium samples containing carbon. The carbon content was 0.013 wt. % C. Measurements were made at 237.5, 238.3, 259.3, and 261.6°C at applied frequencies of 0.155, 0.165, 0.568, and 0.710 cycles per second respectively. Their data may be represented by:

$$D = 0.0046 \exp [-(33,300 \pm 900)/RT].$$

The error in Q is slightly larger than usually found in internal friction work, but this is due to the rapid aging of the carbon peak.

The most recent work of Powers and Doyle,⁽⁴⁸⁾ given in Table 34, reported the diffusion coefficients of carbon in niobium obtained by internal friction and elastic after effect measurements over the temperature range of 140 to 261°C.

Table 34

Diffusion Coefficients for the Diffusion of
Carbon in Niobium as Determined
by Internal Friction Measurements⁽⁴⁸⁾

Method of Measurement	D_0 (cm ² /sec)	Q (cal/mole)
Internal friction	0.0050 ± 0.0050	33,200 ± 900
Elastic After-effects	0.0038 ± 0.0005	33,000 ± 100
Combined	0.0046 ± 0.0007	33,020 ± 180

The log of the relaxation time vs 1/T°K for this data is plotted in Fig. 4. A comparison of this superb data with that of Samsonov and Latysheva once again shows the doubtful validity of the work presented in Refs. 8, 9, and 34.

c. Niobium-Hydrogen

Gulbransen and Andrew⁽⁵⁰⁾ measured the weight gain of niobium heated in hydrogen as a function of time and temperature. The reaction was observed to start at 250°C and the rate increased as the time progressed. At 300°C, the curve of weight gained vs time was linear. At 350°C, the rate decreased as the time progressed. Above 360°C, the sample lost weight as the low temperature hydride decomposed. Between 700 and 900°C, the rate followed a parabolic law and probably was diffusion controlled in this temperature range. No diffusion coefficient was given due to the different reaction rates at the different temperatures.

Albrecht, Goode, and Maillet⁽¹¹⁰⁾ evaluated the absorption of hydrogen by niobium. This was stated to be diffusion controlled (obeyed a parabolic rate law) between 600 and 700°C, and therefore data was taken at 600, 650, and 700°C. The relationship obtained was

$$D = 0.0214 \exp [-(9,370 \pm 600)/RT].$$

The data appears to be very good, but in view of the results of Gulbransen and Andrew, caution should be used in applying the data outside the 600 to 700°C temperature range.

Applying the theory of Ferro⁽⁴⁹⁾ to the diffusion of hydrogen in niobium, the following theoretical diffusion coefficient can be calculated:

$$D = 0.0004 \exp (-18,000/RT).$$

The success of this theoretical treatment in other systems has been exceptional, but the agreement in systems with niobium will be seen to be less than satisfactory.

d. Niobium-Nitrogen

Powers and Doyle⁽¹⁰⁹⁾ carried out internal friction measurements with the torsion pendulum on niobium samples containing 0.0184 and 0.0215 weight percent nitrogen. These two nitrogen contents gave the same diffusion coefficients. Measurements were made at 267.3, 274.4, 285.5, and 295.3°C at applied frequencies of 0.349, 0.542, 1.005, and 1.728 cycles per second respectively. Their data fitted the equation

$$D = 0.0072 \exp [-(34,800 \pm 200)/RT].$$

The diffusion coefficients of nitrogen in niobium obtained by internal friction, elastic after effects, and peak breadth measurements over the temperature range of 150 to 295°C, reported in Powers and Doyle's⁽⁴⁸⁾ most recent work, are shown in Table 35.

Table 35

Niobium-Nitrogen Diffusion Data of Powers and Doyle⁽⁴⁸⁾

Method of Measurement	D_0 (cm ² /sec)	Q (cal/mole)
Internal Friction	0.0081 ± 0.0020	$34,800 \pm 200$
Elastic After-effects	0.0087 ± 0.0008	$35,000 \pm 100$
Combined	0.0086 ± 0.0007	$34,920 \pm 90$
Peak Breadth		$34,500 \pm 100$

The log of the relaxation time vs $1/T^{\circ}\text{K}$ plot for this data is indicated in Fig. 4.

Marx, Baker, and Sivertsen⁽⁵²⁾ extended the temperature range of internal friction measurements by employing a high frequency method. By using both the torsion pendulum and the high frequency method, measurements were made over the temperature range of 285 to 583 $^{\circ}\text{C}$. They reported an activation energy of $Q = 35,700$ cal/mole from this data. This is in fine agreement with the above mentioned work of Powers and Doyle.

Ang⁽⁵¹⁾ made internal friction measurements with the torsion pendulum over the temperature range of 285 to 310 $^{\circ}\text{C}$ and the values are related by:

$$D = 0.0980 \exp (-38,600/RT).$$

The weight gain of a niobium sample heated in nitrogen as a function of time and temperature was determined by Gulbransen and Andrew.⁽⁵⁰⁾ The rate limiting process was assumed to be diffusion, due to the parabolic relationship between weight gained and time over the temperature range investigated (400 to 800 $^{\circ}\text{C}$). A value of $Q = 25,400$ cal/mole was reported.

Albrecht and Goode⁽¹¹¹⁾ measured the absorption of nitrogen by niobium. Their data was found to fit the equation:

$$D = 0.061 \exp (-38,800/RT).$$

The data of Powers and Doyle^(48,109) and of Marx, Baker, and Sivertsen⁽⁵²⁾ represent the best diffusion data for this system. The weight gained and the absorption data are probably quite reliable but are not clear as to the mechanism or mechanisms responsible for the observed data.

Ferro's⁽⁴⁹⁾ calculations for the theoretical values of D_0 and Q for diffusion of nitrogen in niobium gives

$$Q = 20,000 \text{ cal/mole}$$

$$D_0 = 0.02 \text{ cm}^2/\text{sec}.$$

e. Niobium-Oxygen

Diffusion of oxygen in niobium has been measured by internal friction methods, weight gain methods, and microhardness traverses covering the temperature range of 40 to 1000 $^{\circ}\text{C}$. The agreement between all the investigators is very good with the possible exception of the weight gain determinations.

The recent work of Powers and Doyle⁽⁴⁸⁾ on diffusion of oxygen in niobium is very good. They obtained diffusion coefficients by internal friction, elastic after-effects and peak breadth measurements over the temperature range of 40 to 150°C which are given in Table 36.

Table 36

Niobium-Oxygen Diffusion Data by Powers and Doyle⁽⁴⁸⁾

Method of Measurement	D_0 (cm ² /sec)	Q (cal/mole)
Internal friction	0.014 ± 0.004	26,600 ± 200
Elastic after-effects	0.026 ± 0.009	27,000 ± 300
Combined	0.0212 ± 0.0073	26,910 ± 250
Peak breadth		26,700 ± 200

The log of the relaxation time vs 1/T°K for this data is plotted in Fig. 4.

Internal friction work by Ang⁽⁵¹⁾ obtained with the torsion pendulum over the temperature range of 148 to 168°C, fitted the following equation of oxygen diffusion in niobium.

$$D = 0.0147 \exp (-27,600/RT).$$

Marx, Baker, and Sivertsen⁽⁵²⁾ made internal friction measurements over the temperature range of 168 to 377°C. This was done by using both the torsion pendulum and the high frequency methods. They reported an activation energy of 26,000 cal/mole.

Gulbransen and Andrew's⁽⁵⁰⁾ measurements were concerned with the weight gain of a niobium sample heated in oxygen as a function of time and temperature. From this data, diffusion coefficients were calculated for the temperature range of 200 to 375°C and the following relationship was obtained:

$$D = 2 \times 10^{-5} \exp (-22,800/RT).$$

Comparison of this data with the more reliable internal friction measurements showed that this value of Q is a little small and D₀ is too small by 10³.

The concentration gradient of oxygen diffused into niobium was calculated by Jaffee, Klopp, and Sims⁽¹¹²⁾ from microhardness measurements by assuming the

hardness to be linear with the oxygen concentration. Measurements were made at 600, 800, and 1000°C. The average diffusion coefficients at each of these temperatures is listed in Table 37.

Table 37

Niobium-Oxygen Diffusion Data of Jaffee, Klopp and Sims ⁽¹¹²⁾

Temp. (°C)	D (cm ² /sec)
600	2.4×10^{-9}
800	3.5×10^{-8}
1000	2.1×10^{-7}

The data may be expressed as

$$D = 0.00407 \exp (-24,900/RT).$$

A plot of the log D vs 1/T°K values is shown in Fig. 21.

3. Substitutional Diffusion

a. Niobium-Titanium

Grzhimailo ⁽¹¹³⁾ deposited a radio-isotope of titanium onto titanium-niobium alloys of varying composition. The titanium isotope used had a half-life of several seconds so the diffusion of its decay product, Sc⁴⁶ (85 day half-life), was actually being measured. Flat samples of the alloy, 15 mm in diameter and 2 mm thick, were prepared by sintering. The radioactive titanium powder was pressed between two slices of the sintered alloy and diffused at 1000 and 1200°C. The radioactivity was measured at the end of the sample as a function of time. The data in Table 38 was obtained from these measurements.

The activation energy and the diffusion coefficient as a function of composition are shown in Figs. 22 and 23. Two peaks are observed in the activation energy plot which correspond to the composition Ti₃Nb and Ti₂Nb₃. These probably are regions of short range order as these phases are not in the published phase diagram. ⁽¹¹⁴⁾

Corrections were made in this data for the porosity of the sintered material, but some doubt exists as to whether the corrections were adequate. The reported D values are rather large for diffusion between elements of relatively high melting points and two temperatures are hardly adequate for determining Q. The data should definitely be considered questionable.

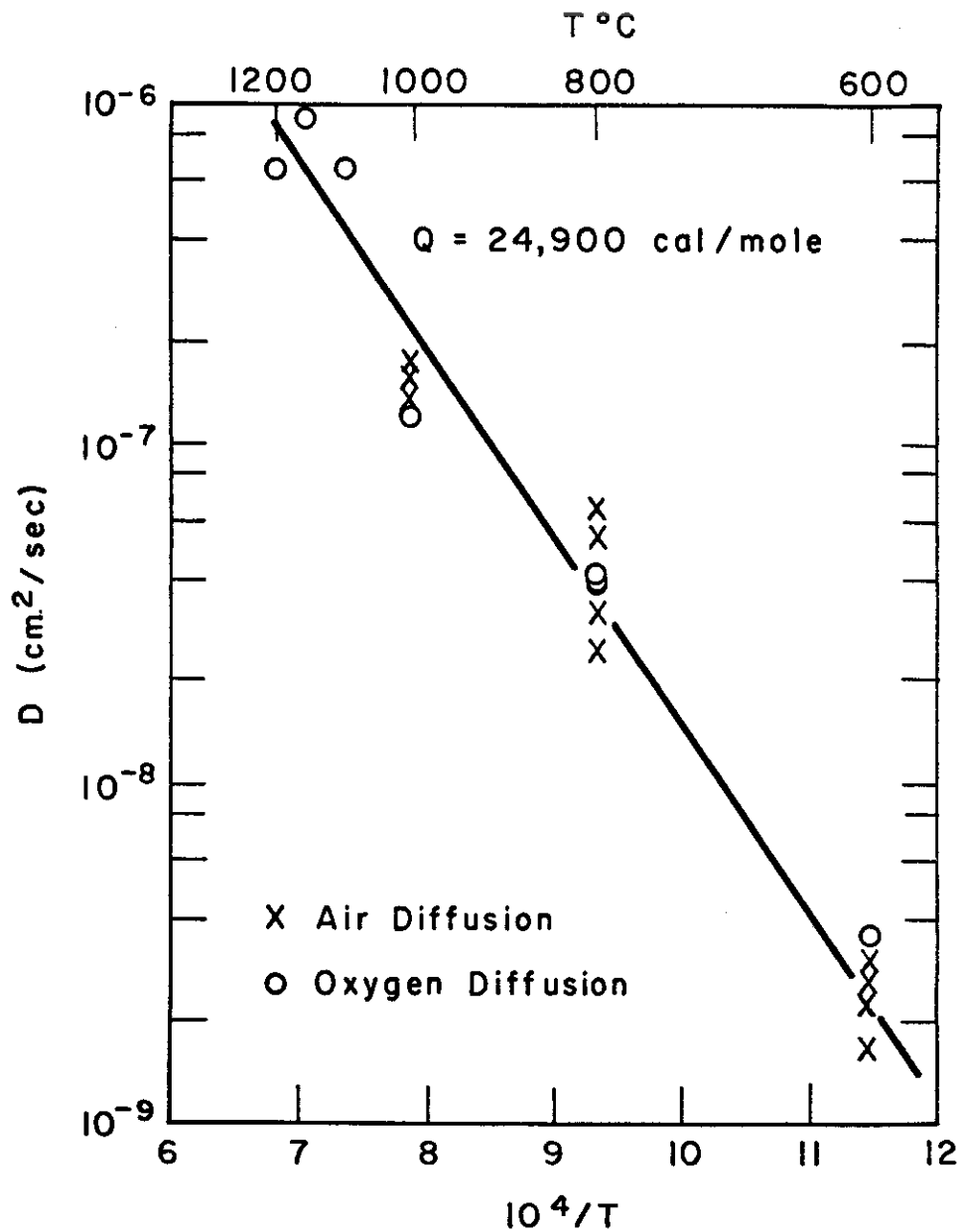


Fig. 21 - Temperature dependence of D for contamination of niobium in oxygen and air. (112)

Contrails

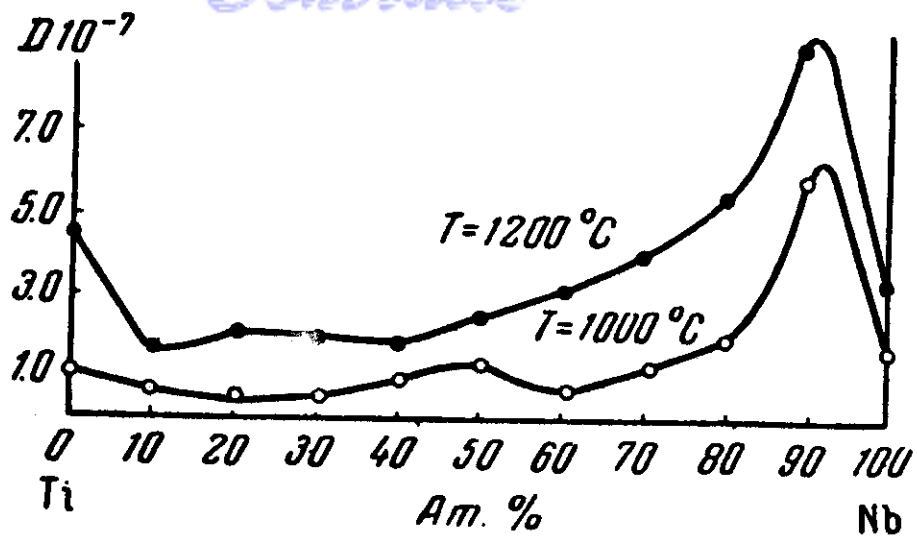


Fig. 22 - Variation of the diffusion coefficient of Sc^{46} with composition for the niobium-titanium system. (113)

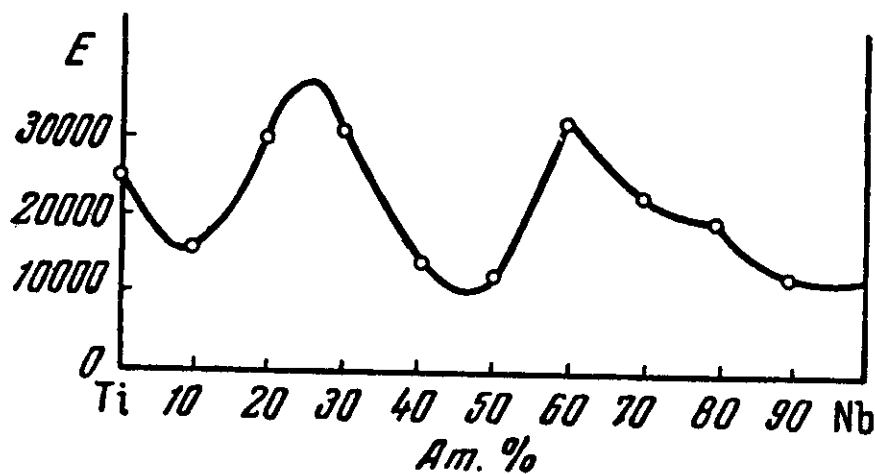


Fig. 23 - Variation of the activation energy for diffusion of Sc^{46} with composition for the niobium-titanium system. (113)

Table 38

Diffusion of Sc⁴⁶ into Various Titanium-Niobium Alloys⁽¹¹³⁾

At. %		D x 10 ⁷ (cm ² /sec)		Q (cal/mole)
Ti	Nb	1000°C	1200°C	
	100	1.125	3.05	13,010
10	90	0.731	8.80	12,160
20	80	0.381	5.11	19,900
30	70	0.521	3.77	22,990
40	60	0.795	2.92	32,790
50	50	1.250	2.32	11,470
60	40	0.481	1.67	13,500
70	30	1.045	1.94	31,500
80	20	1.710	2.00	30,150
90	10	4.506	11.74	15,770
100		1.525	4.52	25,290

b. Niobium-Chromium, Niobium-Iron, and Niobium-Nickel

Diffusion anneals were carried out by Birks and Seebold⁽¹⁰²⁾ between diffusion couples of the pure elements, Nb-Cr, Nb-Fe, and Nb-Ni. No diffusion coefficients were obtained. Concentration gradients were measured on the samples with the electron microbeam probe. The data is very incomplete and of doubtful value, but is given below for the sake of completeness.

Table 39

Phases Found in Niobium-Chromium, Niobium-Iron and
Niobium-Nickel Diffusion Couples

Diffusion System	Temp. (°C)	Time at Temp. (hr)	Width of Diffusion Zone (microns)	Phases Appearing in Diffusion Zone
Nb-Cr	1100	71 167	10	NbCr ₂ , NbCr ₇ NbCr, NbCr ₂ , NbCr ₇
Nb-Fe			25	NbFe ₂
Nb-Ni	1075 1100		25 Melting occurred	Nb ₂ Ni, NbNi, NbNi ₃

c. Niobium-Silicon

Samsonov and Solonnikova⁽²⁹⁾ measured the rate of growth of the NbSi₂ phase as a function of time and temperature. An activation energy for this process is given as $Q = 11,720$ cal/mole. The doubtful validity of this value as the activation energy for diffusion has been demonstrated earlier in this paper.

d. Niobium-Uranium

Diffusion anneals were carried out by Peterson and Ogilvie⁽¹¹⁵⁾ on samples composed of the pure elements at temperatures of 800, 892, and 996°C and at times of 4 to 49 days. The concentration gradients were determined with the electron microbeam probe. In order to determine the diffusion coefficient in the composition range of 0 to 10 at. % Nb the Matano analysis was applied. A previously unreported phase was observed in the diffusion couples, which may be an unstable phase. The data was found to fit the following equations:

for 99.5 at. % U

$$D = 3.4 \times 10^{-6} \exp (-25,800/RT)$$

for 95 at. % U

$$D = 9.6 \times 10^{-7} \exp (-23,400/RT)$$

for 90 at. % U

$$D = 2.4 \times 10^{-7} \exp (-21,800/RT).$$

Intrinsic diffusion coefficients were determined for 99.5 at. % U, which may be represented by the following equations:

$$D_U = 2 \times 10^{-4} \exp (-23,200/RT)$$

$$D_{Nb} = 3.1 \times 10^{-6} \exp (-25,800/RT).$$

This data is plotted as a function of $1/T$ in Figs. 24 and 25. Uranium is seen to diffuse 150 times faster than the niobium at 99.5 at. % U.

A summary of diffusion in niobium is given in Table 40.

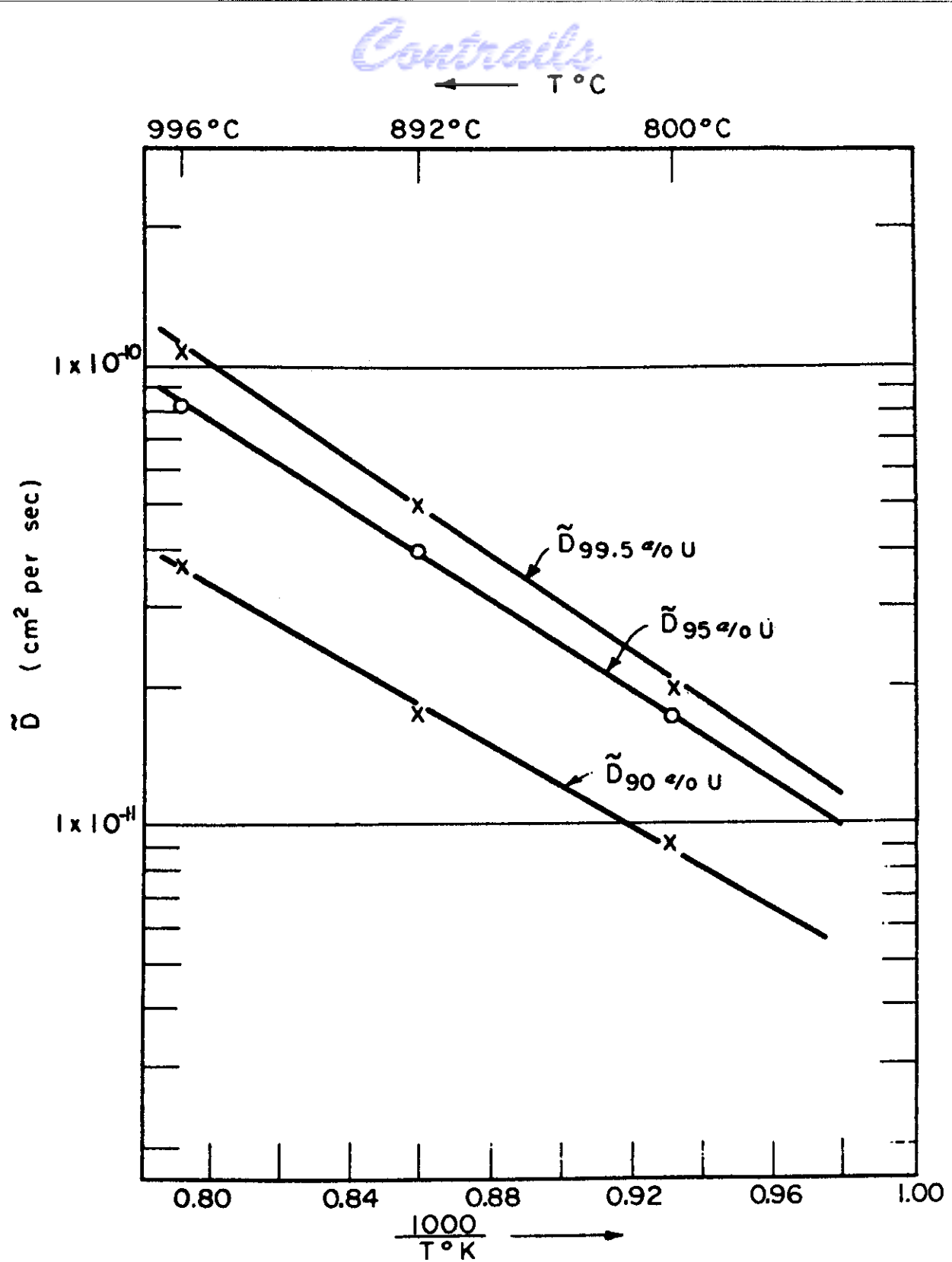


Fig. 24 - \tilde{D} as a function of $1/T$ for uranium-niobium diffusion. (115)

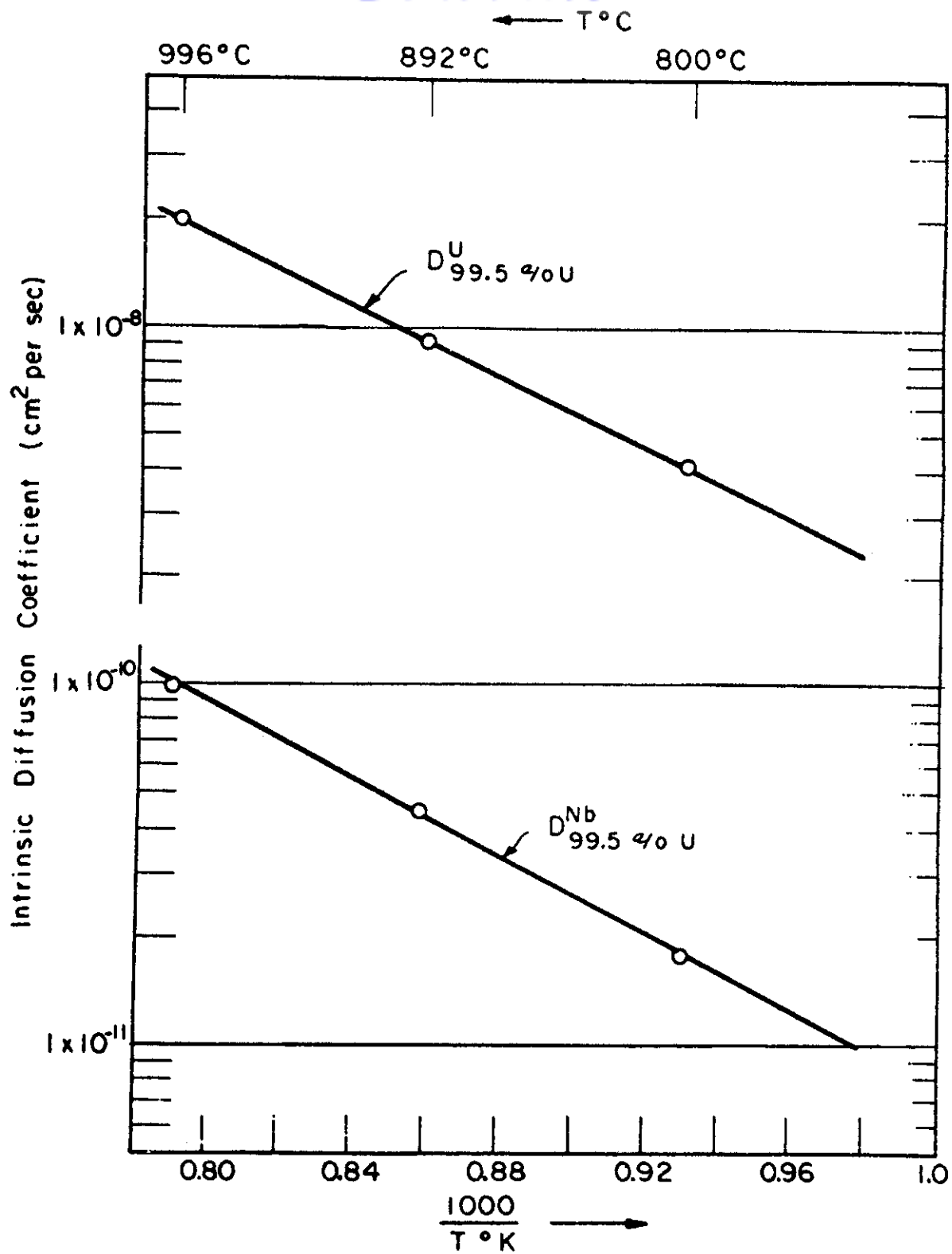


Fig. 25 - Intrinsic diffusion coefficients as a function of $1/T$. (115)

Table 40

Summary of Diffusion Data for Niobium

Diffusing Element	Composition Range (Wt. %)	Temp. (°C)	D (cm ² /sec)	D ₀ (cm ² /sec)	Q (cal/mole)	Reference
Nb		1585-2120		12.4	105,000	94
B	20	1400-2000		4.74 x 10 ³	14,300	8,9
C	0.013	1000-2000		3.14 x 10 ⁴	18,900	8,9
				0.015	27,000	44
		237.5-266.6		0.0046	33,300	109
		140-261		0.004	33,020	48
H		600-700		0.0214	9,370	110
N	0.0184-0.0215	267.3-295.3		0.0072	34,800	109
		150-295		0.0086	34,920	48
		285-583			35,700	52
		285-310		0.0980	38,600	51
		400-800		0.061	25,400	50
O					38,800	111
		40-150		0.0212	26,910	48
		148-168		0.0147	27,600	51
		168-377			26,000	52
		200-375		2 x 10 ⁻⁵	22,800	50
		600	2.4 x 10 ⁻⁹	0.00407	24,900	112
		800	3.5 x 10 ⁻⁸	0.00407	24,900	112
		1000	2.1 x 10 ⁻⁷	0.00407	24,900	112
Ti (Tracer)	0-100	1000	0.4-4.5 x 10 ⁻⁷		11,000-32,800	113
		1200	1.7-11.8 x 10 ⁻⁷			
Si	30				11,720	34
U	99.75 97.5 95.8	800-996		3.4 x 10 ⁻⁶	25,800	115
				9.6 x 10 ⁻⁷	23,400	
				2.4 x 10 ⁻⁷	21,800	

(Cont'd. on next page.)

Table 40 (Cont'd.)

Diffusing Element	Composition Range (Wt. %)	Temp. (°C)	D (cm^2/sec)	D_0 (cm^2/sec)	Q (cal/mole)	Reference
U (intrinsic)	99.75% U	800-996		2×10^{-4}	23,200	115
Nb (intrinsic)	99.75% U	800-996		3.1×10^{-6}	25,800	115
Ta		1100	5×10^{-15}			55
Mo	0-100	1100	$3-7 \times 10^{-14}$			102

III. GROUP II

A. Diffusion in Platinum

1. Self-diffusion

Kidson and Ross⁽⁹³⁾ evaporated radioactive platinum onto the surface of one centimeter diameter rods, 0.5 to 0.25 cm thick. Two such pieces were then welded together with their active surfaces in contact. The samples were diffused in the temperature range 1325 to 1600°C. The samples were sectioned and the activity of the sections was counted. The data is shown below.

Table 41

Diffusion Data for the Self-diffusion
of Platinum⁽⁹³⁾

Temp. (°C)	D (cm ² /sec)
1325	1.746×10^{-10}
1375	3.089×10^{-10}
1450	9.760×10^{-10}
1525	1.822×10^{-9}
1600	4.092×10^{-9}

A plot of log D vs 1/T is shown in Fig. 26. This figure illustrates that the scatter in the data is quite low. The values obtained may be represented by the equation:

$$D = 0.33 \exp (-68,200/RT).$$

2. Interstitial Diffusion

Platinum-Hydrogen

Ham⁽¹¹⁶⁾ measured the rate of flow of hydrogen through platinum foils 0.0133 cm thick at 600, 700, and 800°C. Although the data is treated in a somewhat different manner than normally found in physical metallurgy, the activation energy should be in agreement with that obtained from standard measurements. Q is given as 18,000 cal/mole with very little scatter in the data.

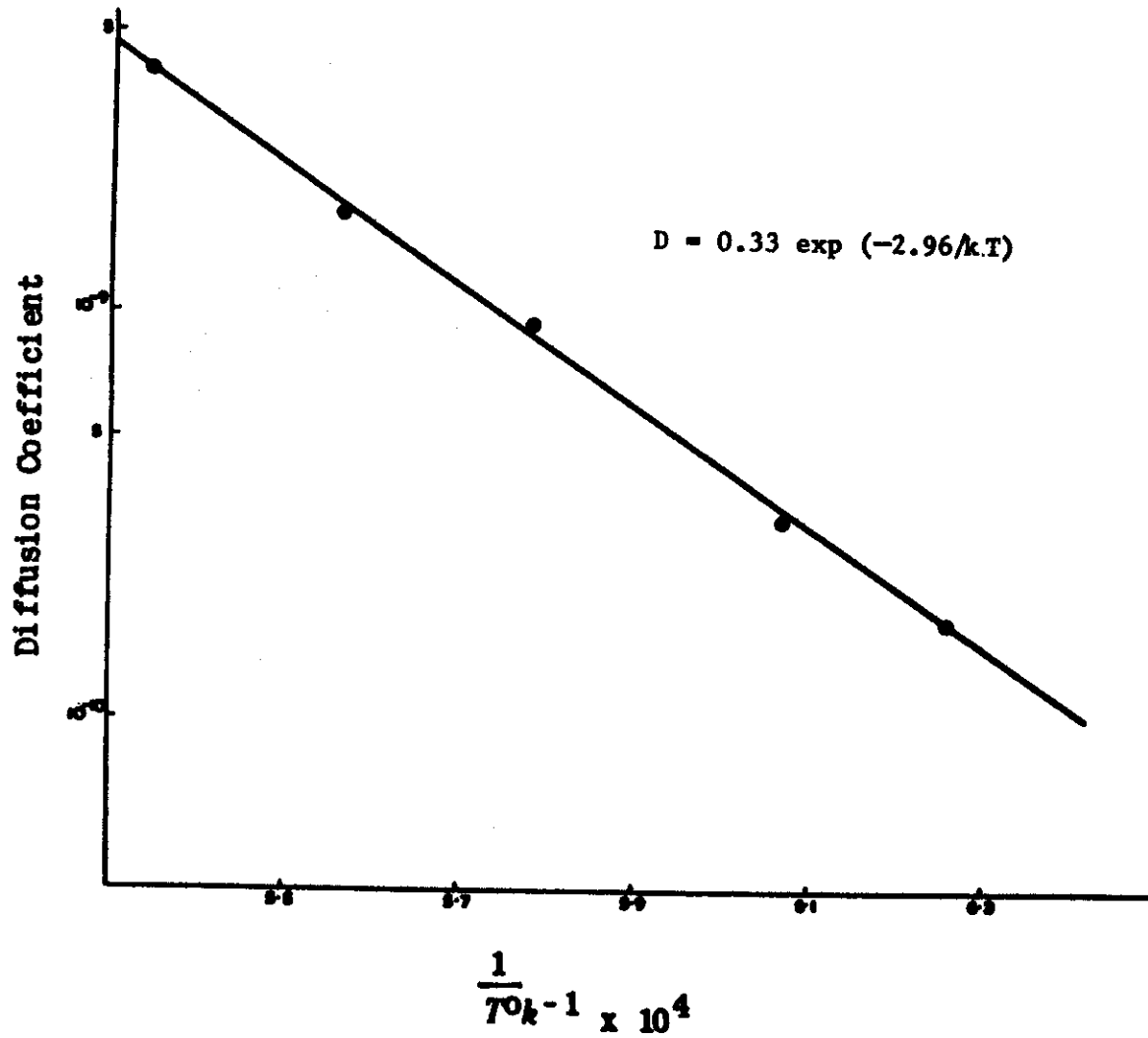


Fig. 26 - Log D vs 1/T for self-diffusion of platinum.(93)

3. Substitutional Diffusion

a. Platinum-Gold

The diffusion between pure platinum and pure gold, at 1002 and 1038°C was reported by Bolk.(117) The samples were bonded, diffused, and sectioned. After the removal of each section (20 to 500 microns), a Laue-back reflection picture was taken and the composition was determined from the lattice spacings. The diffusion coefficient is plotted as a function of composition in Fig. 27. No activation energies were reported as measurements were made at only two temperatures. However, intrinsic diffusion coefficients were determined and are listed in Table 42.

Table 42

Intrinsic Diffusion Coefficients in
Platinum-Gold System(117)

Temp. (°C)	D_{Au} (cm ² /sec)	D_{Pt} (cm ² /sec)	% Gold at Marker Interface
1002	2.50×10^{-9}	5.3×10^{-11}	94.8
1038	3.49×10^{-9}	4.1×10^{-11}	96.2

A sharp discontinuity was found in the concentration vs distance plots, corresponding to the two phase region, $\alpha_1 + \alpha_2$ in the phase diagram reported by Darling, Mintern, and Chaston.(118)

Jost⁽¹¹⁹⁾ studied the diffusion of gold from an electrolytically plated layer into an alloy of 80 wt. % Au - 20 wt. % Pt. The diffusion was carried out in a single phased region. No measurements were made as to the effect of composition on the diffusion rate. The reported data is given in Table 43.

Table 43

Platinum-Gold Diffusion Data at High
Gold Concentrations(119)

Temp. (°C)	D (cm ² /sec)
740	4.7×10^{-12}
824	2.2×10^{-11}
927	6.2×10^{-11}
986	$1.7-2.8 \times 10^{-10}$

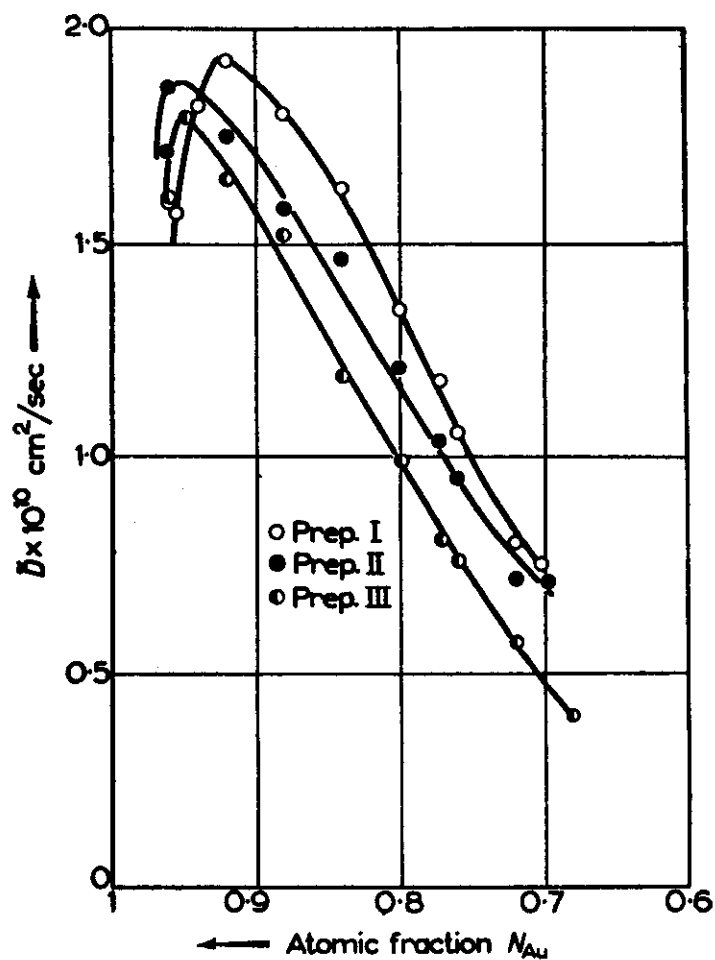


Fig. 27 - The dependence of D on composition. I and II diffused at 1038°C , III diffused at 1002°C . (117)

This data may be found to fit the equation:

$$D = 1.24 \times 10^{-3} \exp (-39,000/RT).$$

This value for D at 986°C agrees quite well with that obtained by Bolk for 1002°C.

Jedele⁽¹²⁰⁾ annealed pure gold - pure platinum diffusion couples for 5 days at 900°C. His sectioning technique was not good enough to pick up the discontinuity; consequently, he plotted the penetration-composition curve as a continuous line from which he deduced a much faster diffusion of platinum into gold than of gold into platinum. Due to this obvious error, the data will not be given here. It should be mentioned that Matano⁽¹²¹⁾ used this data to calculate the diffusion coefficient as a function of composition, which, consequently, is also in error.

b. Platinum-Copper

The diffusion of platinum in copper was investigated by Matano⁽¹²²⁾ over the concentration range of 2.4 to 3.5 at. % Pt (7 to 10 wt. % Pt). The specimens were ground away in steps. After each step the lattice parameter of the ground surface was determined by x-ray diffraction, from which the composition was determined. The data is reported in Table 44.

Table 44

Platinum-Copper Diffusion Data at High
Copper Concentrations⁽¹²²⁾

Temp. (°C)	D (cm ² /sec)
490	5.8×10^{-13}
580	4.5×10^{-12}
700	1.3×10^{-11}
850	3.5×10^{-11}
960	$1.1-2.3 \times 10^{-10}$

The equation

$$D = 1.0 \times 10^{-6} \exp (-21,900/RT)$$

represents the relationship for the values obtained.

Kubaschewski and Ebert⁽¹²³⁾ carried out diffusion in the platinum-copper system at high platinum concentration. Pure platinum was bonded with a 95 wt. % Pt-5 wt. % Cu (13.9 at. % Cu) alloy and diffused at temperatures from 1041 to 1401°C. Layers were machined off and x-ray diffraction patterns recorded. From these patterns the composition was determined from previously prepared standards. The values found are shown in Table 45.

Table 45
Platinum-Copper Diffusion at High
Platinum Concentrations⁽¹²³⁾

Temp. (°C)	D (cm ² /sec)
1041	2.2×10^{-11}
1150	1.1×10^{-10}
1152	1.6×10^{-10}
1213	1.4×10^{-10}
1241	6.7×10^{-10}
1350	1.5×10^{-9}
1401	1.7×10^{-9}

This data may be represented by the equation:

$$D = 4.9 \times 10^{-2} \exp (-55,700/RT).$$

In the last two references, superb data has been reported for the high platinum and low platinum portions of the copper-platinum system. This may well be sufficient for some alloy development purposes but for academic reasons, the diffusion data and especially the activation energy data, may be far more interesting in the region of the ordered Cu₃Pt and CuPt phases.

c. Platinum-Nickel

Kubaschewski and Ebert⁽¹²³⁾ also studied the diffusion in the high platinum portion of the platinum-nickel system. Pure platinum was bonded to an alloy of 94.8 wt. % Pt - 5.2 wt. % Ni and diffused at temperatures from 1043 to 1401°C. The composition along the diffusion couple was determined from x-ray diffraction patterns of machined sections. The data obtained is given in Table 46.

Table 46

Diffusion Data for the Platinum-Nickel System
at High Platinum Concentrations(123)

Temp. (°C)	D (cm ² /sec)
1043	5.3×10^{-11}
1149	1.8×10^{-10}
1241	4.9×10^{-10}
1374	1.5×10^{-9}
1401	1.6×10^{-9}

These values may be expressed as

$$D = 7.9 \times 10^{-4} \exp (-43,100/RT).$$

The data appears to be very good with less than a normal amount of scatter in the log D vs 1/T curve.

A summary of diffusion in platinum is given in Table 47.

B. Diffusion in Hafnium

1. Self-diffusion

The self-diffusion of hafnium has not been measured. However, estimates of the activation energy may be obtained from melting point and heat of fusion relations.

The best value for the melting point of hafnium is 2222°C as determined by Deardorff and Hayes.(124) (This value is considered best as their hafnium contained the least amount of impurities, the main impurity usually being zirconium.) From LeClaire's relation,(58) the activation energy for self-diffusion in hafnium is $Q = 94,800$ cal/mole. The plot of activation energy for self-diffusion vs melting point shown in Fig. 8 enables Q to be estimated for hafnium as $Q = 94,000$ cal/mole.

Nachtrieb and Handler(59) stated the empirical formula $Q = 16.5 \Delta H_f$ where ΔH_f is the heat of fusion. Kelley(125) gives $\Delta H_f = 5,790$ cal from which Q is calculated to be $Q = 95,500$ cal/mole.

Table 47
Summary of Diffusion Data for Platinum

Diffusing Element	Composition Range (wt. %)	Temp. (°C)	D (cm^2/sec)	D_0 (cm^2/sec)	Q (cal/mole)	Reference
Pt (self)		1325	1.746×10^{-10}	0.33	68,200	93
		1375	3.089×10^{-10}			
		1450	9.760×10^{-9}			
		1525	1.822×10^{-9}			
		1600	4.092×10^{-9}			
H		600-800			18,000	116
Au	70-100	1002	$1.8-0.4 \times 10^{-10}$			117
		1038	$1.9-0.7 \times 10^{-10}$			
Au (intrinsic)	94.8 96.2	1002	2.5×10^{-9}			117
		1038	3.5×10^{-9}			
Pt (intrinsic)	94.8% Au 96.2% Au	1002	5.3×10^{-11}			117
		1038	4.1×10^{-11}			
Au	80	740	4.7×10^{-12}	1.24×10^{-3}	39,000	119
		824	2.2×10^{-11}			
		927	6.2×10^{-11}			
		986	$1.7-2.8 \times 10^{-10}$			
Cu	90-93	490	5.8×10^{-13}	1.0×10^{-6}	21,900	114
		580	4.5×10^{-12}			
		700	1.3×10^{-11}			
		850	3.5×10^{-11}			
		960	$1.1-2.3 \times 10^{-10}$			
Cu	0-5	1041	2.6×10^{-11}	4.9×10^{-2}	55,700	123
		1150	1.1×10^{-10}			
		1213	1.4×10^{-10}			
		1241	6.7×10^{-9}			
		1350	1.5×10^{-9}			
		1401	1.7×10^{-9}			

(Cont'd. on next page.)

Table 47 (Cont'd.)

Diffusing Element	Composition Range (wt. %)	Temp. (°C)	D (cm ² /sec)	D_0 (cm ² /sec)	Q (cal/mole)	Reference
N ₁	0-5.2	1043	5.3×10^{-11}	7.9×10^{-4}	43,100	123
		1149	1.8×10^{-10}			
		1241	4.9×10^{-10}			
		1374	1.5×10^{-9}			
		1401	1.6×10^{-9}			

From these different estimated values, the value $Q = 95,000$ cal/mole may be taken as a reasonable estimate for the activation energy for self-diffusion in hafnium until a good experimental value is obtained.

2. Interstitial Diffusion

Hafnium-Oxygen

The hafnium-oxygen system is the only hafnium system in which diffusion measurements have been made. Pemsler⁽¹²⁶⁾ measured the rate of diffusion of oxygen in hafnium by observing the rate of dissolution of oxide films into the metal in vacuum. Samples containing 1.45 wt. % Zr were electrolytically oxidized in a solution of KOH to a known layer thickness. The size of the oxide layer was measured by the weight gained by the sample. The color of the oxide (a measure of its thickness) was observed during the diffusion in vacuum. The parabolic rate of disappearance of the oxide film on the hafnium suggests that the rate-controlling step is the diffusion of oxygen in hafnium. Different orientations of the grains caused the rate of disappearance to vary by as much as a factor of two.

To calculate diffusion coefficients, Pemsler had to assume values for the density of oxygen-saturated metal, the density of monoclinic hafnia, and the solubility of oxygen in hafnium. The theoretical density of 10.22 g/cm^3 was used for the monoclinic HfO_2 . The value of density for the oxygen saturated metal was taken arbitrarily as 13.5 g/cm^3 . No data for the solubility of oxygen in hafnium are known, so the diffusion coefficients were calculated for three assumed values of oxygen, 20, 30, and 40 atomic percent. These values should bracket the actual value as the solubility of oxygen in titanium-oxygen is 34 atomic percent oxygen and zirconium-oxygen is 29 atomic percent oxygen. The diffusion coefficients may be expressed by the following equations:

for 20 at. % O

$$D = 1.4 \exp [-(51,850 \pm 200)/RT]$$

for 30 at. % O

$$D = 0.47 \exp [-(51,850 \pm 200)/RT]$$

for 40 at. % O

$$D = 0.14 \exp [-(51,850 \pm 200)/RT].$$

The experimental measurements have been performed with good precision but the lack of knowledge of certain values limits the precision of the resulting D values.

Smeltzer and Simnad⁽¹²⁷⁾ studied the oxidation of hafnium containing 5 weight percent zirconium in pure oxygen at 760 mm Hg pressure in the temperature

range 35 to 1200°C by observing the weight gain as a function of time. Only the parabolic region of the curve were used for diffusion constants. Thomas and Hayes⁽¹²⁸⁾ plotted the weight gained per unit area vs 1/T for Smeltzer and Simnad's data where the parabolic rate law is obeyed. From this, they calculated an activation energy $Q = 56,000$ cal/mole which is in good agreement with that obtained by Pemsler.

C. Diffusion in Zirconium

1. Self-diffusion

The self-diffusion of zirconium may be estimated from the melting point and heat of fusion relations as no diffusion measurements have been made. From LeClaire's relation,⁽⁵⁸⁾ the activation energy for self-diffusion in zirconium is $Q = 81,000$ cal/mole. From the plot of activation energy for self-diffusion vs melting point shown in Fig. 8, Q may be estimated for zirconium as $Q = 80,000$ cal/mole.

Using Nachtrieb and Handler's empirical formula⁽⁵⁹⁾ and Kelley's value⁽¹²⁵⁾ of $\Delta H_f = 4,900$ cal, Q is calculated to be $Q = 80,800$ cal/mole.

These values are probably fairly close to the true value for beta zirconium. The activation energy for self-diffusion in alpha-zirconium will be somewhat different, probably larger.

2. Interstitial Diffusion

a. Zirconium-Carbon

Samsonov and Latysheva^(8,9) determined the diffusion coefficients for diffusion of carbon in zirconium in the range 1000 to 1600°C by applying the analysis outlined under the tungsten-boron system (page 3) to the growth of the zirconium-carbon phase. The data may be described by the equation

$$D = 4.52 \times 10^3 \exp [-(17,900 \pm 5,600)/RT].$$

Table 48

Zirconium-Carbon Diffusion Data Using the Samsonov and Latysheva Technique^(8,9)

Temp. (°C)	D (C - C ₂)	Q (cal/mole)	D ₀ (cm ² /sec)	C - C ₂ (g/cm ³)	D (cm ² /sec)
1000	0	17,900 ± 5600	1810 ± 340	0.401	4.52 x 10 ³ exp ($\frac{-17,900}{RT}$)
1200	2.4420				
1400	4.1366				
1500	5.8312				
1600	8.1622				

Contrails

b. Zirconium-Hydrogen

Mallett and Albrecht⁽¹²⁹⁾ measured the diffusion of hydrogen into zirconium containing 0.02 weight percent hafnium. The samples were degassed in vacuum and then heated in a hydrogen atmosphere for various times at temperatures of 305 to 610°C. Layers were machined off and analyzed for hydrogen. The diffusion data is shown below.

Table 49

Diffusion of Hydrogen in Alpha-Zirconium at
Low Hafnium Content⁽¹²⁹⁾

Temp. (°C)	D x 10 ⁶ (cm ² /sec)	Temp. (°C)	D x 10 ⁶ (cm ² /sec)
305	1.7	486	6.9
350	2.0	567	9.7
410	3.7	610	13.0
446	5.2		

These results are shown in a plot of log D vs 1/T in Fig. 28. The data may be represented by the equation:

$$D = 7.0 \times 10^{-4} \exp [-(7,060 \pm 260)/RT].$$

Surface films can easily lead to erroneous diffusion data when the diffusing element is in the gaseous phase. Great care was taken in this work to reduce these effects.

Earlier data by Schwartz and Mallett⁽¹³⁰⁾ on diffusion of hydrogen in zirconium was obtained for zirconium containing 1 weight percent hafnium. The values are given in Table 50.

Table 50

Diffusion of Hydrogen in Alpha-Zirconium
Containing 1% Hafnium⁽¹³⁰⁾

Temp. (°C)	D x 10 ⁶ (cm ² /sec)
400	6
500	10
600	16

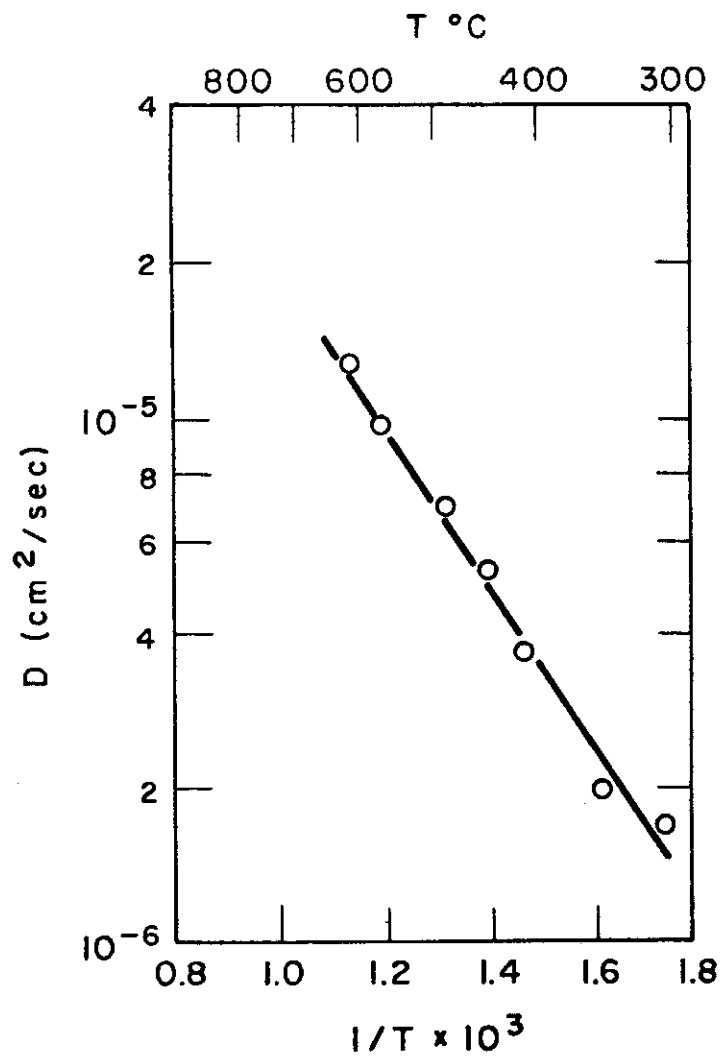


Fig. 28 - Temperature variation of diffusion coefficient for hydrogen in zirconium.(129)

This data is not as complete nor as reliable as the more recent data reported in Ref. 129.

Sawatzky⁽¹⁹¹⁾ obtained cylindrical specimens of 5 to 6 ppm of hydrogen by vacuum degassing at 830°C. These samples were then abraded with 600-A carbide paper and subsequently heated for various times at different temperature in a hydrogen atmosphere at 200 mm pressure. Turnings were removed from the diameter of the specimen and the radial distribution of hydrogen was determined. Table 51 lists the values reported.

Table 51

Diffusion Data for Hydrogen Diffusion in Zircaloy-2⁽¹⁹¹⁾

Temp. (°C)	D x 10 ⁶ (cm ² /sec)
261	0.80
315	1.70
358	2.94
408	4.71
458	5.49
515	10.3
560	15.8

This data may be represented by the equation:

$$D = 2.7 \times 10^{-3} \exp [-(8,380 \pm 400)/RT].$$

The agreement of this data with that of Mallett and Abrecht is quite good, differing by less than a factor of two over the temperature range investigated. This small difference may well be due to the small amounts of tin, iron, and chromium in the Zircaloy.

The measurement of the weight gain as a function of time for zirconium heated in hydrogen by Gulbransen and Andrew⁽¹³¹⁾ showed a parabolic relationship. The reaction was reported to be very slow at 250°C and quite fast at 300°C. The effect of pressure was also studied. The reaction was found to be very sensitive to surface films and pre-treatment. No values are given for the diffusion coefficient or the activation energy.

c. Zirconium-Nitrogen

Mallett, Belle and Cleland⁽¹³²⁾ investigated the diffusion of nitrogen from the gaseous phase into beta-zirconium containing 0.015 weight percent hafnium. The samples were degassed in vacuum and then heated in nitrogen in the temperature range of 920 to 1640°C. Layers were removed and analyzed for nitrogen. The data is tabulated below.

Table 52

Zirconium-Nitrogen Diffusion Data for Beta-Zirconium
of Low Hafnium Content⁽¹³²⁾

Temp. (°C)	D x 10 ⁷ (cm ² /sec)	Temp. (°C)	D x 10 ⁷ (cm ² /sec)
920	0.55	1305	7.7
975	0.72	1305	11.0
1030	1.3	1305	6.3
1085	1.5	1420	14.0
1085	1.3	1420	17.0
1140	1.9	1475	25.0
1195	3.4	1530	35.0
1195	3.1	1530	39.0
1195	6.3	1640	51.0

These values are plotted in Fig. 29, and may be related by the equation:

$$D = 1.5 \times 10^{-2} \exp [-(30,700 \pm 1,000)/RT].$$

In an earlier publication, Mallett, Baroody, Nelson and Papp⁽¹³³⁾ reported the diffusion of nitrogen into beta-zirconium containing 1.8 to 2.2 weight percent hafnium. This investigation was carried out over the temperature range of 900 to 1600°C using the same technique as reported in Ref. 132. The data is summarized in Table 53. These results are represented by the equation:

$$D = 3 \times 10^{-2} \exp [-(33,600 \pm 1,600)/RT].$$

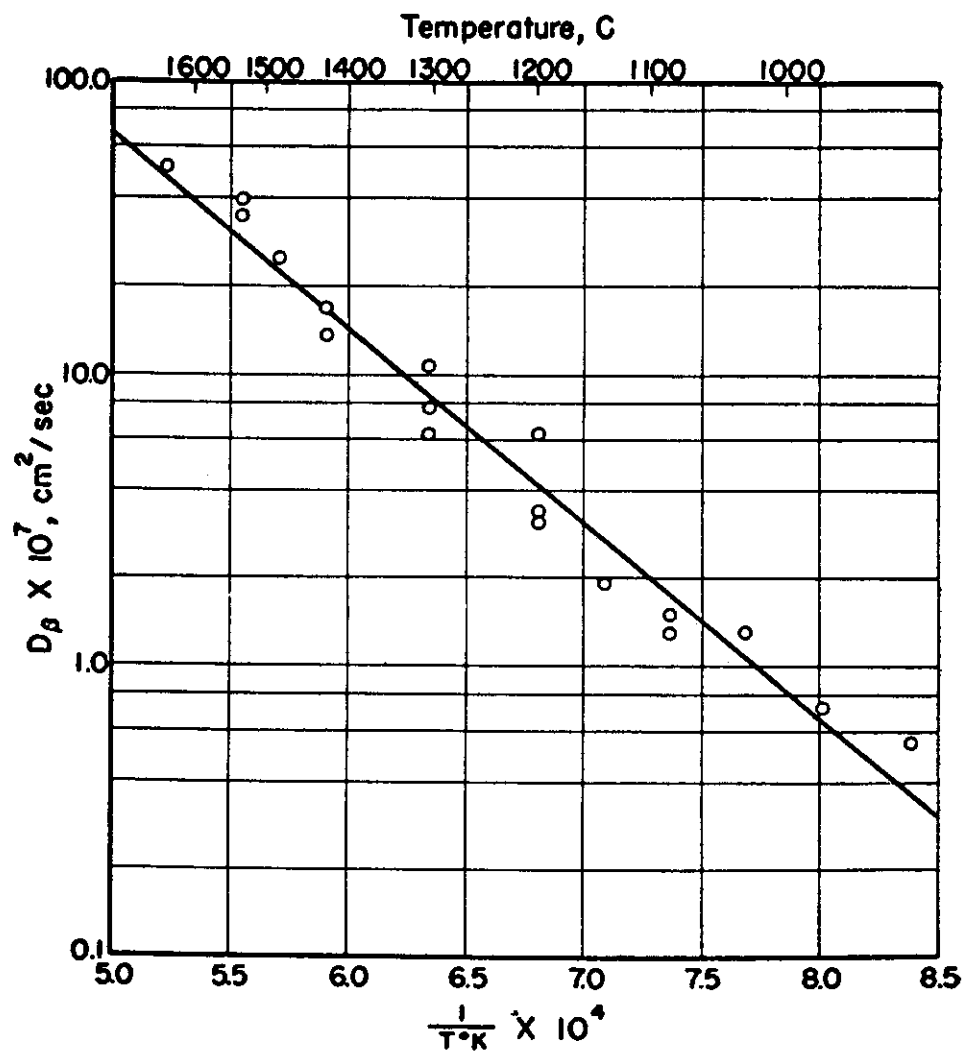


Fig. 29 - Variation of the diffusion coefficient with temperature for diffusion of nitrogen in zirconium.(132)

Zirconium-Nitrogen Diffusion Data for Beta-Zirconium
Containing 1.8-2.2% Hafnium⁽¹³³⁾

Temp. (°C)	D x 10 ⁷ (cm ² /sec)	Temp. (°C)	D x 10 ⁷ (cm ² /sec)
900	0.1	1200	2.4
1000	0.4	1200	5.0
1000	0.5	1300	6
1100	1.1	1400	11
1100	2.7	1500	17
		1600	27

Good agreement is shown with the previously reported data of Mallett, Belle, and Cleland. The slight discrepancy found may be a real effect due to the different hafnium contents.

Wasilwski⁽¹³⁴⁾ reported that the diffusion of nitrogen in beta-zirconium fits the equation:

$$D = 3.5 \times 10^{-2} \exp (-33,800/RT).$$

This work has not been published but is given as a private communication in Ref. 132. Further comments as to experimental procedure, temperature range, or degree of accuracy of this work cannot be made until publication of this work. The superb agreement between this work and the excellent work of the two previously mentioned investigations speaks well for all three.

Gulbransen and Andrew⁽¹³¹⁾ measured the weight gain as a function of time for alpha-zirconium heated in nitrogen. Parabolic curves were obtained in the temperature range of 600 to 825°C. However, the data at 400 and 500°C does not fit the diffusion equation. The activation energy for the rate limiting step (assumed to be diffusion) is given as $Q = 39,200$ cal/mole. This larger activation energy would be expected for diffusion in the alpha phase. The work in the zirconium-oxygen system showed that the diffusion coefficients as determined by Gulbransen and Andrew are in very bad agreement with the data obtained by more reliable techniques. This leads one to doubt this value for diffusion of nitrogen in alpha-zirconium. In the zirconium-oxygen system, $Q_\alpha \approx 1.5 Q_\beta$. Hence, a reasonable value for the activation energy for diffusion of nitrogen in alpha-zirconium may be taken as $Q = 45,000$ cal/mole and D_0 may be assumed to be around $4 \text{ cm}^2/\text{sec}$.

Contrails

d. Zirconium-Oxygen

Pemsler⁽¹³⁵⁾ measured the rate of diffusion of oxygen in alpha-zirconium by observing the rate of dissolution of oxide films into the metal in vacuum. The samples were oxidized electrolytically in a solution of KOH. The thickness of the initial oxide layer was measured by the weight gained by the sample, and the color of the oxide was observed during the diffusion in vacuum. There is a parabolic rate of disappearance of the oxide film on the zirconium which suggests that the rate-controlling process is the diffusion of oxygen into the metal. Variation of the rate of disappearance by as much as a factor of two among the different oriented grains was observed.

To calculate diffusion coefficients, Pemsler had to assume a value for the density of oxygen-saturated metal. The other quantities which must be known for this calculation, the density of zirconia and the solubility of oxygen in alpha-zirconium, had been determined experimentally. The data obtained is listed in Table 54.

Table 54

Diffusion of Oxygen in Alpha-Zirconium⁽¹³⁵⁾

Temp. (°C)	D (cm ² /sec)
400	1.34×10^{-16}
482	1.21×10^{-14}
510	2.79×10^{-14}
542	1.38×10^{-13}
585	5.62×10^{-13}

These experimental points are plotted in Fig. 30, and may be described by the equation:

$$D = 9.4 \exp [-(51,780 \pm 220)/RT].$$

Measurements of surface effects may often lead to large errors due to the presence of surface films of grease or entrapped gases. Sufficient care was taken to minimize these effects making this data quite reliable.

Mallett, Albrecht, and Wilson⁽¹³⁶⁾ examined the diffusion of oxygen in alpha and beta Zircaloy in the temperature range of 1000 to 1500°C. For the determination of the diffusion coefficient in the alpha phase, the movement of the

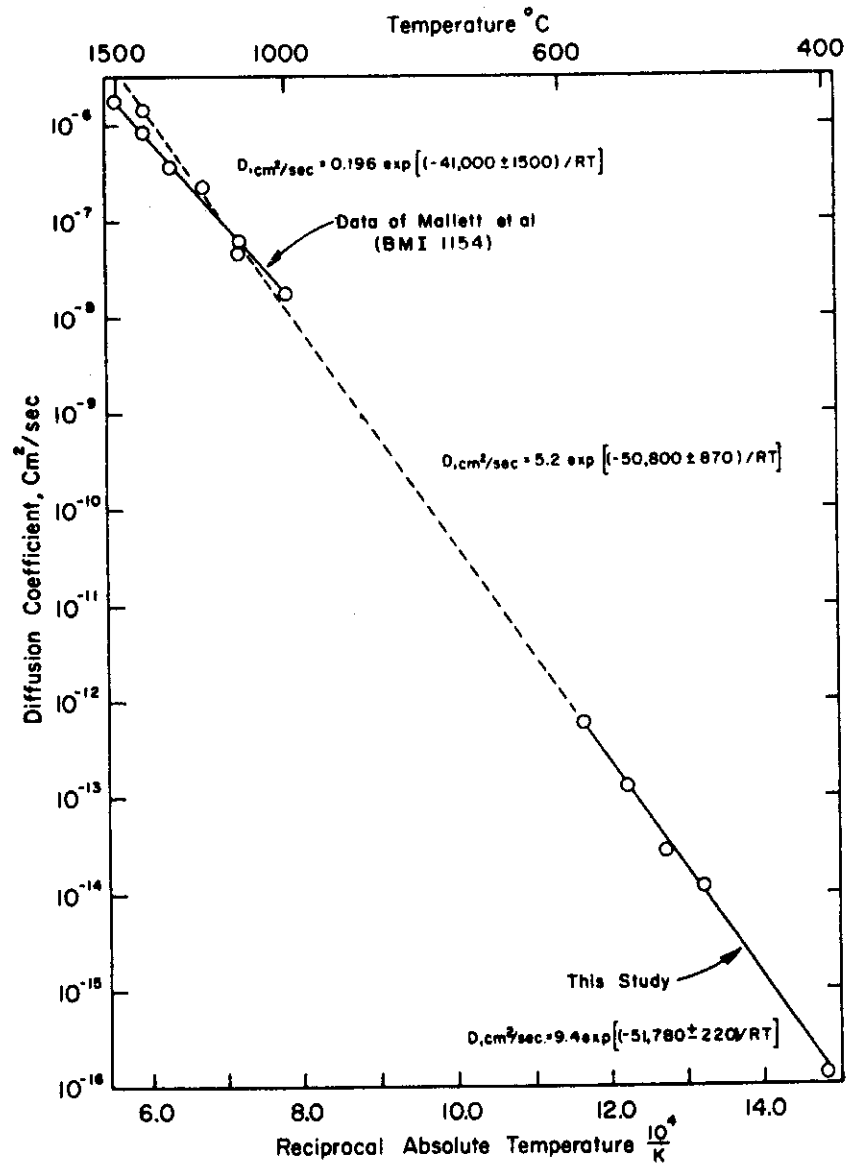


Fig. 30 - Temperature dependence of the diffusion coefficient of oxygen in zirconium. (135)

alpha-beta phase boundary was observed as a function of time at the different temperatures. Their diffusion coefficient may be represented by the equation:

$$D_{\alpha-Zr} = 0.196 \exp [-41,000 \pm 1,500/RT].$$

This data is plotted in Fig. 30. Due to the alloying elements in Zircaloy and the higher oxygen contents of this investigation, precise agreement with the data of Pemsler would not be expected. Although the D_0 and Q values of this investigation are considerably different from those of Pemsler's, the agreement is pretty good as seen in Fig. 30.

The concentration gradients for the oxygen-beta zirconium diffusion were determined by sectioning and chemical analysis of samples. The data achieved may be represented by the equation:

$$D_{\beta-Zr} = 0.0453 \exp [-(28,200 \pm 2,400)/RT].$$

Tresco⁽¹³⁷⁾ obtained an estimate of the diffusion coefficient at 1280°C by following the homogeneity of a zirconium sample to which a known amount of oxygen had been added. The time was noted for complete diffusion through a known volume. This gave a minimum value of

$$D = 5.25 \times 10^{-6} \text{ cm}^2/\text{sec at } 1280^\circ\text{C}$$

for diffusion of oxygen in beta-zirconium which agrees very well with the data of Mallett, Albrecht, and Wilson.

Other investigators, Gulbransen and Andrew,⁽¹³¹⁾ measured the weight gained by a zirconium sample heated in oxygen. The reaction followed a parabolic rate law throughout the temperature range of 200 to 425°C. Their data was found to fit the equation:

$$D = 5.3 \times 10^{-8} \exp (-18,200/RT).$$

This is in very poor agreement with the more reliable data of Refs. 135 and 136. Since the data appears to have been taken with good precision, the reaction measured probably was not diffusion.

3. Substitutional Diffusion

a. Zirconium-Nickel

Allison and Samelson⁽¹³⁸⁾ investigated the diffusion of zirconium in an alloy of 0.08 weight percent zirconium - remainder nickel in

the temperature range 800 to 970°C. Their method consisted of measuring the weight gain caused by surface oxidation of the zirconium in a wet hydrogen ambient, and identifying the surface oxide by means of electron diffraction. Since the grain size was less than 10^{-3} mm, considerable grain boundary diffusion was found. The observed diffusion coefficient fitted the equation:

$$D = 1 \times 10^{-5} \exp (-26,700/RT).$$

It is not clear what mechanism was actually being evaluated by these measurements. It could have been lattice or grain boundary diffusion of oxygen into the sample, diffusion of zirconium to the surface, hydride formation, or surface film reaction with the gas, or many others. Therefore, this method is not very useful for diffusion coefficient determinations.

b. Zirconium-Titanium

Martens⁽¹³⁹⁾ reported preliminary work on the diffusion of zirconium-95 tracer into zirconium-titanium alloys over the temperature range of 825 to 1150°C. An activation energy of approximately 23,000 cal/mole is reported.

c. Zirconium-Uranium

A very complete and accurate investigation of the diffusion in the zirconium-uranium system was carried out by Adda, Philibert, and Faraggi.⁽¹⁴⁰⁾ Pressure bonded diffusion couples were prepared between the pure elements and annealed in the temperature range 550 to 1075°C. The concentration gradients were determined with the electron microbeam probe, and the diffusion coefficients and the activation energies were then determined as a function of the concentration. This data is given in Table 55 and may be seen in Figs. 31 and 32. Intrinsic diffusion coefficients were also measured. This data is summarized in Table 56 and is shown graphically in Fig. 33.

In a more recent paper, Adda, Mairy, and Andreu⁽¹⁹²⁾ reported the uranium and zirconium intrinsic diffusion coefficients as a function of composition. This was accomplished by bonding a series of uranium foils with fine tungsten wire between them to a similar set of zirconium foils. By measuring the movements of the tungsten wire, a whole series of intrinsic diffusion coefficients can be determined from one sample. The concentration gradient was determined with the electron microbeam probe. The experimental values of D_U and D_{Zr} are plotted as a function of composition for 950 and 1000°C in Fig. 34. It may be noted in this figure that at compositions of 0 to 10 atomic percent uranium, D_{Zr} is greater than D_U while at compositions of 10 to 100 atomic percent uranium, D_{Zr} is less than D_U . This means that there are several separate regions of sources and sinks for vacancies.

Smith⁽¹⁴¹⁾ measured the diffusion of zirconium in liquid uranium at 1270°C and reported that $D = (1.9 \pm 0.9) \times 10^{-4}$ cm²/sec.

A summary of diffusion in zirconium is given in Table 57.

Table 55

Zirconium-Uranium Diffusion Coefficients for
Various Zirconium Concentrations⁽¹⁴⁰⁾

Concentraion (at. % Zr)	Activation Energy (cal/mole)	Frequency Factor D_0 (cm ² /sec)
10	32,000	9.5×10^{-4}
20	28,600	1.3×10^{-4}
30	26,300	3.5×10^{-5}
40	27,400	4.0×10^{-5}
50	29,700	8.0×10^{-5}
60	29,700	6.3×10^{-5}
70	29,700	5.5×10^{-5}
80	34,300	3.2×10^{-4}
90	41,000	7.8×10^{-3}
95	47,000	8.7×10^{-2}

Table 56

Intrinsic Diffusion Coefficients for the
Zirconium-Uranium System⁽¹⁴⁰⁾

Temp. (°C)	950	1000	1040	1075
At. % Zr	12.5	11.5	11.0	9.5
Intrinsic D_U	7.7×10^{-9}	1.6×10^{-8}	2.1×10^{-8}	3.7×10^{-8}
Intrinsic D_{Zr}	6.5×10^{-10}	1.0×10^{-9}	2.3×10^{-9}	2.9×10^{-9}

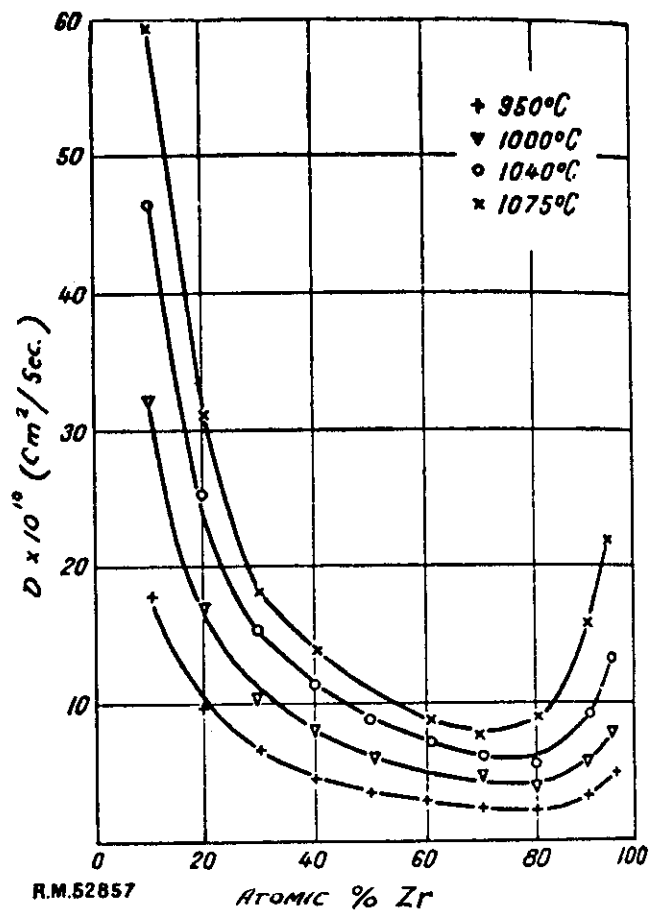


Fig. 31 - Variation of the diffusion coefficient with composition for the zirconium-uranium system.(140)

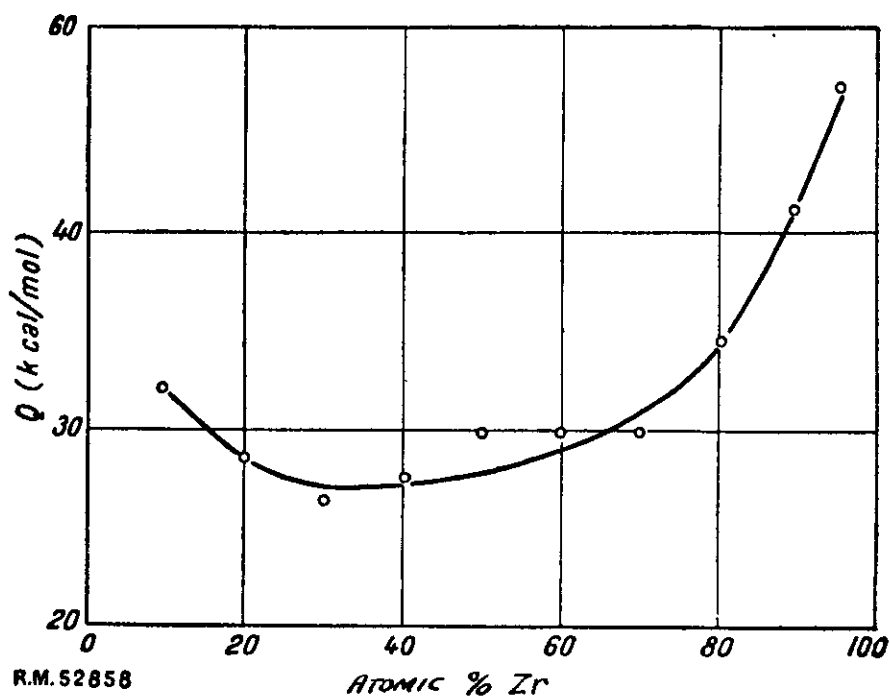


Fig. 32 - Variation of the activation energy for diffusion with composition for the zirconium-uranium system.(140)

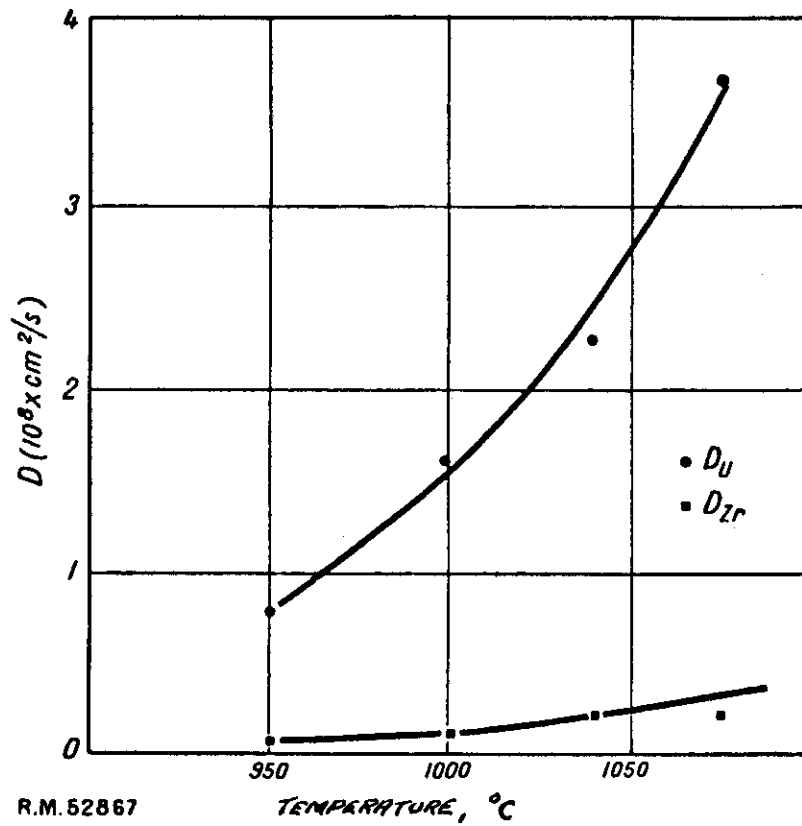


Fig. 33 - Variation of the intrinsic diffusion coefficients with temperature for the zirconium-uranium system.⁽¹⁴⁰⁾

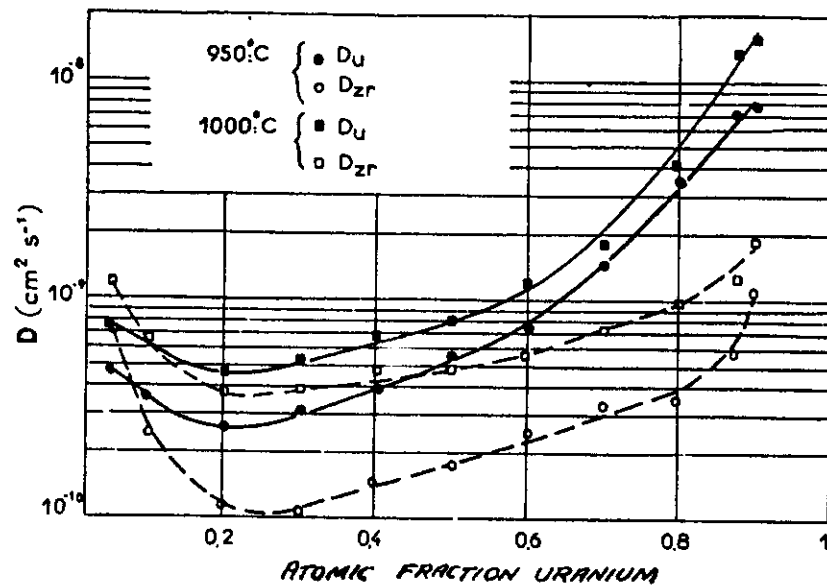


Fig. 34 - Variation of the intrinsic diffusion coefficients with composition for the zirconium-uranium system. (192)

Table 57

Summary of Diffusion Data for Zirconium

Diffusing Element	Composition Range (wt. %)	Temp. (°C)	D (cm^2/sec)	D_0 (cm^2/sec)	Q (cal/mole)	References
Zr (self)	Estimate from melting point Estimate from heat of fusion				81,000 80,000 80,800	
C	6	1000-1600		4.52×10^3	17,900	8,9
H	$(\alpha\text{-Zr})$	305	1.7×10^{-6}	7.0×10^{-4}	7,060	129
		350	2.0×10^{-6}			
		410	3.7×10^{-6}			
		446	5.2×10^{-6}			
		486	6.9×10^{-6}			
		567	9.7×10^{-6}			
		610	13.0×10^{-6}			
H	(Zircaloy-2)	400	6×10^{-6}	2.7×10^{-3}	8,380	191
		500	10×10^{-6}			
		600	16×10^{-6}			
		261	0.8×10^{-6}			
		315	1.7×10^{-6}			
		358	2.94×10^{-6}			
		408	4.71×10^{-6}			
		458	5.49×10^{-6}			
		515	10.3×10^{-6}			
		560	15.8×10^{-6}			
N	$(\beta\text{-Zr})$	920	5.5×10^{-8}	1.5×10^{-2}	30,700	132
		1085	1.5×10^{-7}			
		1195	3.4×10^{-7}			
		1305	7.7×10^{-7}			
		1475	2.5×10^{-6}			
		1640	5.1×10^{-6}			

(Cont'd. on next page)

Table 57 (Cont'd.)

Diffusing Element	Composition Range (wt. %)	Temp. (°C)	D (cm^2/sec)	D_o (cm^2/sec)	Q (cal/mole)	References
N	(β-Zr)	900	1×10^{-8}	3×10^{-2}	33,600	133
		1100	2.7×10^{-7}			
		1300	6×10^{-7}			
		1600	2.7×10^{-6}			
O	(α-Zr)	600-825		3.5×10^{-2}	33,800	134
					39,200	131
	(α-Zr)	400	1.34×10^{-16}	9.4	51,780	135
		482	1.21×10^{-14}			
		510	2.79×10^{-14}			
		542	1.38×10^{-13}			
		585	5.62×10^{-13}			
	(β-Zr)	1000-1500		0.196	41,000	136
		1000-1500		0.0453	28,200	136
		1280	5.25×10^{-6}			137
	(α-Zr)	200-425		5.3×10^{-8}	18,200	131
	99.92	800-970		1×10^{-5}	26,700	138
Ti		825-1150			23,000	139
U	90	950-1075		9.5×10^{-4}	32,000	140
	80			1.3×10^{-4}	28,600	
	70			3.5×10^{-5}	26,300	
	60			4.0×10^{-5}	27,400	
	50			8.0×10^{-5}	29,700	
	40			6.3×10^{-5}	29,700	
	30			5.5×10^{-5}	29,700	
	20			3.2×10^{-4}	34,300	
	10			7.8×10^{-3}	41,000	
	5			8.7×10^{-2}	47,000	

(Cont'd. on next page)

Table 57 (Cont'd.)

Diffusing Element	Composition Range (wt. %)	Temp. (°C)	D^D (cm ² /sec)	$D_{O_2}^D$ (cm ² /sec)	Q (cal/mole)	References
Liquid U		1270	1.9×10^{-4}			141
W		1727	3.24×10^{-9}	1.1	78,000	11

IV. GROUP III

A. Diffusion in Vanadium

1. Self-diffusion

The self-diffusion of vanadium has not been measured; however, estimates may be made on the basis of the relationships of LeClaire⁽⁵⁸⁾ and Nachtrieb and Handler.⁽⁵⁹⁾

From LeClaire's empirical formula,⁽⁵⁸⁾ the activation energy for self-diffusion in vanadium is calculated as $Q = 82,500$ cal/mole. From the plot of activation energy for self-diffusion vs melting point shown in Fig. 8, Q may be estimated as $Q = 81,500$ cal/mole.

Nachtrieb and Handler's⁽⁵⁹⁾ equation, using Kelley's value of $\Delta H_f = 5,050$ cal/mole, give $Q = 83,300$ cal/mole.

2. Interstitial Diffusion

a. Vanadium-Carbon

Powers and Doyle⁽¹⁴²⁾ carried out internal friction and elastic after-effect measurements in the temperature range of 60 to 160°C on carbon doped vanadium samples and obtained the relation:

$$D = 0.0047 \pm 0.0006 \exp [-(27,300 \pm 100)/RT].$$

The data looks extremely good as reflected in the authors estimate of their error.

A year later the same authors⁽⁴⁸⁾ reported similar values obtained by the same techniques. This data fitted the equation:

$$D = 0.0045 \pm 0.0005 \exp [-(27,290 \pm 80)/RT].$$

The log of the relaxation time vs $1/T^\circ K$ for this data is plotted in Fig. 4.

b. Vanadium-Nitrogen

An early report by Powers⁽¹⁴³⁾ described internal friction measurements made at 254.2, 263.8, and 279.2°C using the torsion pendulum. A peak due to diffusion of nitrogen in vanadium was found at 272°C for a frequency of 1 cps. The activation energy is given as $Q = 34,100$ cal/mole.

Stanley and Wert⁽¹⁴⁴⁾ determined the diffusion of nitrogen in vanadium from internal friction measurements with the torsion pendulum at frequencies

of 1.2 to 0.7 cps. Their data may be represented by the equation:

$$D = 0.018 \exp (-35,100/RT).$$

At higher nitrogen concentrations, a nitrogen-nitrogen interaction peak becomes apparent which may lead to spurious results.

The more recent measurements of Powers and Doyle⁽⁴⁸⁾ were obtained from internal friction, elastic after-effects, and peak breadth measurements over the temperature range of 140 to 270°C. The values obtained are presented below.

Table 58

Vanadium-Nitrogen Diffusion Data of Powers and Doyle⁽⁴⁸⁾

Method of Measurement	D_0 (cm ² /sec)	Q (cal/mole)
Internal friction	0.016 ± 0.016	34,600 ± 900
Elastic after-effects	0.0090 ± 0.0022	34,000 ± 200
Combined	0.0092 ± 0.0021	34,060 ± 220
Peak breadth		34,200 ± 300

The log of the relaxation time vs 1/T°K for this data is plotted in Fig. 4. The data is extremely good and is probably the most reliable for diffusion of nitrogen in vanadium.

The theoretical values calculated by Ferro⁽⁴⁹⁾ for diffusion of nitrogen in vanadium is given by:

$$D = 0.038 \exp (-22,000/RT).$$

The agreement of Ferro's theoretical values with the very reliable experimental values is not as good in this system as it was for previous systems found in this paper.

c. Vanadium-Oxygen

Early data of Powers⁽¹⁴³⁾ on diffusion of oxygen in vanadium, obtained with the torsion pendulum at temperatures of 172.4, 180.5, and 193.4°C gave the activation energy as Q = 28,600 cal/mole.

Powers and Doyle⁽¹⁴²⁾ examined diffusion in the vanadium-oxygen system by use of internal friction and elastic after-effect measurements using the torsion pendulum in the temperature range of 72 to 190°C. The data may be represented by the equation:

$$D = 0.019 \pm 0.002 \exp [-(29,300 \pm 100)/RT].$$

The high degree of accuracy of this work may be seen in the small errors reported in the above equation.

Stanley and Wert⁽¹⁴⁴⁾ also obtained a diffusion coefficient using internal friction measurements performed with the torsion pendulum in the frequency range of 0.7 to 1.2 cps. Their data is described by the equation:

$$D = 0.003 \exp (-28,200/RT).$$

The most recent measurements of Powers and Doyle⁽⁴⁸⁾ were carried out over the temperature range of 72 to 190°C using internal friction and elastic after-effect relationships. The data is listed in Table 59.

Table 59

Diffusion Coefficients for the Diffusion of Oxygen
in Vanadium as Determined by Internal
Friction Measurements⁽⁴⁸⁾

Method of Measurement	D_0 (cm ² /sec)	Q (cal/mole)
Internal friction	0.026 ± 0.010	$29,600 \pm 300$
Elastic after-effects	0.011 ± 0.004	$28,900 \pm 300$
Combined	0.0130 ± 0.0032	$29,010 \pm 190$

The plot of the log of the relaxation times vs $1/T^{\circ}K$ for this data is shown in Fig. 4. The high degree of accuracy of the work published in this reference has been stressed previously.

Ferro's theoretical values of $D_0 = 0.018$ and $Q = 19,000$ cal/mole are in rather poor agreement with the experimental results for this system.

3. Substitutional Diffusion

a. Vanadium-Iron

Stanley and Wert⁽¹⁸⁶⁾ determined the diffusion constants in an alloy of iron and 18% vanadium over a wide temperature range by a combination of radioactive tracer and internal friction measurements. Measurements were made over a considerable temperature range on both sides of the Curie temperature. In the paramagnetic region, the diffusion results may be described by the equations:

$$D_{(Fe^{59})} = 7 \exp (-61,700/RT)$$

$$D_{(V^{48})} = 4 \exp (-58,500/RT).$$

Below the Curie temperature, the internal friction data showed that diffusion was 100 times slower than the above two equations would indicate. Part of the effect is due to a change in the activation energy and part due to the change in D_0 . This same effect of a change in the diffusion coefficient at the Curie temperature has been observed in the diffusion of Ni^{63} into pure iron⁽¹⁸⁷⁾ and in the self-diffusion in iron.⁽¹⁸⁸⁾

b. Vanadium-Titanium

Diffusion between pure titanium and two different titanium-vanadium alloys, 15 weight percent vanadium and 7.5 weight percent vanadium, was investigated by Goold.⁽¹⁰⁶⁾ Samples were diffused at temperatures in the range 900 to 1248°C. The samples were then sectioned and chemically analyzed, and diffusion coefficients were determined as a function of concentration by means of the Matano analysis. ThO_2 markers were included in some samples in order to determine the intrinsic diffusion coefficients. D as a function of atomic percent vanadium is shown in Fig. 35. For 2 atomic percent vanadium, D is given by the equation:

$$D = 6.0 \times 10^{-3} \exp [-(39,600 \pm 4,700)/RT].$$

At 1250°C, the intrinsic diffusion coefficients for 96.5 atomic percent titanium are:

$$D_{Ti} = 1.31 \times 10^{-9}$$

$$D_V = 14.9 \times 10^{-9}$$

A summary of diffusion in vanadium is given in Table 60.

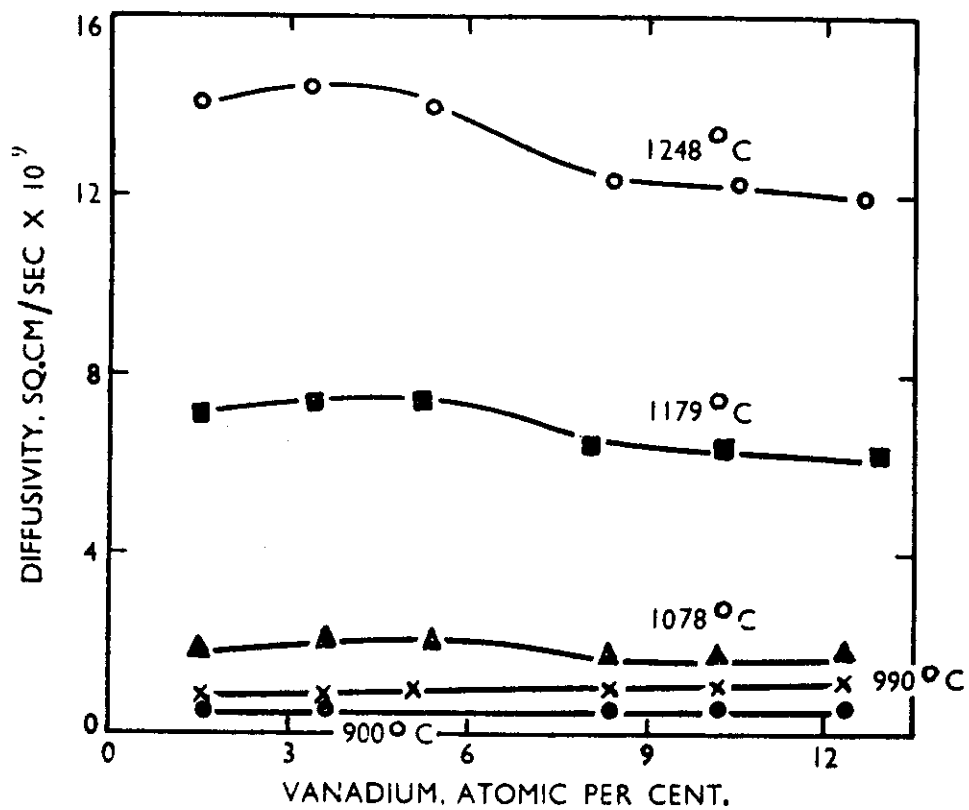


Fig. 35 - Variation of the interdiffusion coefficient with composition for the vanadium-titanium system.(106)

Table 60

Summary of Diffusion Data for Vanadium

Diffusing Element	Composition Range (wt. %)	Temp. (°C)	D^D (cm ² /sec)	D_0 (cm ² /sec)	Q (cal/mole)	References
V (self)	Estimate from melting point Estimate from heat of fusion				82,500 81,500 83,300	
C		60-160		0.0047 0.0045	27,300 27,290	142 48
N		254-279 140-270		0.018 0.0092	34,100 35,100 34,060	143 144 48
O		172-193 72-190 72-190		0.019 0.003 0.0130	28,600 29,300 28,200 29,010	143 142 144 48
Ti (intrinsic)	85-100 96.5	900-1248 1250	$Ti = 1.31 \times 10^{-9}$ $V = 14.9 \times 10^{-9}$	6×10^{-3}	39,600	106
⁵⁹ Fe	82% Fe			7	61,700	186
⁴⁸ V	82% Fe			4	58,500	186

B. Diffusion in Chromium

1. Self-diffusion

Paxton and Gondolf⁽¹⁴⁵⁾ measured the self-diffusion coefficient for chromium in the temperature range of 950 to 1250°C by vacuum-condensation deposition of Cr⁵¹ on pure chromium discs. Self-diffusion coefficients were evaluated by surface activity before and after annealing and by progressive grinding, fresh surfaces were exposed on which activity measurements were made. The data may be represented by the equation:

$$D = 0.0001 \exp (-52,700/RT).$$

Both the D_0 and the Q values are much lower than one would expect for a vacancy diffusion process. Pound, Bitler, and Paxton⁽¹⁴⁶⁾ have proposed that the ring mechanism^(147,148) is the operating mechanism for self-diffusion in chromium. [Rothman, Lloyd, and Harkness⁽¹⁴⁹⁾ have also suggested that the ring mechanism is operating in self-diffusion in gamma uranium. Excessively low values of D_0 and Q have been obtained for self-diffusion in gamma uranium by three different investigations in three different countries,^(149,150,151) all of their results agreeing within experimental error.] Hence, the often doubted ring mechanism is beginning to receive experimental support. Although the activation energies to be expected for the ring mechanism have not been calculated for chromium or uranium, D_0 values have been calculated on the basis of this mechanism. These calculated values agree qualitatively with the experimental values obtained for self-diffusion in gamma uranium.⁽¹⁴⁹⁾

2. Interstitial Diffusion

a. Chromium-Boron

Samsonov and Solonnikova,⁽³⁴⁾ using the technique described under the tungsten-boron system (page 3) have determined the "diffusion coefficient" of boron in chromium from the measured rates of growth of the CrB₂ phase. The only data reported is the activation energy $Q = 20,520$ cal/mole. Although no data points are given from which to judge the validity of this work, previous comparison of data reported in this reference with data from more reliable techniques has shown that this data is of questionable value for diffusion purposes.

b. Chromium-Carbon

Samsonov and Solonnikova⁽³⁴⁾ have also measured the diffusion of carbon into chromium. An activation energy of $Q = 26,000$ cal/mole is stated for this process. The comments made on the chromium-boron system concerning the usefulness of this data as diffusion data also apply to this system.

3. Substitutional Diffusion

a. Chromium-Cobalt

Weeton⁽¹⁵²⁾ measured the diffusion of chromium in alpha-cobalt-chromium alloys over the composition range of 0 to 35 weight percent chromium by pressure bonding alloys of different composition and diffusing them in the temperature range of 1000 to 1360°C. The temperature of diffusion and the composition of the different diffusion couples is given in Table 61.

Table 61

Chromium Concentration of Chromium-Cobalt
Diffusion Specimens⁽¹⁵²⁾

Temp. (°C)	1360		1300		1150		1000	
	C ₁	C ₂	C ₁	C ₂	C ₁	C ₂	C ₁	C ₂
Intital composition (% Cr)	0	22.20	0	28.00	13.15	38.65	0	24.92
	9.6	28.06	9.60	41.15	0	28.06	9.80	39.97
	0	28.00	9.98	39.20				
			0	28.15				

C₁ = Chromium content of low chromium side.

C₂ = Chromium content of high chromium side.

Sections were machined off and chemically analyzed. The diffusion coefficient was found to be constant within a factor of two over the composition range investigated, hence, the Grube analysis was used. The values were found to fit the equation:

$$D = 0.443 \exp (-63,600/RT).$$

The data points in the log D vs 1/T plot have more than a normal amount of scatter. This may well be due to the various compositions studied in this reference.

Gruzin and Noskow⁽¹⁵³⁾ examined the diffusion of Co⁶⁰ into various cobalt-chromium and cobalt-nickel-chromium alloys. A Co⁶⁰ layer, 0.005-mm thick, was electrolytically deposited onto thin discs of the alloys and diffused in the temperature range of 1100 to 1350°C. Two to four measurements were made at each temperature. The results are shown in Table 62.

Table 62

Diffusion of Co⁶⁰ in Cobalt-Chromium and Cobalt-Nickel-Chromium Alloys⁽¹⁵³⁾

Temp. (°C)	D x 10 ¹¹ (cm ² /sec)			
	Co-Cr (4% Cr)	Co-Cr (7% Cr)	Co-Ni-Cr (26% Ni - 9% Cr)	Co-Ni-Cr (26% Ni - 18% Cr)
1100	2.7	1.7	2.1	2.5
1120	3.2	3.8		
1150		3.1	4.7	4.9
1160	5.2	6.8	7.1	
1200	9.7	9.4	12.2	11.7
1220	15.0	24.0	22.2	
1250	21.5	24.0	23.5	29.5
1280	36.0	47.0	51.0	
1300	33.5	38.8	36.8	40.0
1320	58.0		62.0	
1350	80.8	135.0	20.0	

The D₀ and Q values obtained from this data are shown in Table 63.

Table 63

Frequency Factor and Activation Energy for Diffusion of Co⁶⁰ in Cobalt-Chromium and Cobalt-Nickel-Chromium Alloys⁽¹⁵³⁾

Composition		D (cm ² /sec)	Q (cal/mole)
Co-Cr	4% Cr	0.67	65,800
Co-Cr	7% Cr	56.3	79,300
Co-Ni-Cr	26% Ni - 9% Cr	6.3	72,100
Co-Ni-Cr	26% Ni - 18% Cr	0.4	64,200

Below 1160°C a great deal of grain boundary diffusion was observed. The Fisher⁽¹⁵⁴⁾ analysis was used to obtain the grain boundary diffusion data shown in Table 64. The grain boundary width was taken as one lattice spacing.

Table 64
Grain-Boundary Diffusion of Co⁶⁰ in Cobalt-Chromium and
Cobalt-Nickel-Chromium Alloys⁽¹⁵³⁾

Temp. (°C)	D _{G.B.} x 10 ⁸ (cm ² /sec)		
	Co-Cr (4% Cr)	Co-Cr (7% Cr)	Co-Ni-Cr (26% Ni - 9% Cr)
980	8.3	7.5	4.9
1040	69	64	14
1100	160	160	57
1160	400	650	170
Q (cal/mole)			
	55,000	74,000	67,000

The data appears to be very good and quite complete. No mention was made as to the sectioning or counting procedures. However, in the past Gruzin has preferred to measure the activity of the surface of the specimen after various diffusion times.

b. Chromium-Iron

The early data by Hicks⁽¹⁵⁵⁾ and Bardenheuer and Muller⁽¹⁵⁶⁾ is very incomplete. More recent data, by Ueda⁽¹⁵⁷⁾ and Gruzin,^(24,158) is much more precise and complete.

In the work of Hicks⁽¹⁵⁵⁾ electrolytic iron specimens were packed in chromium powder and heated at 1200°C in vacuum. The concentration vs distances curves were determined by measuring the lattice spacings by x-ray diffraction after the removal of known layer thicknesses. He found that

$$D = (1.7-8.1) \times 10^{-9} \text{ at } 1200^{\circ}\text{C}.$$

Bardenheuer and Muller⁽¹⁵⁶⁾ measured the diffusion between pure chromium and pure iron at 1150 and 1350°C. The samples were sectioned and chemically

analyzed. No measurements were made as to the variation of the diffusion coefficient with changing composition. The data is listed in Table 65.

Table 65

Chromium-Iron Diffusion Data for 1150 and 1350°C⁽¹⁵⁶⁾

Temp. (°C)	D (cm ² /sec)
1150	6.8×10^{-10}
1350	$2.2-5.3 \times 10^{-8}$

Taking an average value of $D = 3.2 \times 10^{-8}$ cm²/sec at 1350°C, this data may be shown to fit the equation:

$$D = 218 \exp (-69,500/RT).$$

With measurements at only two temperatures, the activation energy and D_0 values are very uncertain.

Ueda⁽¹⁵⁷⁾ measured the diffusion of chromium in iron by plating chromium onto iron wires and measuring the growth of the plated layer as a function of time and temperature. The following analysis was used to determine the diffusion coefficient:

$$1 - \frac{C_x}{C_0} = \frac{2}{\sqrt{\pi}} \int_0^{\frac{x}{2\sqrt{Dt}}} e^{-y^2} dy,$$

which gives $x^2 = 4A Dt$, where A depends on $\frac{C_x}{C_0}$. Taking the solubility limit as $C_x = 14\%$ and $C_0 = 100/2 = 50\%$, then $A = 0.584$. From measured penetrations (x) at given times (t) the following values of D , listed in Table 66, were determined. A $\log D$ vs $1/T$ plot of this data is shown in Fig. 36. The curve shows very little scatter in the data points. The activation energy is reported as $Q = 61,800$ cal/mole from which one may calculate the relation:

$$D = 127 \exp (-61,800/RT).$$

Contrails

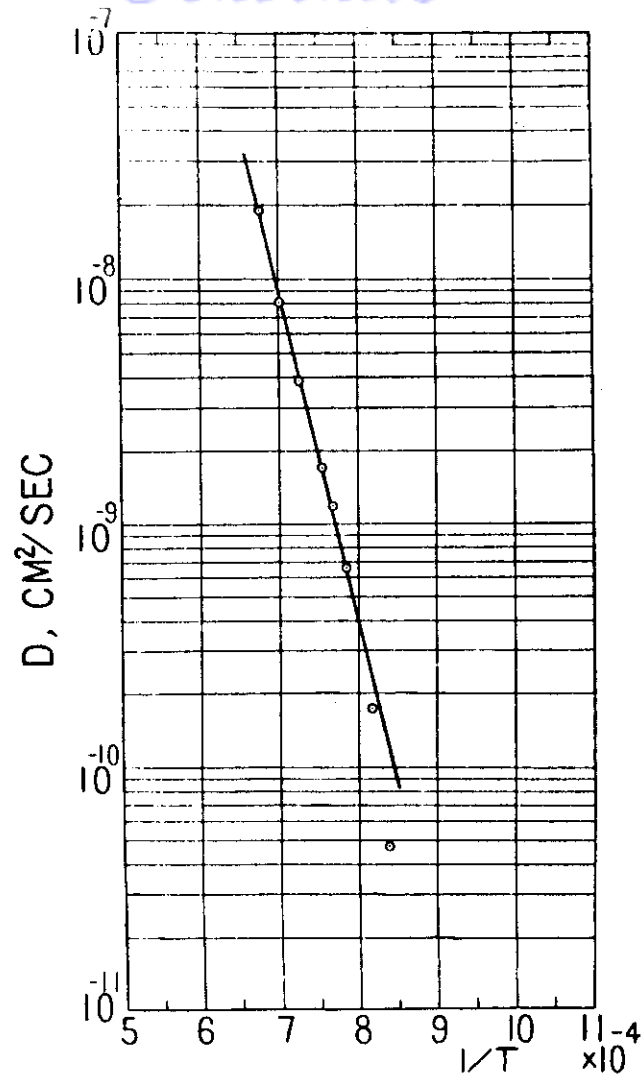


Fig. 36 - Influence of temperature on the interdiffusion coefficient of chromium in iron.(157)

Diffusion in the Chromium-Iron System ⁽¹⁵⁷⁾

Temp. (°C)	D (cm ² /sec)	Temp. (°C)	D (cm ² /sec)
920	1.3×10^{-10}	1050	1.6×10^{-9}
950	2.4×10^{-10}	1100	4.0×10^{-9}
1000	6.6×10^{-10}	1150	8.6×10^{-9}
1030	1.1×10^{-9}	1200	1.9×10^{-8}

This data represents an average diffusion coefficient over the concentration range of 0 to 14% chromium. No calculations can be made from such data as to the variation of the diffusion coefficient with composition.

Gruzin ⁽²⁴⁾ studied the diffusion of Cr ⁵¹ into alpha-iron, gamma-iron, and a 0.82% carbon steel. The diffusion anneals were carried out in the temperature range of 750 to 1250°C. The data is shown in Table 67.

Table 67

Data on the Diffusion of Cr ⁵¹ into Iron and Steel ⁽²⁴⁾

Temp. (°C)	D x 10 ¹² (cm ² /sec)	
	Iron	0.82% C steel
750	0.5	1.4
800	4.9	2.0
850	19.0	---
875	---	5.7
900	14.0	---
950	24.0	13
1000	44	18
1050	58	33
1100	23	39
1150	90	67
1200	130	190
1250	870	370

These values may be described by the following equations:

$$D_{\alpha\text{Fe}} = 3 \times 10^4 \exp (-82,000/RT)$$

$$D_{\gamma\text{Fe}} = 1.8 \times 10^4 \exp (-97,000/RT)$$

$$D_{\gamma\text{steel}} = 10 \exp (-75,000/RT).$$

The experimental points were obtained by reliable techniques and show a normal amount of scatter in the log D vs 1/T plots.

Gruzin⁽¹⁵⁸⁾ also measured the diffusion of an electrolytical deposited Fe⁵⁹ tracer into Fe - 3.98 wt. % Cr and Fe - 7.90 wt. % Cr alloys over the temperature range of 1100 to 1250°C. The alloy samples were melted and homogenized for 20 to 30 hours at 1100 to 1200°C. The diffusion coefficients were found to be as stated in Table 68.

Table 68
Data on the Diffusion of Fe⁵⁹ into Chromium-Iron
Alloys of 4% and 8% Chromium⁽¹⁵⁸⁾

Temp. (°C)	D (cm ² /sec)	
	8% Cr	4% Cr
1100	1.1 x 10 ⁻¹¹	3.3 x 10 ⁻¹¹
1150	2.2 x 10 ⁻¹¹	7.2 x 10 ⁻¹¹
1200	9.0 x 10 ⁻¹¹	1.5 x 10 ⁻¹⁰
1250	2.1 x 10 ⁻¹⁰	3.6 x 10 ⁻¹⁰

This data is shown in Fig. 37. The activation energy and D₀ values are given in Table 69. Gruzin believed that the activation energy should vary linearly with composition. Therefore, he felt that the lower value of Q for the 4% Cr alloys was due to hydrogen in the metal and accordingly made a correction for the hydrogen content which gave him a Q = 75,000 cal/mole. The hydrogen content for his alloy is not given nor does he describe the method for "correcting" for it.

The data in general is quite good as seen by the small amount of scatter in the data plotted in Fig. 37. However, the correction for the hydrogen content does not seem necessary nor valid.

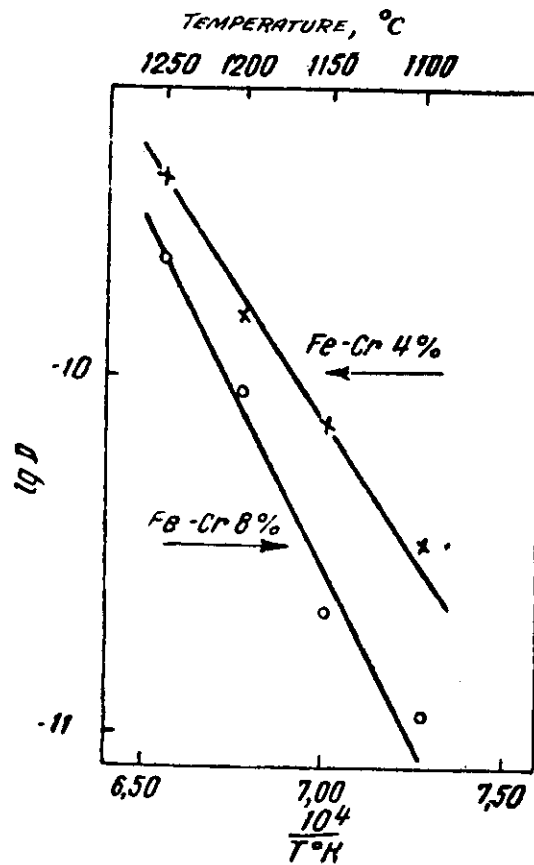


Fig. 37 - Log D vs $1/T$ for diffusion of Fe^{59} in Fe - 4% Cr and Fe - 8% Cr Alloys.(158)

Frequency Factor and Activation Energy for
Diffusion of Fe⁵⁹ in Several
Iron-Chromium Alloys (158)

Composition	Q (cal/mole)	D (cm ² /sec)
Fe - 8% Cr	90,000	600
Fe - 4% Cr	69,000	4
Pure Fe (Ref. 84)	68,000	0.7
Fe - 4% Cr (corrected for H ₂ content)	75,000	20.0

c. Chromium-Silicon

Samsonov and Solonnikova⁽³⁴⁾ using their previously described method (page 3) determined the "diffusion coefficient" of silicon in chromium from the measured rates of growth of the CrSi₂ phase. The only data reported is the activation energy Q = 10,250 cal/mole. This value seems to be extremely low when compared to the activation energy for diffusion in any of the other chromium systems. The doubtful validity of the data given in this reference for use as diffusion data has been expanded upon earlier.

d. Chromium-Titanium

Mortlock and Tomlin⁽¹⁵⁹⁾ evaporated Cr⁵¹ onto discs of a Ti - 18% Cr alloy. These discs were then put together so that the Cr⁵¹ formed the middle layer of a sandwich arrangement, the samples were diffused at 1000 and 1047°C. Autoradiographs were taken and measured with a high resolution scanning microphotometer. The log of the photographic density was plotted vs the square of the distance which yielded very fine straight lines. The results found are tabulated in Table 70. A further extension of this work was performed in a rather interesting way by Mortlock and Tomlin.⁽¹⁶⁰⁾ Cr⁵¹ was evaporated onto commercially pure titanium and diffused at 1055°C. The same sample was then analyzed by three different techniques. First, an autoradiograph was taken. Then, the sample was sectioned. After the removal of each section, the activity at the end of each sample was counted. The machined sections were also dissolved and their activity counted. A comparison of the three techniques can be noted in the following data. The agreement is surprisingly good between the three techniques.

Table 70

Diffusion Data for the Diffusion of Cr⁵¹ into an Alloy of Ti - 18% Cr⁽¹⁵⁹⁾

Temp. (°C)	D x 10 ⁹ (cm ² /sec)
1000	2.0
1000	2.0
1000	2.2
1000	1.8
1047	3.9

Table 71

Data on the Diffusion of Cr⁵¹ into Pure Titanium⁽¹⁶⁰⁾

Method	D at 1055°C (cm ² /sec)
Autoradiographic	7.4 x 10 ⁻⁹
Counting transverse sections	7.8 x 10 ⁻⁹
Counting dissolved layers	7.0 x 10 ⁻⁹

More recently, Mortlock and Tomlin⁽¹⁸⁹⁾ have extended their autoradiographic technique to a range of temperatures for several different titanium-chromium alloys. Cr⁵¹ was vacuum deposited onto finely ground end faces of samples 1 cm in diameter and 0.5 cm in length. The samples were clamped together in a sandwich arrangement with the active faces in the middle. Diffusion anneals were made at temperatures in the range 926 to 1178°C on samples of iodide titanium, commercial titanium, Ti + 10% Cr alloy, and Ti + 18% Cr alloy. The concentration-penetration curves for the chromium tracer were determined from autoradiographs after correction for the gamma-rays emitted along with the beta-particles by Cr⁵¹. The results may be expressed as follows.

Table 72

Frequency Factor and Activation Energy for Diffusion
of Cr⁵¹ into Pure Titanium and Several
Chromium-Titanium Alloys (189)

Solvent Metal	D_0 (cm ² /sec)	Q (cal/mole)
Commercial Ti	0.005	35,300 ± 2,700
Iodide Ti	0.010	37,700 ± 2,200
Ti + 10% Cr	0.02	40,200 ± 3,900
Ti + 18% Cr	0.09	44,500 ± 1,600

The fine accuracy of this work is reflected in the small errors reported for the activation energies.

e. Chromium-Uranium

Mosse, Levy and Adda⁽¹⁹³⁾ reported diffusion measurements in dilute alloys of chromium in gamma-uranium in the temperature range 900 to 1000°C. A dilute uranium-chromium alloy was bonded to pure uranium and diffused at a temperature such that the alloy was in the two-phase field of gamma plus liquid. By measuring the movement of the interface of the gamma plus liquid-gamma boundary, the diffusion coefficient was determined. A knowledge of the solidus composition at the temperature of diffusion was also necessary. The data may be seen in Table 73.

Table 73

Data on the Diffusion of Chromium in Uranium
at Low Chromium Concentrations

Temp. (°C)	D (cm ² /sec)
900	3.1 x 10 ⁻⁷
925	5.0 x 10 ⁻⁷
950	6.7 x 10 ⁻⁷
975	8.0 x 10 ⁻⁷
1000	9.4 x 10 ⁻⁷

These values fit the equation:

$$D = 0.7 \exp (-34,000/RT).$$

A summary of diffusion in chromium is given in Table 74.

C. Diffusion in Titanium

1. Self-diffusion

Because of the lack of a suitable radioisotope, self-diffusion in titanium has not been measured experimentally. Estimates of the activation energy for self-diffusion in titanium can be made from measurements of the heat of fusion, the melting point, and the air contamination of commercial titanium.

From the relation of LeClaire,⁽⁵⁸⁾ $Q = 38 T_m$, the activation energy for self-diffusion in titanium is $Q = 73,600$ cal/mole. From the plot of activation energy for self-diffusion vs melting point shown in Fig. 8, Q is estimated as $Q = 72,200$ cal/mole.

Nachtrieb and Handler's formula,⁽⁵⁹⁾ $Q = 16.5 \Delta H_f$, and Kelley's data of $\Delta H_f = 4,460$ cal/mole yields an estimated value for Q as $Q = 73,600$ cal/mole.

Although the values reported for ΔH_f and T_m were measured for beta-titanium, Kaufman calculated a melting temperature of 1670°C for alpha-titanium which is practically the same as the accepted value of 1667°C for beta-titanium. Hence, the activation energy for self-diffusion in titanium would be expected to be about the same for the two phases of titanium.

Reynolds, Ogden, and Jaffee⁽¹⁶¹⁾ found the activation energy for air contamination of commercial titanium to be $Q = 75,300$ cal/mole. In order to explain this high activation energy, they proposed a mechanism requiring counter current diffusion of titanium atoms and oxygen atoms, in which self-diffusion of titanium created vacancies that would aid the diffusion of oxygen. This explanation appears more feasible than postulating interstitial mechanism. If this model is true, then this observed activation energy should be in good agreement with the activation energy for self-diffusion in titanium. The agreement with the above empirical estimates is quite good.

Since high temperature creep is usually diffusion controlled, and on many occasions the activation energies for the two processes have been observed to be identical,⁽¹⁶²⁾ such a comparison would be interesting. Orr, Sherby, and Dorn⁽⁵⁷⁾ have calculated the activation energy for high temperature creep of titanium from the experimental data of Cuff and Grant.⁽¹⁶³⁾ They found $Q = 60,000$ cal/mole which is somewhat smaller than the above estimates of the activation energy for self-diffusion in titanium.

Table 74

Summary of Diffusion Data for Chromium

Diffusing Element	Composition Range (wt. %)	Temp. (°C)	D (cm ² /sec)	D_0 (cm ² /sec)	Q (cal/mole)	References
Cr (self)		950-1250		0.0001	52,700	145
B	17				20,520	34
C	13				26,000	34
Co	65-100	1000-1360		0.443	63,600	152
⁶⁰ Co tracer	93 96	1100-1350 1100-1360		56.3 0.67	79,300 65,800	153
Co-Ni	26 Ni, 9 Cr 26 Ni, 18 Cr	1100-1350 1100-1350		6.3 0.4	72,100 64,200	153
γFe		1200	$1.7-8.1 \times 10^{-9}$			155
	0-100	1150 1350	6.8×10^{-10} $2.2-5.3 \times 10^{-8}$	218	69,500	156
				127	61,800	157
⁵¹ Cr tracer	100% αFe 100% γFe	750-900 950-1250		3×10^4 1.8×10^4	82,000 97,000	124
	99.18% Fe 0.82% C	950-1250		10	75,000	124
⁵⁹ Fe tracer	96 92	1100-1250		4 600	69,000 90,000	158
Si	52				10,250	34
Ti	82	1000 1047	2×10^{-9} 3.9×10^{-9}			159

(Cont'd. on next page)

Table 74 (Cont'd.)

Diffusing Element	Composition Range (wt.%)	Temp. (°C)	D (cm^2/sec)	D_0 (cm^2/sec)	Q (cal/mole)	References
Cr^{51} tracer	100% Ti	1055	7.4×10^{-9}			160
	100% Ti	926-1178		0.010	37,700	189
	Ti + 10% Cr			0.02	40,200	
	Ti + 18% Cr			0.09	44,500	
U	98	900	3.1×10^{-7}	0.7	34,000	193
		925	5.0×10^{-7}			
		950	6.7×10^{-7}			
		975	8.0×10^{-7}			
		1000	9.4×10^{-7}			

2. Interstitial Diffusion

a. Titanium-Boron

Samsonov and Latysheva,^(8,9) using the technique described under the tungsten-boron system (page 3), determined the "diffusion coefficient" of boron in titanium from the measured rates of growth of the TiB₂ phase. Their data fitted the equation:

$$D = 2.15 \times 10^4 \exp [-(9,150 \pm 2,800)/RT]$$

over the temperature range of 800 to 1200°C. The data is given in Table 75.

Table 75

Titanium-Boron Diffusion Data Using the
Samsonov and Latysheva Technique^(8,9)

Temp. (°C)	D (C - C ₂)	Q (cal/mole)	D ₀ (cm ² /sec)	C - C ₂ (g/cm ³)	D (cm ² /sec)
800	54.7000	9,150 ± 2,800	7,880 ± 1,230	0.333	2.15 x 10 ⁴ exp ($\frac{-9,150}{RT}$)
1000	112.4350				
1100	150.0640				
1200	178.6530				

b. Titanium-Carbon

Samsonov and Latysheva^(8,9) measured the growth of the TiC phase as a function of time over the temperature range of 800 to 1400°C. By applying the analysis described under the tungsten-boron system (page 3) they obtained:

$$D = 2.44 \times 10^3 \exp [-(17,500 \pm 5,670)/RT].$$

The data is shown in Table 76.

Wagner, Bucur, and Steinberg⁽¹⁶⁴⁾ determined the diffusion of carbon in titanium by a more reliable and standard procedure than that used by Refs. 8 and 9. Discs of high purity titanium (0.038% C) were pressure bonded to discs of carbon-titanium alloys containing 0.4 to 1.37% C. These carbon alloys consisted of two phases. The samples were annealed in the temperature range of 736 to 1150°C, sectioned and chemically analyzed. Three to six specimens were run

at each temperature. Over the composition range used, the diffusion coefficient was found to be constant. The mathematical analysis of C. Wagner⁽¹⁶⁵⁾ was used to determine the diffusion coefficient. The data is reported in Table 77.

Table 76

Titanium-Carbon Diffusion Data^(8,9)

Temp. (°C)	D (C - C ₂)	Q (cal/mole)	D ₀ (cm ² /sec)	C - C ₂ (g/cm ³)	D (cm ² /sec)
800	0	17,500 ± 5,670	1,060 ± 230	0.436	$2.44 \times 10^3 \exp \left(\frac{-17,500}{RT} \right)$
1000	3.2205				
1200	7.2885				
1300	11.3904				
1400	20.2270				

Table 77

Data on the Diffusion of Carbon in
Alpha and Beta-Titanium⁽¹⁶⁴⁾

Temp. (°C)	Average D at Each Temp. (cm ² /sec)	Ti Phase
736	2×10^{-9}	α
782	5×10^{-9}	α
835	1.3×10^{-8}	α
950	2.5×10^{-7}	β
1050	1.0×10^{-6}	β
1150	4.0×10^{-6}	β

These values may be expressed as:

for α-Ti

$$D = 5.06 \exp (-43,500/RT)$$

for β-Ti

$$D = 108 \exp (-48,400/RT).$$

c. Titanium-Hydrogen

Kusamichi, Yagi, Yukawa, and Noda^(166,167) determined the diffusion of hydrogen in titanium from measurements of the emission of hydrogen from commercially pure titanium. Rod-shaped titanium specimens were degassed in vacuum at 700, 750, 800, 850, and 900°C and the evolved hydrogen was collected and measured. From the data, the diffusion coefficient of hydrogen in alpha-titanium was calculated to be:

$$D = 0.27 \times 10^{-2} \exp (-14,200/RT).$$

Wasilewski and Kehl⁽¹⁶⁸⁾ have diffused hydrogen radially into cylinders of high purity titanium. Turnings were taken off the diameter and the concentration of hydrogen was determined. From the measured concentration gradients, the diffusion coefficients were evaluated, and were found to fit the equations:

for α -Ti

$$D = 1.8 \times 10^{-2} \exp (-12,380/RT)$$

for β -Ti

$$D = 1.95 \times 10^{-2} \exp (-6,640/RT).$$

This data appears to be very good and quite complete.

Koster, Bangert, and Evers⁽¹⁶⁹⁾ found an internal friction peak in quenched alpha-titanium which has a magnitude directly proportional to the hydrogen content. This peak was interpreted as due to the stress induced interstitial diffusion of hydrogen in the alpha solid solution. The peak has an activation energy of $Q = 15,000$ cal/mole which is in fair agreement with the values obtained for hydrogen in alpha-titanium in Refs. 166, 167, and 168.

For diffusion of hydrogen in an alloy of 4% Al, 4% Mn, and 92% Ti (C-130AM)⁻⁹ at room temperature, Daniels, Harmon, and Troiano⁽¹⁷⁰⁾ reported that $D = 1.9 \times 10^{-9}$ cm²/sec. This value falls between the extrapolated diffusion coefficients of Wasilewski and Kehl⁽¹⁶⁸⁾ for hydrogen diffusion in alpha and beta titanium.

The agreement on the diffusion coefficient of hydrogen in titanium among the different authors is quite good, with the data of Wasilewski and Kehl⁽¹⁶⁸⁾ probably being the most accurate.

d. Titanium-Nitrogen

Wasilewski and Kehl⁽¹⁷¹⁾ measured the diffusion of nitrogen in alpha-titanium, beta-titanium, and titanium nitride by diffusing nitrogen into 0.350-inch diameter rods of high purity titanium over the temperature range of 900 to 1570°C. Turnings were taken off the diameter and the concentration of

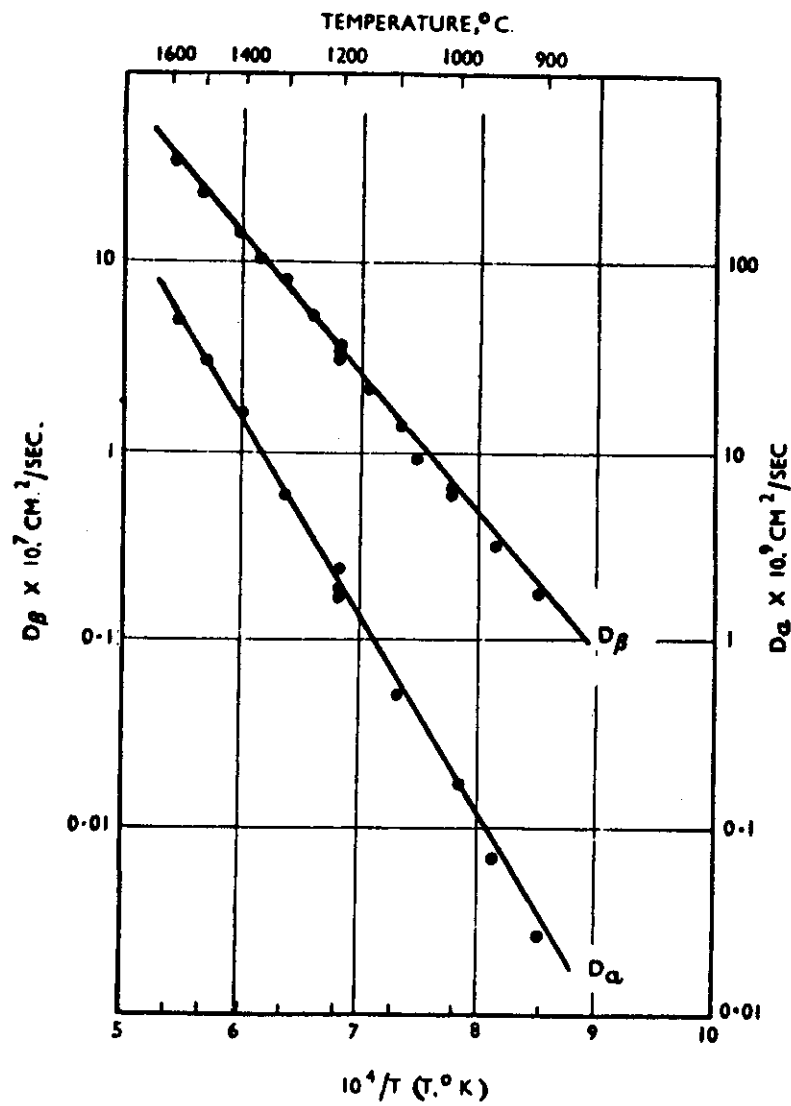


Fig. 38 - Temperature variation of the diffusion coefficient of nitrogen in alpha and beta-titanium. (171)

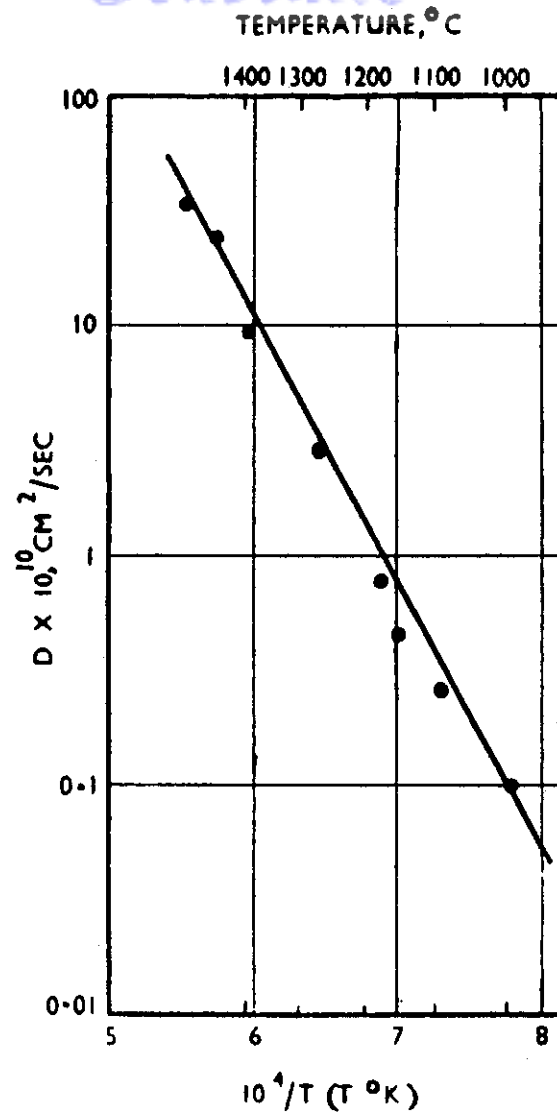


Fig. 39 - Temperature variation of the diffusion coefficient of nitrogen in titanium nitride.(171)

nitrogen determined. The diffusion coefficient was found to be independent of the concentration in each phase. The experimental points for the diffusion of nitrogen in alpha and beta titanium are given in a log D vs 1/T plot shown in Fig. 38. This data may be described by the equations:

$$D_{\alpha} = 1.2 \times 10^{-2} \exp [-(45,250 \pm 2,250)/RT]$$

$$D_{\beta} = 3.5 \times 10^{-2} \exp [-(33,800 \pm 1,400)/RT].$$

The diffusion of nitrogen in titanium nitride may be represented by the equation:

$$D = 5.4 \times 10^{-3} \exp [-(52,000 \pm 3,500)/RT].$$

This data is shown in Fig. 39.

These values were obtained by a reliable technique and may be considered quite accurate as demonstrated by the small amount of scatter in the data points as seen in Figs. 38 and 39.

Gulbransen and Andrew⁽¹⁷²⁾ measured the weight gained by a sample of commercially pure titanium heated in purified nitrogen. The measurements were made as a function of time and gas pressure over the temperature range of 550 to 850°C. The rate controlling mechanism followed a parabolic rate law and therefore was assumed to be a diffusion process which was evaluated as having an activation energy of $Q = 36,300$ cal/mole. This value is considerably smaller than the more reliable value for diffusion of $Q = 45,250$ cal/mole reported in Ref. 171.

e. Titanium-Oxygen

For the diffusion of oxygen in beta-titanium over the temperature range of 950 to 1414°C, Wasilewski and Kehl⁽¹⁷¹⁾ diffused oxygen into 0.350-inch diameter rods of high purity titanium. Sections were machined off the diameter of the specimen and chemically analyzed for oxygen. The diffusion coefficient was found to be constant over the investigated concentration range. Because of undue complications arising from surface layers of oxide, no diffusion coefficients were determined for oxygen diffusion in alpha-titanium. The data for oxygen diffusion in beta-titanium may be described by the equation:

$$D = 1.6 \exp [-(48,200 \pm 3,200)/RT].$$

This data is shown in a log D vs 1/T plot of Fig. 40. The fine accuracy of this work is demonstrated by the small amount of scatter in the data points as seen in Fig. 40.

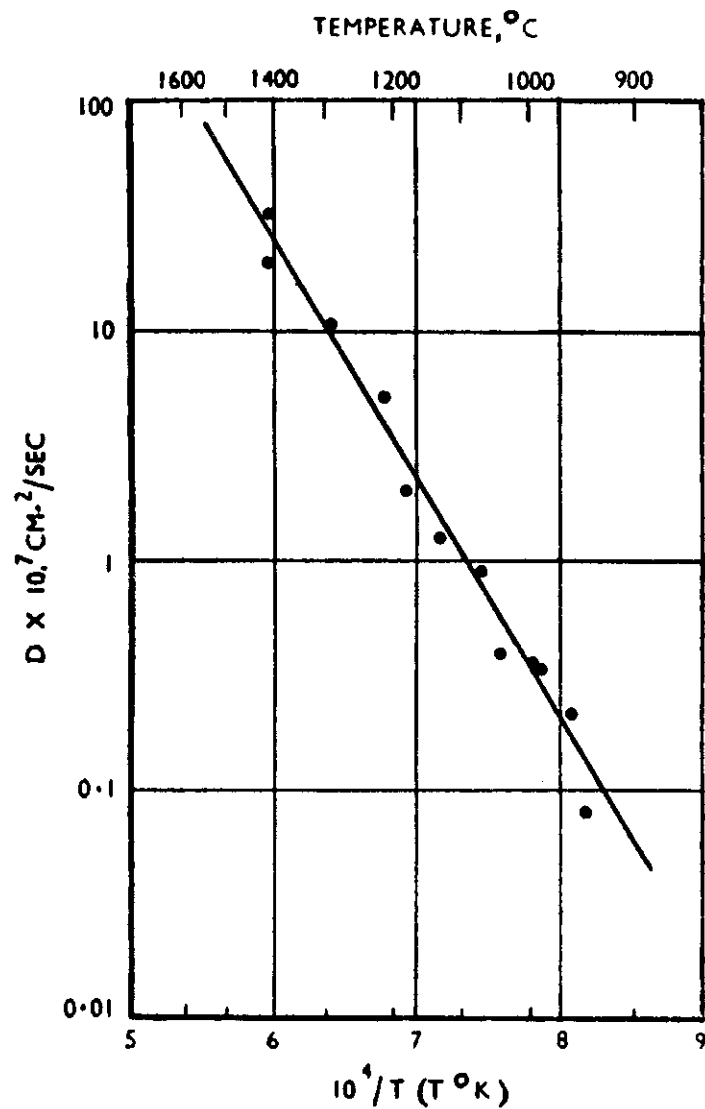


Fig. 40 - Temperature variation of the diffusion coefficient of oxygen in beta-titanium. (171)

Pratt, Bratina, and Chalmers⁽¹⁷³⁾ used a low-frequency torsion pendulum technique to study internal friction in alpha-titanium and in titanium-oxygen solid solutions containing up to 4.5 atomic percent oxygen. A relaxation peak was found with an activation energy of $Q = 48,000$ cal/mole. This peak has been attributed to the diffusion of oxygen in alpha-titanium. Using this value of Q , Reynolds and Jaffee⁽¹⁷⁴⁾ calculated $D_0 = 0.4$ cm²/sec from the Dushman-Langmuir equation.

Roe, Palmer, and Opie⁽¹⁷⁵⁾ obtained experimental values of the diffusion coefficient for diffusion of oxygen in titanium which are in sharp disagreement with the results of Refs. 171 and 173. Samples of titanium were cut from 1/4-inch diameter titanium 75A bar stock, polished and packed tightly in TiO₂ powder. These samples were heated for various times up to 117 hours at temperatures of 700 to 1150°C. Microhardness measurements were made across the diameter of a polished cross section of each of the diffused specimens. From these microhardness measurements, the concentration gradient was evaluated. The diffusion coefficients determined for the inward diffusion of oxygen were compared with measurements of outward diffusion obtained by submerging a piece of oxygen doped titanium in a bath of liquid calcium. The agreement between the two techniques is good although there is much more scatter in the data for outward diffusion than for inward diffusion.

The data may be represented by the equations:

for α -Ti

$$D = 5.08 \times 10^{-3} \exp (-33,500/RT)$$

for β -Ti

$$D = 3.14 \times 10^4 \exp (-68,700/RT).$$

This data is shown in Fig. 41.

A possible explanation of the excessively large activation energy for diffusion of oxygen in beta-titanium was proposed by Parr in the written discussion of Ref. 175. Parr suggested that since this value of $Q = 68,700$ cal/mole is very close to that which would be expected for self-diffusion in titanium; perhaps the oxygen atoms occupy substitutional sites and diffuse by a substitutional mechanism in the case of beta-titanium. In the case of alpha-titanium, the oxygen atoms may occupy interstitial sites and diffuse by an interstitial mechanism. This possibility is substantiated by the fact that the octahedral holes in alpha titanium are about 40% larger than the holes in the beta structure.

Although this data was obtained with good accuracy, as may be seen in the small amount of scatter in the inward diffusion data (Fig. 41), a large discrepancy exists between this data and the equally good data reported in Ref. 171. Since this work used less pure titanium than Ref. 171 (which was shown to be very important in the work of Gupta⁽¹⁷⁷⁾ et al. reported in the coming pages) and since diffusion of oxygen in TiO₂ may possibly be a controlling mechanism in this work, the use of the data of Wasilewski and Kehl is recommended.⁽¹⁷¹⁾

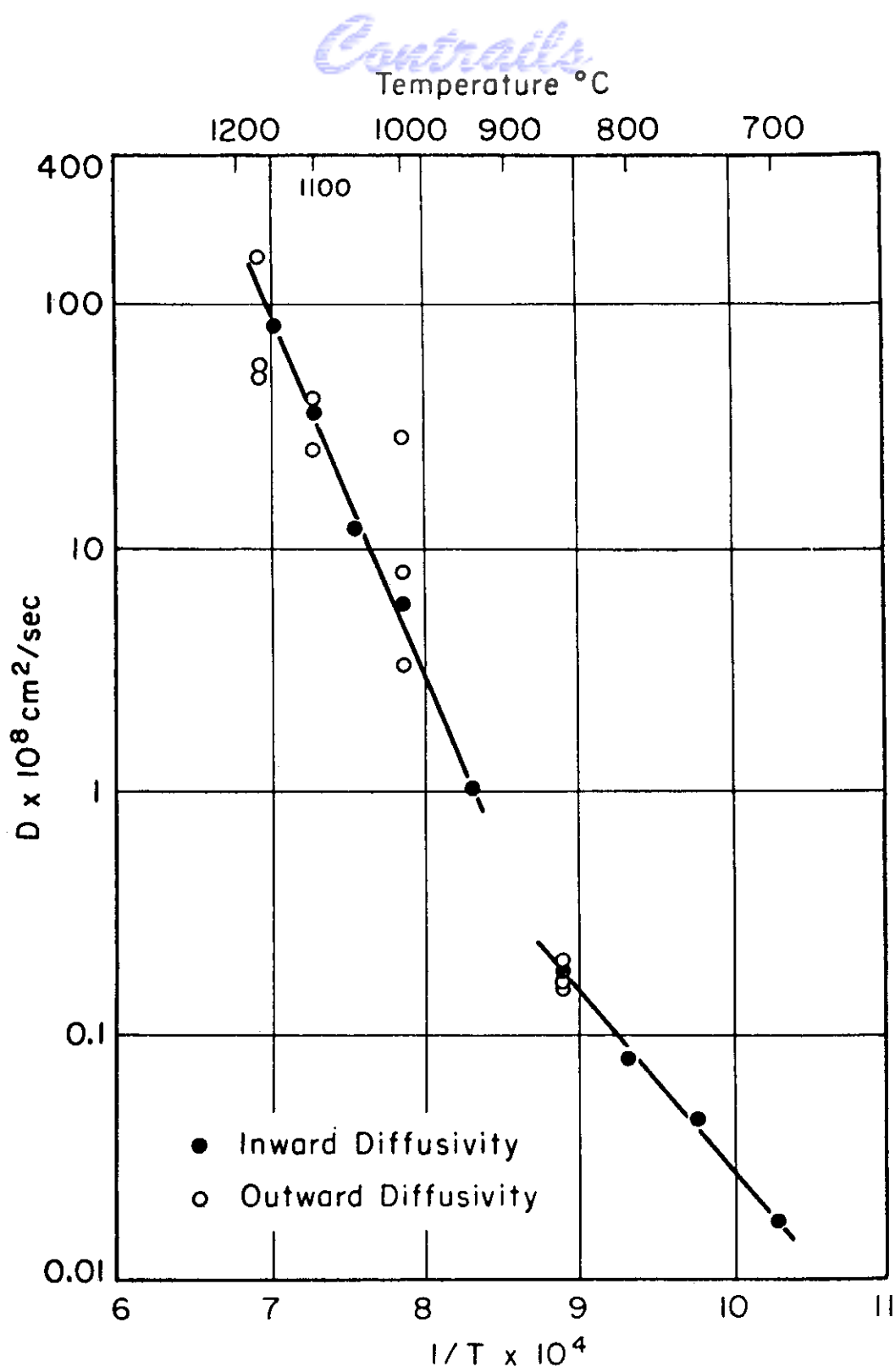


Fig. 41 - Diffusivity of oxygen in alpha and beta-titanium. (175)

Claisse and Koenig⁽¹⁷⁶⁾ measured the diffusion of oxygen into beta-titanium under the influence of an electric field. Specimens of 1/4-mm diameter wire were oxidized in a local area and then heated with a d.c. current passing through the specimen. The concentration gradient was determined at various time intervals by measuring the resistance of the wire over a 1/2-mm length at different positions along the wire. These measurements were made at six temperatures in the range 1127 to 1347°C. The results may be expressed by the equation:

$$D = 8.3 \times 10^{-2} \exp [-(31,200 \pm 2,000)/RT].$$

A negative excess of 0.4 electron units was found to be carried by the oxygen atoms. This data seriously disagrees with all of the previously reported diffusion data.

Gulbransen and Andrew's⁽¹⁷²⁾ data notoriously disagrees with the data of other investigators. They examined the weight gained by titanium samples of commercial purity (0.77% carbon) and by iodide titanium while heated in purified oxygen. Measurements were made at a gas pressure of 7.6 cm of Hg and in the temperature range of 250 to 600°C. Their data may be given by the relation:

$$D = 1 \times 10^{-6} \exp (-26,000/RT).$$

These authors have made similar investigations on many systems reported in this paper. Their work has always been conducted with extreme care and fine experimental procedure. However, their results seldom agree with diffusion data obtained by more reliable methods. This may lead to the conclusion that weight gain measurements are not governed solely by the diffusion mechanism.

f. Titanium-Oxygen-X

Large disagreements between different investigations, all of which are performed with great care and a high degree of finesse, are blamed on experimental error. The error in good experimental work, even in the field of diffusion, can seldom be blamed for much more than a small fraction of these large disagreements. Small quantities of a third element are often responsible for a large portion of these disagreements. This can be seen in the work of Gupta and Weinig.⁽¹⁷⁷⁾ They used internal-friction measurements to study the diffusion of oxygen in alpha-titanium containing various small additions of a third element. The data is listed in Table 78. This illustrates the fact that variations in the activation energy for diffusion of oxygen in alpha-titanium of 34,000 to 67,000 cal/mole may be produced by the addition of 0.10% of various third elements.

Table 78

Data on Oxygen Diffusion in Titanium Containing
Small Amounts of a Third Element⁽¹⁷⁷⁾

Solute (at. %)	Oxygen (at. %)	Q (cal/mole)
0.10 V	2.0	34,000
0.10 Zr	2.0	48,000
0.10 Al	2.0	39,000
0.10 Nb	2.0	39,000
0.06 Zr	2.0	67,000
0.10 Zr	2.0	48,000
0.50 Zr	2.0	--

3. Substitutional Diffusion

a. Titanium-Aluminum

Goold⁽¹⁰⁶⁾ performed diffusion measurements on samples composed of pure titanium and one of two different titanium-aluminum alloys, 4 weight percent aluminum or 8 weight percent aluminum. Samples were diffused at six different temperatures in the range 983 to 1250°C. The diffusion coefficients were determined as a function of concentration by means of the Matano analysis. The intrinsic diffusion coefficients were measured in some samples by use of ThO₂ markers. D as a function of atomic percent aluminum is shown in Fig. 42. For 2 atomic percent aluminum, D is given by the equation:

$$D = 1.4 \times 10^{-5} \exp [-(21,900 \pm 3,700)/RT].$$

Similarly for 12 atomic percent aluminum,

$$D = 9.0 \times 10^{-5} \exp [-(25,500 \pm 4,800)/RT].$$

At 1250°C, the intrinsic diffusion coefficients for 96.2 atomic percent titanium are:

$$D_{Ti} = 4.6 \times 10^{-9} \text{ cm}^2/\text{sec}$$

$$D_{Al} = 14.11 \times 10^{-9} \text{ cm}^2/\text{sec}.$$

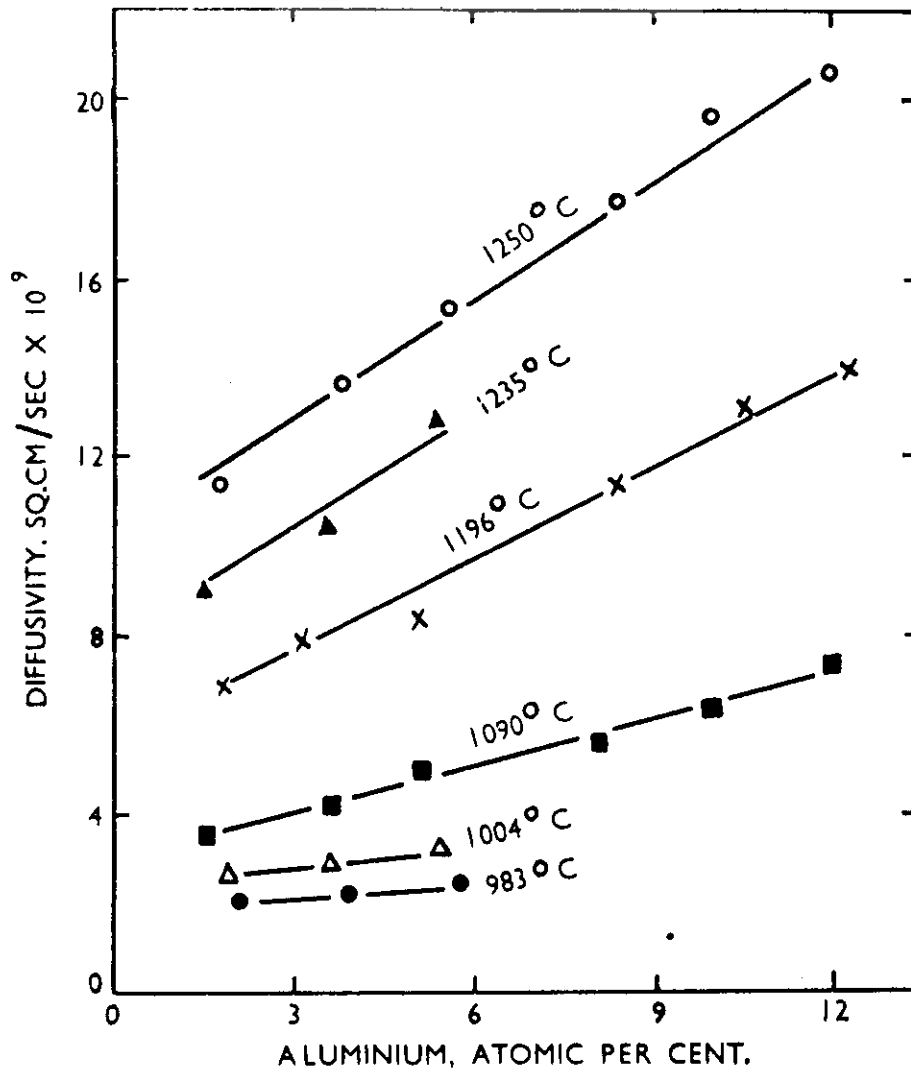


Fig. 42 - Variation of the interdiffusion coefficient with composition for the titanium-aluminum system. (106)

Since aluminum stabilizes the alpha phase in titanium, it was possible to determine the diffusivity of aluminum in alpha-titanium by employing a couple composed of the alloys 4 weight percent aluminum and 8 weight percent aluminum, heated at 834 and 900°C. Diffusion at these temperatures was too low to use the Matano method for calculating results, so the Grube analysis was used. The results fitted the equation:

$$D = 1.6 \times 10^{-5} \exp (-23,700/RT).$$

The data is quite complete, however, the errors reported for the activation energies are rather large.

b. Titanium-Iron

The diffusion of titanium in alpha and gamma iron at low titanium concentration was measured by Moll and Ogilvie.(178) Pressure bonded diffusion couples were prepared between pure iron and one of two different iron-titanium alloys, 2.13 weight percent titanium or 2.45 weight percent titanium, and these samples were diffused for various times at temperature in the range of 1075 to 1225°C. The concentration gradients were evaluated by a linear x-ray absorption technique. The observed rate of movement of the alpha-gamma interface determined the diffusion of titanium in alpha iron. This data is given in Table 79.

Table 79

Titanium-Iron Diffusion Data for Alloys of
Low Titanium Concentration(178)

Composition	Temp. (°C)	D (cm ² /sec)
2.13% Ti	1075	9.80×10^{-10}
	1150	2.27×10^{-9}
	1225	8.28×10^{-9}
2.45% Ti	1075	8.80×10^{-10}
	1150	2.09×10^{-9}
	1225	7.92×10^{-9}
2.47% Ti	1216	6.40×10^{-9}

The equation

$$D_{\alpha} = 3.15 \exp (-59,200/RT)$$

represents these points. Values for the diffusion coefficient of titanium in gamma iron were calculated by applying a Matano analysis to the concentration curves within the gamma phase region. The temperature variation of the diffusion coefficient may be described by the equation:

$$D_{\gamma} = 0.15 \exp (-60,000/RT).$$

These results on the activation energy for the interdiffusion of titanium in alpha-iron, at low titanium concentrations, are essentially the same as the activation energy for self-diffusion of iron in alpha-iron.⁽⁹⁰⁾ This result correlates with the theory of Zener⁽¹⁷⁹⁾ for diffusion in body-centered cubic alloys of low solute concentration. Also the scatter in the points on a log D vs 1/T is very reasonable for the alpha iron data. An evaluation of the gamma iron data is not possible since no data points were given.

c. Titanium-Manganese

Goold⁽¹⁰⁶⁾ carried out diffusion measurements on samples composed of pure titanium and one of two different titanium-manganese alloys, 8.5 weight percent manganese or 17 weight percent manganese. Samples were diffused at five different temperatures in the range 830 to 1190°C. After diffusion anneals at temperatures up to approximately 1000°C, 0.35 inch was machined off the diameter of the sample before taking the turnings for analysis. Due to the large manganese losses from the alloys by volatilization above 1000°C, the normal methods of analysis were not adequate. Instead, the radial distribution of manganese in the alloys was determined after diffusion. From this data, the diffusion coefficients were calculated. Excellent agreement between the two techniques was obtained on the same sample annealed at 926°C. D as a function of composition is shown in Fig. 43. For 8 atomic percent manganese, D is given by the equation:

$$D = 1.0 \times 10^{-3} \exp [-(35,200 \pm 1,800)/RT].$$

The data is quite complete and its reproducibility is represented by the reasonable error reported for the activation energy.

d. Titanium-Nickel

Swalin and Martin⁽³²⁾ prepared pressure welded diffusion couples of pure nickel and a Ni - 0.9% Ti alloy. Spectrophotometric analysis of lathe turnings was used to determine the concentration gradient. The data is given in Table 80. This data fitted the equation:

$$D = 0.86 \exp (-61,400/RT).$$

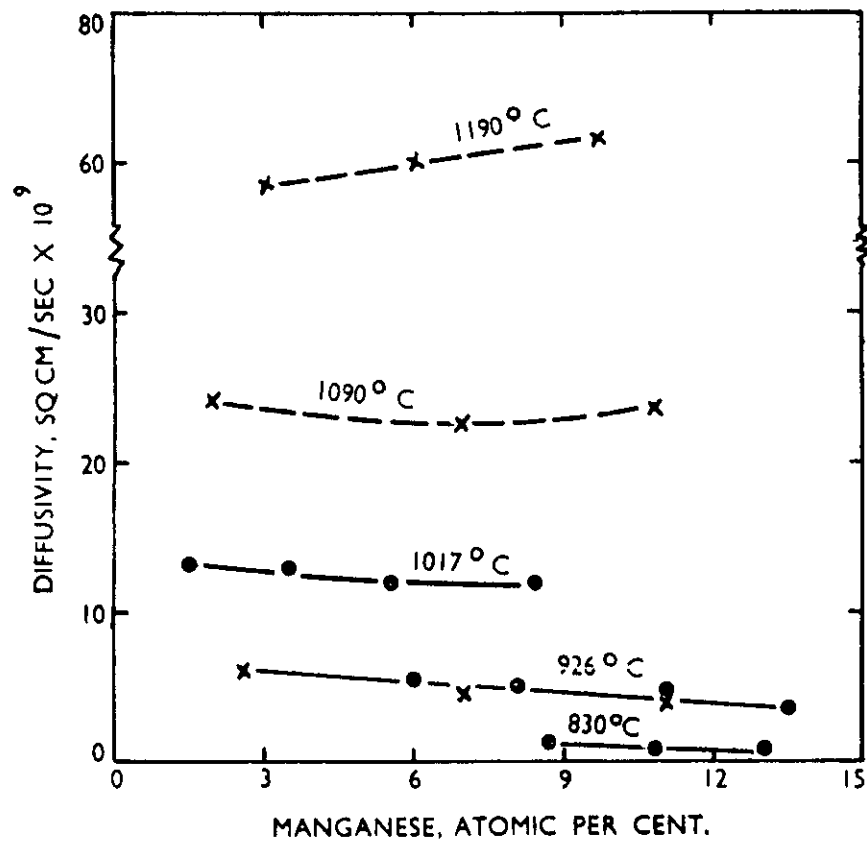


Fig. 43 - Variation of the interdiffusion coefficient with composition for the titanium-manganese system.⁽¹⁰⁶⁾

o = determined from transverse turnings

x = determined from circumferential turnings

Data on Diffusion in the Titanium-Nickel System at
Low Titanium Concentrations⁽³²⁾

Temp. (°C)	D (cm ² /sec)
1104	1.53×10^{-10}
1150	3.23×10^{-10}
1202	6.19×10^{-10}
1214	8.75×10^{-10}
1239	1.15×10^{-9}
1282	1.96×10^{-9}

A plot of $\log D$ vs $1/T$ is shown in Fig. 44. These values are very good as may be seen by the small amount of scatter in the data in Fig. 44. The authors estimated their error in the activation energy at ± 1000 cal/mole.

e. Titanium-Silicon

Samsonov and Solonnikova⁽³⁴⁾ reported a value for the activation energy for diffusion of silicon in titanium, determined from measurements of the growth of the $TiSi_2$ phase as $Q = 5,690$ cal/mole. The doubtful applicability to diffusion of the data of these authors has previously been discussed in this paper.

f. Titanium-Tin

Goold⁽¹⁰⁶⁾ measured the diffusion in couples composed of pure titanium and one of two different titanium-tin alloys, 10 weight percent (4.3 atomic percent) tin or 20 weight percent (9.2 atomic percent) tin. Samples were diffused at five different temperatures in the range 1004 to 1250°C. The diffusion coefficients were determined as a function of concentration by means of the Matano analysis. ThO_2 markers were included in some samples in order to determine the intrinsic diffusion coefficients. D as a function of atomic percent tin is shown in Fig. 45. For 1 atomic percent tin, D may be expressed by the equation:

$$D = 8.4 \times 10^{-7} \exp [-(15,300 \pm 3,800)/RT].$$

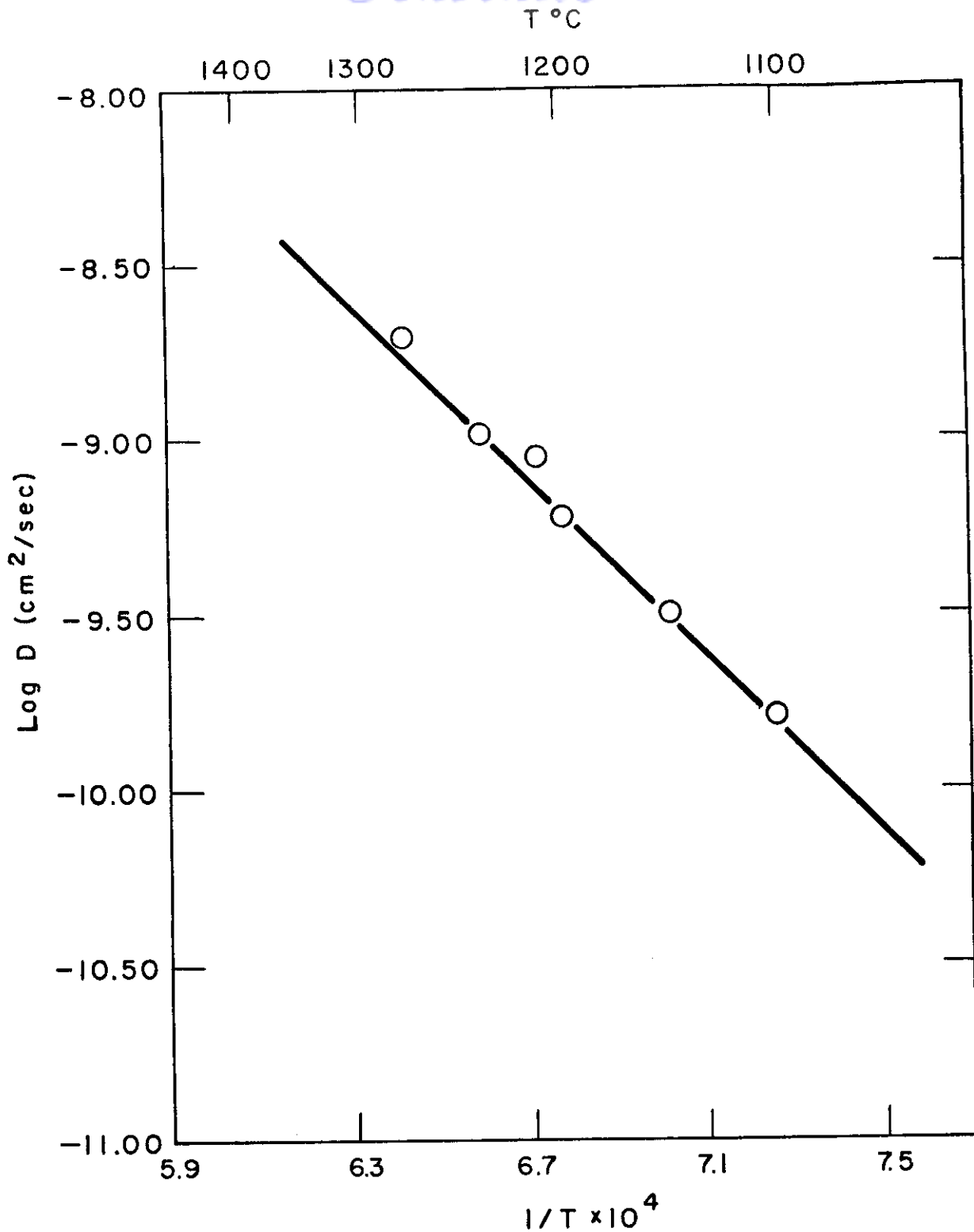


Fig. 44 - Log D vs $1/T$ is plotted for diffusion in titanium-nickel alloys of high nickel concentration.(32)

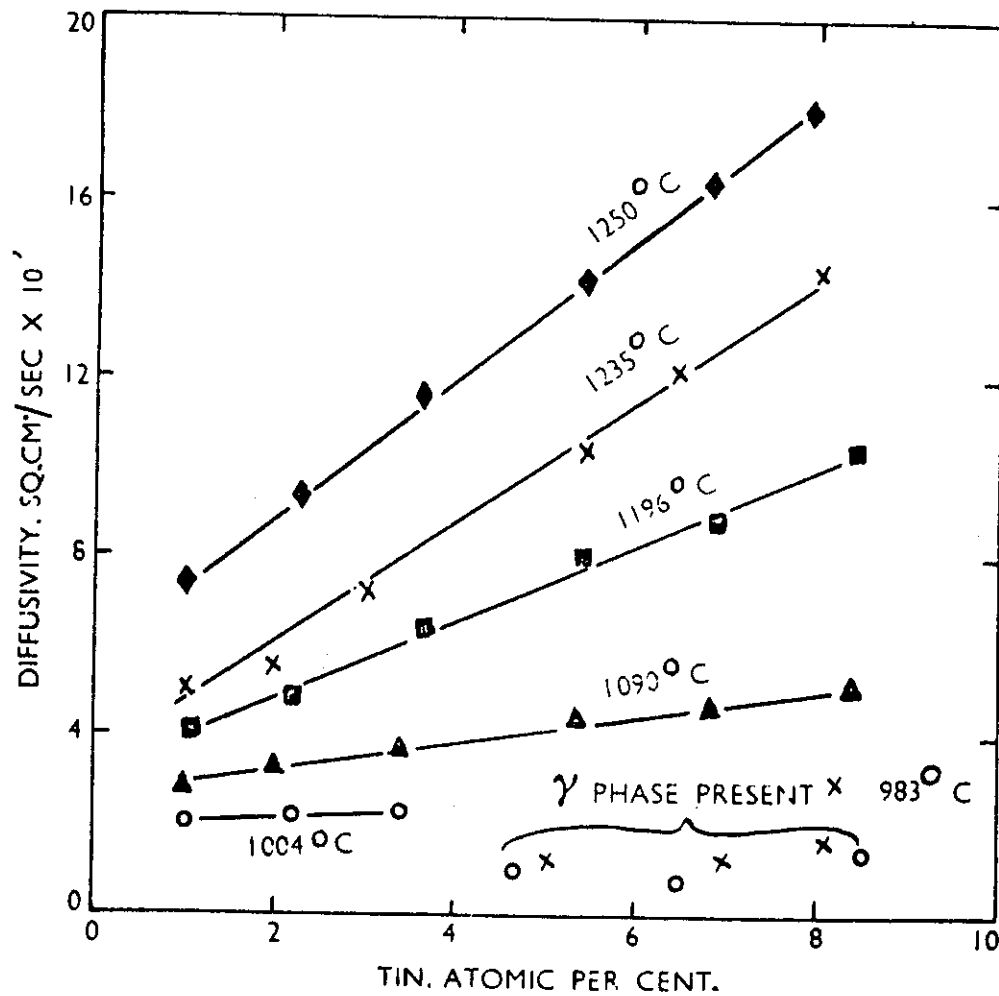


Fig. 45 - Variation of the interdiffusion coefficient with composition for the titanium-tin system. (106)

Similarly for 8 atomic percent tin:

$$D = 2.7 \times 10^{-4} \exp [-(29,800 \pm 8,300)/RT].$$

At 1250°C, the intrinsic diffusion coefficients for 98 atomic percent titanium were:

$$D_{Ti} = 2.65 \times 10^{-9} \text{ cm}^2/\text{sec}$$

$$D_{Sn} = 9.18 \times 10^{-9} \text{ cm}^2/\text{sec}.$$

Since tin stabilizes the alpha phase in titanium, it was possible to determine the diffusivity of tin in alpha-titanium by using a diffusion couple composed of the alloy 10 weight percent tin and 20 weight percent tin, heated at 834°C. The diffusion at this temperature was too small to use the Matano analysis, so the Grube analysis was used. This data yielded the diffusion coefficient:

$$D = 0.5 \times 10^{-10} \text{ cm}^2/\text{sec}.$$

The data is very complete; however, the errors reported for the activation energy (~25%) are excessively large.

f. Titanium-Uranium

A very complete and accurate investigation of the diffusion in the titanium-uranium system was performed by Adda and Philibert.⁽¹⁸⁰⁾ Pressure bonded diffusion couples were prepared between pure uranium and pure titanium. Diffusion anneals were carried out between 950 and 1075°C. The concentration gradients were determined with the electron microbeam probe, and the diffusion coefficients and the activation energies were determined as a function of composition. This data is given in Table 81 and can be seen in Figs. 46 and 47. Intrinsic diffusion coefficients were also measured. This data is summarized in Table 82 and is shown graphically in Fig. 48.

4. Substitutional Diffusion in Ternary and Higher Order Titanium Systems

a. Titanium-Iron-Cobalt

Gruzin and Noskow⁽¹⁵³⁾ investigated the diffusion of Co⁶⁰ into an alloy of 81% cobalt, 15% iron, and 4% titanium. A Co⁶⁰ layer, 0.005 mm thick was electrolytically deposited onto thin discs of the alloy and diffused at the temperatures 1100 and 1200°C. Two to four measurements were made at each temperature. An average of the different measurements for the two temperatures investigated are tabulated in Table 83.

Table 81

Titanium-Uranium Diffusion Coefficients for Various Titanium-Concentrations (180)

Concentration (at. % U)	D (cm ² /sec)				Q (cal/mole)	D ₉ (cm ² /sec)
	950°C	1000°C	1050°C	1075°C		
5	1.7 x 10 ⁻⁹	2.6 x 10 ⁻⁹	4.5 x 10 ⁻⁹	5.7 x 10 ⁻⁹	30,200	4.6 x 10 ⁻⁴
10	1.0 x 10 ⁻⁹	1.6 x 10 ⁻⁹	3.1 x 10 ⁻⁹	3.4 x 10 ⁻⁹	33,800	1.1 x 10 ⁻³
20	4.6 x 10 ⁻¹⁰	7.1 x 10 ⁻¹⁰	1.3 x 10 ⁻⁹	1.9 x 10 ⁻⁹	37,500	2.2 x 10 ⁻³
30	2.3 x 10 ⁻¹⁰	5.7 x 10 ⁻¹⁰	8.9 x 10 ⁻¹⁰	1.1 x 10 ⁻⁹	39,400	2.6 x 10 ⁻³
40	2.7 x 10 ⁻¹⁰	4.2 x 10 ⁻¹⁰	8.6 x 10 ⁻¹⁰	1.2 x 10 ⁻⁹	39,400	2.6 x 10 ⁻³
50	2.9 x 10 ⁻¹⁰	4.6 x 10 ⁻¹⁰	1.1 x 10 ⁻⁹	1.5 x 10 ⁻⁹	42,000	9.5 x 10 ⁻³
60	6.2 x 10 ⁻¹⁰	8.6 x 10 ⁻¹⁰	1.7 x 10 ⁻⁹	2.6 x 10 ⁻⁹	38,400	4.0 x 10 ⁻³
70	1.1 x 10 ⁻⁹	1.5 x 10 ⁻⁹	3.1 x 10 ⁻⁹	4.1 x 10 ⁻⁹	34,800	1.6 x 10 ⁻³
80	1.9 x 10 ⁻⁹	2.8 x 10 ⁻⁹	5.5 x 10 ⁻⁹	6.5 x 10 ⁻⁹	33,000	1.4 x 10 ⁻³
90	3.4 x 10 ⁻⁹	5.4 x 10 ⁻⁹	1.2 x 10 ⁻⁸	1.25 x 10 ⁻⁸	36,600	1.1 x 10 ⁻²

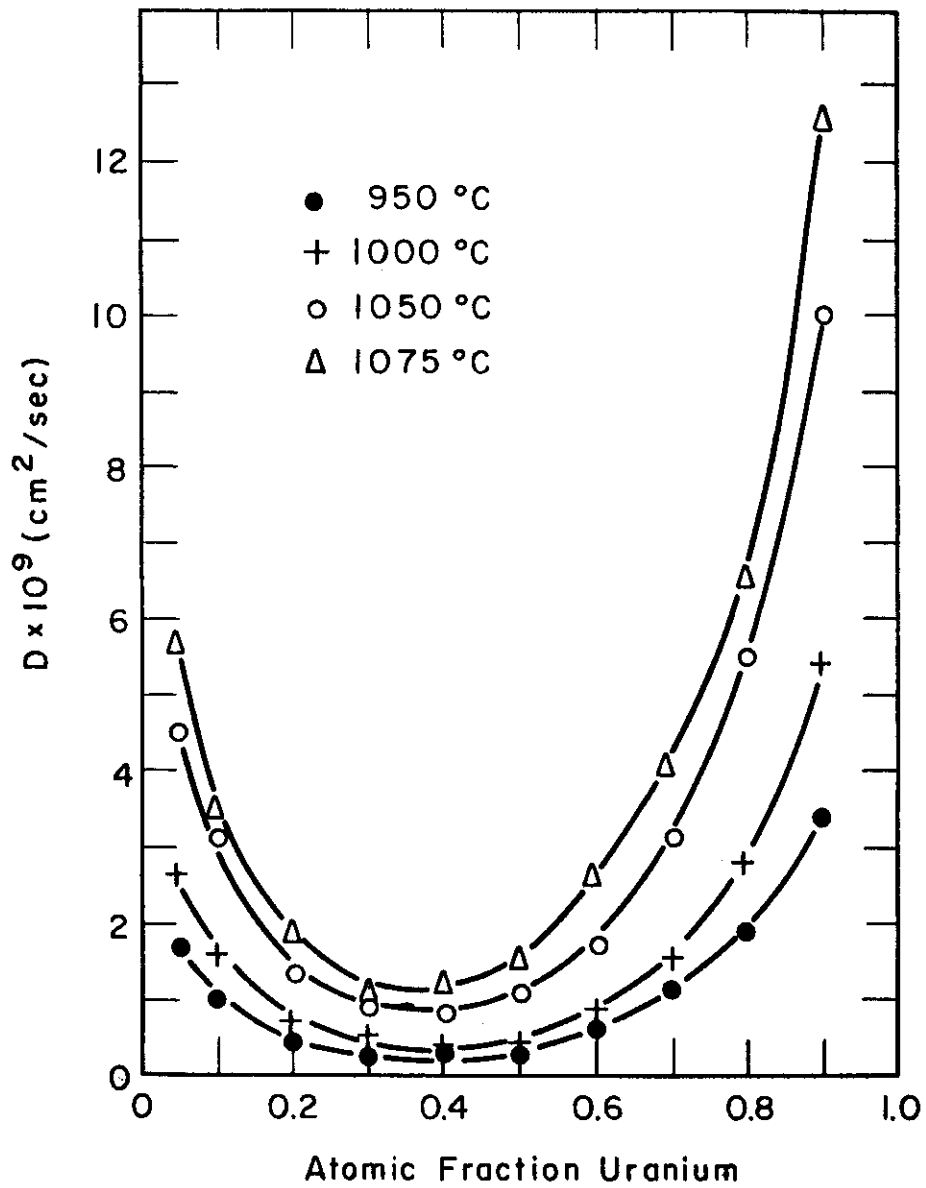


Fig. 46 - D vs composition for uranium-titanium system.(180)

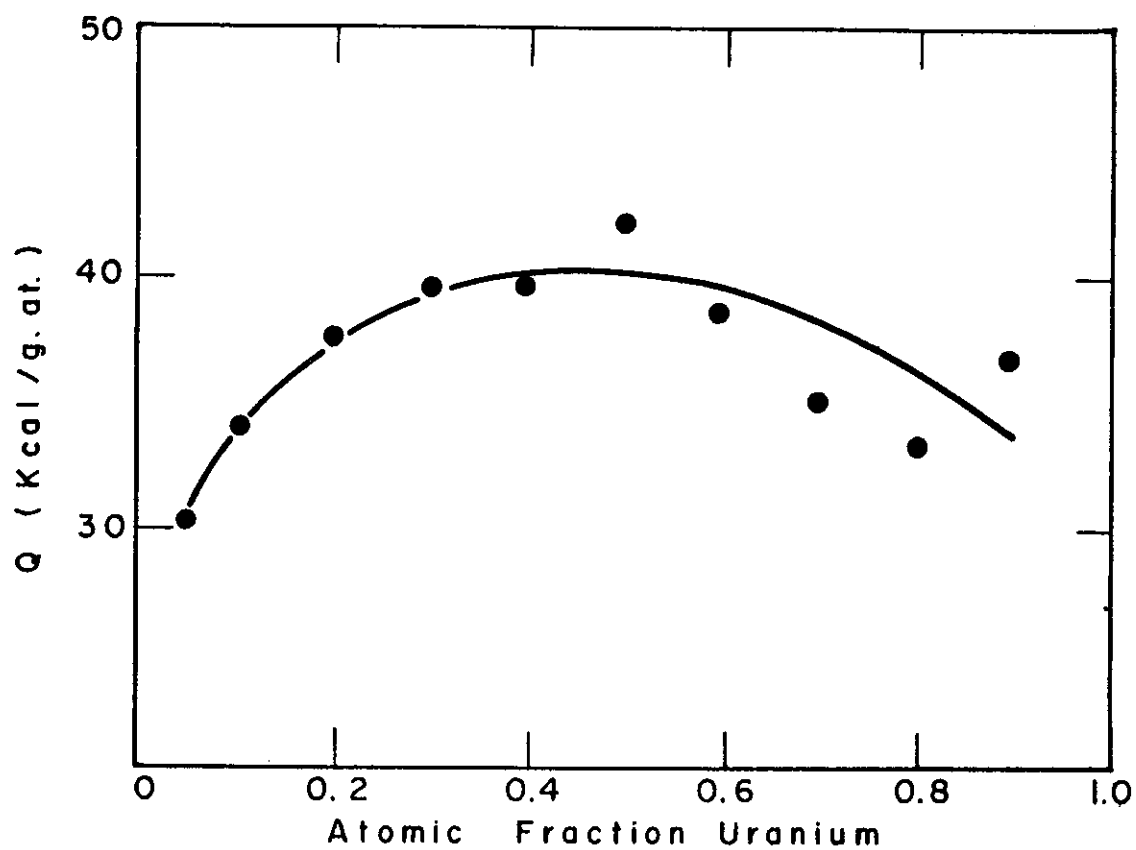


Fig. 47 - Dependence of Q on composition for the uranium-titanium system.(180)

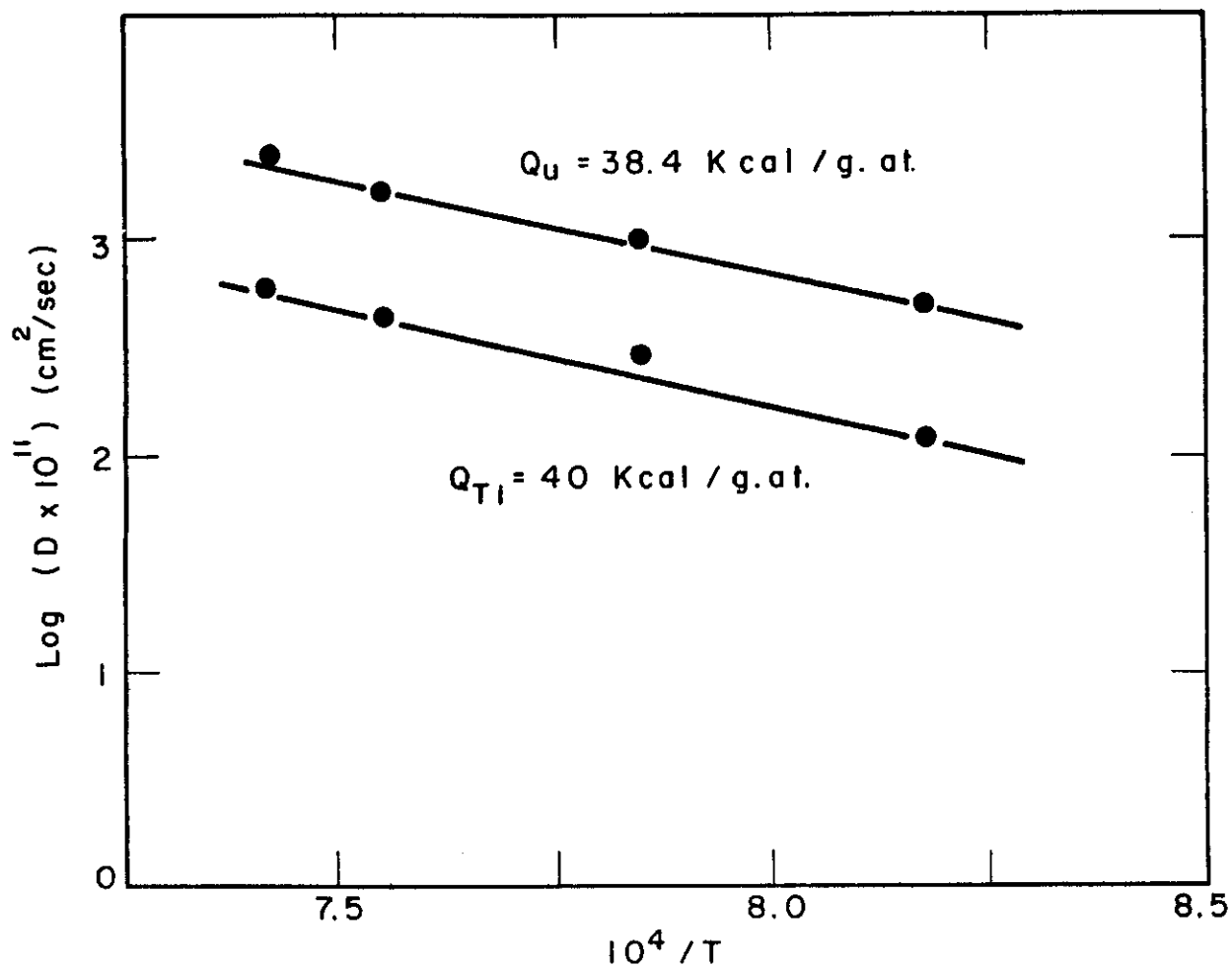


Fig. 48 - Temperature Dependence of intrinsic diffusion coefficients for uranium-titanium system.(180)

Table 82

Intrinsic Diffusion Coefficients in the
Titanium-Uranium System(180)

Temp. (°C)	950	1000	1050	1075
At. % U	82	82	82	83.5
Intrinsic D_U	4.7×10^{-9}	9.5×10^{-9}	1.6×10^{-8}	2.2×10^{-8}
Intrinsic D_{Ti}	1.2×10^{-9}	2.9×10^{-9}	4.1×10^{-9}	5.8×10^{-9}

Table 83

Data on the Diffusion of Co^{60} in an Alloy of
81% Cobalt, 15% Iron and 4% Titanium(153)

Temp. (°C)	D (cm ² /sec)
1100	7.5×10^{-11}
1200	19.0×10^{-11}

This data may be expressed by the equation:

$$D = 0.008 \exp (-51,200/RT).$$

There is a large uncertainty in the equation for the temperature variation of the diffusion coefficient since measurements were made at only two temperatures.

b. Titanium-Nickel-Chromium-Tungsten-Aluminum

Kornilov and Shinyaev⁽¹⁸¹⁾ measured the diffusion of Fe^{59} in alloys of Ni-Ti, Ni-Ti-Cr, and Ni-Ti-Cr-W-Al. These alloys were nickel base, in saturated solid solution; however, the actual compositions were not given. Fe^{59} was electrolytically deposited on 20 mm diameter discs, 2 to 3 mm thick, and diffusion anneals were performed in the temperature range of 920 to 1250°C. After diffusion, layers were etched off the surface of the alloy discs and the activity of the Fe^{59} was measured. The data is reported in Table 84. The experimental values are plotted as log D vs 1/T shown in Fig. 49. The accuracy of the data appears to be very good as seen in the small amount of scatter in the data of Fig. 49.

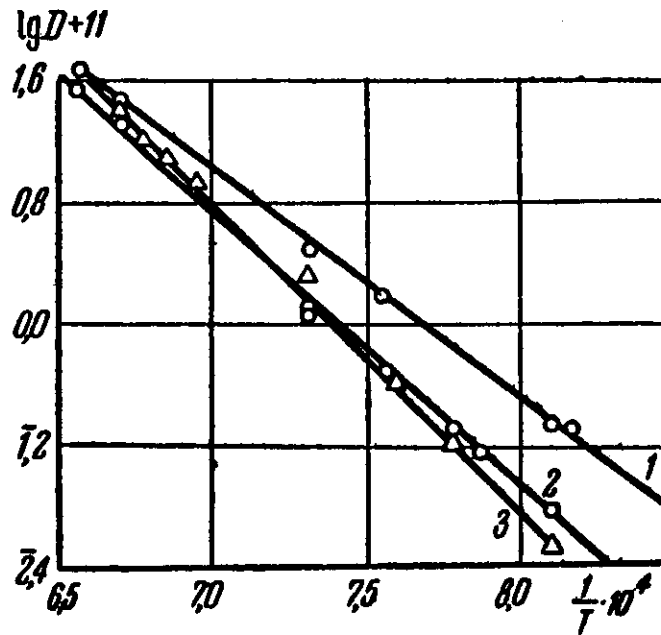


Fig. 49 - Temperature dependence of the diffusion coefficient of Fe^{59} in alloys of the systems: (1) Ni-Ti, (2) Ni-Ti-Cr, (3) Ni-Ti-Cr-W-Al. (181)

Frequency Factor and Activation Energy for Diffusion of Fe⁵⁹ in
Ni-Ti, Ni-Cr-Ti, and Ni-Cr-W-Al-Ti Alloys⁽¹⁸¹⁾

Alloy	Q (cal/mole)	D ₀ (cm ² /sec)
Ni	50,700	9.2 x 10 ⁻³
Ni-Ti	73,100	1.6 x 10 ⁻¹
Ni-Cr-Ti	84,000	4.45 x 10 ²
Ni-Cr-W-Al-Ti	91,300	8.2 x 10 ³

c. Iron-Nickel plus a Third Element
(Ti, V, Nb, B or Mo)

It was previously shown that small additions of a third element can greatly alter the measured diffusion coefficient for the interstitial diffusion of oxygen in titanium. Similar measurements were made for the substitutional diffusion of Fe⁵⁹ in a series of iron-nickel alloys with small additions of a third element (titanium, vanadium, niobium, molybdenum or boron).

Bokshtein, Kazakova, Kishkin, and Mirsky⁽¹⁸²⁾ diffused Fe⁵⁹ into alloy samples, 29 x 9 x 7 mm in size, at temperatures of 1000, 1100, 1150, and 1200°C. The alloy compositions and the diffusion data are presented in Table 85. The composition and temperatures were chosen so that all measurements were made in the face-centered cubic gamma-iron phase. The samples were sectioned with a "specially designed machine" which removed whole slices, probably much like a microtome. The data appears to be very good since very little scatter in the data points is shown in the log D vs 1/T plots.

Arkharov, Efremova, Ivanovskaya, Shtol'ts, and Yunikov^(183,184) found that nickel diffused through the grain boundaries of Armco iron to a depth of 0.16 mm after an anneal at 1300°C. Under the same conditions, 0.004% boron completely eliminated the grain boundary penetration of nickel, 0.2 to 0.3% molybdenum practically eliminated it, 0.12% niobium reduced it to 0.04 mm, 0.27% titanium reduced it to 0.06 mm, and 0.2% vanadium reduced it to 0.11 mm.

Investigations such as these are few and far between. With a better knowledge of the minor constituents in diffusion couples and their effect on the diffusion coefficient, one might be able to show a far better correlation between the data of different investigators.

A summary of diffusion in titanium is given in Table 86.

Table 85

Diffusion Data for Iron-Nickel Base Alloys⁽¹⁸²⁾

(Major Constituent is Iron)

% Ni	Third Element	Wt. % of Third Element	$D \times 10^{-11} \text{ (cm}^2/\text{sec)}$			D_0 (cm^2/sec)	Q (cal/mole)
			1200°C	1100°C	1000°C		
11.8	--	----	12.6	3.02	0.479	1.21	66,600
24.3	--	----	16.0	3.63	0.795	3.5×10^{-1}	62,200
25.02	Mo	0.40	15.9	3.49	0.795	3.09	68,000
		1.80	14.5	2.40	0.250	4.33×10^1	77,500
		4.25	13.8	1.26	0.06	2.2×10^4	96,000
24.10	Nb	0.3	16.6	3.17	0.252	1.26×10^3	85,200
		1.3	15.9	3.02	0.252	4.91×10^3	89,000
		3.25	14.8	1.75	0.110	3.48×10^4	95,500
24.35	Ti	0.2	14.5	2.89	0.417	2.38	67,600
		1.88	17.4	2.52	0.347	1.5×10^4	92,000
24.7	V	2.05	19.1	6.31	0.754	3.5×10^{-2}	55,200
		4.92	17.4	5.25	1.26	2.16×10^{-3}	48,000

Table 86

Summary of Diffusion Data for Titanium

Diffusing Element	Composition Range (wt. %)	Temp. (°C)	D (cm ² /sec)	D ₀ (cm ² /sec)	Q (cal/mole)	References
Ti (self)	Estimate from melting point Estimate from heat of fusion				73,600 72,200 73,600	
B	25	800-1200		2.15 x 10 ⁻⁴	9,150	8,9
C	15	800-1400		2.44 x 10 ⁻³	17,500	8,9
C (α-Ti) (β-Ti)	0.4-1.37	736-835 950-1150		5.06 108	43,500 48,400	164
H (α-Ti) (α-Ti) (β-Ti) (α-Ti) (α-Ti)		700-900 R.T.	1.9 x 10 ⁻⁹	0.27 x 10 ⁻² 1.8 x 10 ⁻² 1.95 x 10 ⁻²	14,200 12,380 6,640 15,000	166,167 168 168 169 170
N (α-Ti) (β-Ti) (TiN) (α-Ti)		900-1570 900-1570 550-850		1.2 x 10 ⁻² 3.5 x 10 ⁻³ 5.4 x 10 ⁻³	45,250 33,800 52,000 36,300	171 171 171 172
O (β-Ti) (α-Ti) (α-Ti) (β-Ti) (β-Ti) (β-Ti)		950-1414 700-1150 700-1150 1127-1347 250-600		1.6 0.4 5.08 x 10 ⁻³ 3.14 x 10 ⁻⁴ 8.3 x 10 ⁻² 1 x 10 ⁻⁶	48,200 48,000 33,500 68,700 31,200 26,000	171 173 175 175 176 172
Al (β-Ti)	1.5 7.5	983-1250		1.4 x 10 ⁻⁵ 9.0 x 10 ⁻⁵	21,900 25,500	106
(intrinsic)	96.2% Ti	1250	D _{Ti} = 4.6 x 10 ⁻⁹ D _{Al} = 14.11 x 10 ⁻⁹			106

(Cont'd. on next page)

Table 86 (Cont'd.)

Diffusing Element	Composition Range (wt. %)	Temp. (°C)	D (cm^2/sec)	D_0 (cm^2/sec)	Q (cal/mole)	References
Al (α -Ti)	6	834-900		1.6×10^{-5}	23,700	106
α -Fe	99.0-100	1075-1225		3.15	59,200	178
γ -Fe	97.5-99	1075-1225		0.15	60,000	178
Mn	8	830-1190		1.0×10^{-3}	35,200	106
Ni	99	1104-1282		0.86	61,400	32
Si	60				5,690	34
Sn (β -Ti)	$\frac{1}{7}$	1004-1250	0.5×10^{-10} $D_{Ti} = 2.65 \times 10^{-9}$ $D_{Ti} = 9.18 \times 10^{-9}$ D_{Sn}	8.4×10^{-7} 2.7×10^{-4}	15,300 29,800	106
(α -Ti)	15	834				
(intrinsic)	98% Ti	1250				
U	5 10 20 30 40 50 60 70 80 90	950-1075		4.6×10^{-4} 1.1×10^{-3} 2.2×10^{-3} 2.6×10^{-3} 2.6×10^{-3} 9.5×10^{-3} 4.0×10^{-3} 1.6×10^{-3} 1.4×10^{-2} 1.1×10^{-2}	30,200 33,800 37,500 39,400 39,400 42,000 38,400 34,800 33,000 36,600	180
(intrinsic)	82% U				$Q_U = 38,400$ $Q_{Ti} = 40,000$	
Mo	0-8	938-1248	$D_{Ti} = 6.72 \times 10^{-9}$ $D_{Ti} = 3.95 \times 10^{-9}$ D_{Mo}	1.0×10^{-5}	24,000	106
(intrinsic)	4	1250				

(Cont'd. on next page)

Table 86 (Cont'd.)

Diffusing Element	Composition Range (wt. %)	Temp. (°C)	D (cm^2/sec)	D (cm^2/sec)	Q (cal/mole)	References
Nb	0-100	1000	$0.4-4.5 \times 10^{-7}$			113
(Ti tracer)		1200	$1.7-11.8 \times 10^{-7}$		11,000-32,800	113
Zr		825-1150			23,000	139
V	0-15	900-1248				
(intrinsic)	3.5	1250	$D_{\text{Ti}} = 1.31 \times 10^{-9}$ $D_{\text{V}} = 14.9 \times 10^{-9}$	6×10^{-3}	39,600	106
Cr	18	1000 1047	2×10^{-9} 3.9×10^{-9}			159

V. REFERENCES

1. V. P. Vasiler and S. G. Chernomorchenko, Zavod, Lab. Vol. 22, p. 688 (1956).
2. E. W. Muller, Z. Physik, Vol. 126, p. 642 (1949).
3. C. Herring, J. Appl. Phys., Vol. 21, p. 301 (1950).
4. J. L. Boling and W. W. Dolan, J. Appl. Phys., Vol. 29, p. 556 (1958).
5. I. L. Sokolovskaia, Soviet Physics (Tech. Phys.) Vol. 1, p. 1147 (1956).
6. J. P. Barbour, F. M. Charbonnier, W. W. Dolan, W. P. Dyke, E. E. Martin and J. K. Trolan, Phys. Rev., Vol. 117, p. 1452 (1960).
7. P. C. Bettler and F. M. Charbonnier, Phys. Rev., Vol. 119, p. 85 (1960).
8. G. V. Samsonov and V. P. Latysheva, Fiz Metal i Metalloved, Vol. 2, No. 2, p. 309 (1956).
9. G. V. Samsonov and V. P. Latysheva, Doklady Akad, Nauk S.S.S.R., Vol. 109, p. 582 (1956).
10. G. V. Samsonov, Doklady Akad, Nauk S.S.S.R., Vol. 93, p. 859 (1953).
11. G. S. Kreimer, L. D. Efron and E. A. Voranova, Zhur, Tekh. Fiz., Vol. 22, p. 858 (1952).
12. M. Pirani and J. Sandor, J. Inst. Metals, Vol. 73, p. 385 (1947).
13. C. Zwikker, Physica, Vol. 7, p. 189 (1927).
14. R. Klein, J. Chem. Phys., Vol. 22, p. 1406 (1954).
15. R. Gomer, J. Phys. Chem., Vol. 63, p. 468 (1959).
16. R. Wortman, R. Gomer and R. Lundy, J. Chem. Phys., Vol. 24, p. 161 (1956).
17. R. Gomer and J. K. Hulm, J. Am. Chem. Soc., Vol. 75, p. 4114 (1953).
18. E. W. Muller, Z. Elektrochem., Vol. 59, p. 372 (1955).
19. E. W. Muller, Z. Physik, Vol. 108, p. 668 (1938).
20. J. A. Becker, Bell System Tech. J., Vol. 30, p. 907 (1951).
21. S. Dushman, D. Dennison and N. B. Reynolds, Phys. Rev., Vol. 29, p. 903 (1927).

22. I. Langmuir and J. B. Taylor, Phys. Rev., Vol. 40, p. 463 (1932).
23. V. P. Vasiler, I. F. Kamardin, V. I. Skatskii, S. G. Chernomorchenko and G. N. Shuppe, Trudy Sredneaziat Gosudarst. Univ. im. V.I. Lenina, Vol. 65, No. 12, p. 47 (1955).
24. P. L. Gruzin, Doklady Akad. Nauk S.S.S.R., Vol. 94, p. 681 (1954).
25. J.A.M. Van Liempt, Rec. Trav. Chim, Pays-Bas, Vol. 64, p. 239 (1945).
26. G. Grube and K. Schneider, Z. Anorg. Chem., Vol. 168, p. 17 (1927).
27. G. Grube and A. Jedele, Z. fur Elektrochemie, Vol. 38, p. 799 (1932).
28. C. Matano, Japan J. Phys., Vol. 8, p. 109 (1933).
29. R.C.L. Bosworth, Proc. Roy. Soc. London, Vol. 154, p. 112 (1936).
30. J.A.M. Van Liempt, Rec. Trav. Chim, Pays-Bas, Vol. 51, p. 114 (1932).
31. J.A.M. Van Liempt, Rec. Trav. Chim, Pays-Bas, Vol. 60, p. 634 (1941).
32. R. A. Swalin and A. Martin, Trans. AIME, Vol. 206, p. 567 (1956).
33. H. W. Allison and G. E. Moore, J. Appl. Phys., Vol. 29, p. 842 (1958).
34. G. P. Samsonov and L. A. Solonnikova, Physics of Metals and Metallography, Vol. 5, No. 3, p. 177 (1957).
35. S. Dushman and I. Langmuir, Phys. Rev., Vol. 20, p. 113 (1922).
36. I. Langmuir, Phys. Rev., Vol. 22, p. 357 (1923).
37. I. Langmuir, J. Franklin Inst., Vol. 217, p. 543 (1934).
38. G. R. Fonda, A. H. Young and A. Walker, Physics, Vol. 4, p. 1 (1933).
39. W. H. Brattain and J. A. Becker, Phys. Rev., Vol. 43, p. 428 (1933).
40. R. L. Eager and D. B. Langmuir, Phys. Rev., Vol. 89, p. 911 (1953).
41. P. L. Gruzin and V. I. Meshkov, Vestnik Akad. Nauk Kazakh S.S.S.R., Vol. 11, No. 4, p. 85 (1955).
42. P. L. Gruzin and V. I. Meshkov, Problemy Metallovedeniza i Fiziki Metallov, Vol. 4, p. 570 (1955).
43. T'ing-Sui Ke, Phys. Rev., Vol. 74, p. 9 (1948).
44. C. A. Wert, J. Appl. Phys., Vol. 21, p. 1196 (1950).
45. R. W. Powers, Acta Met., Vol. 3, p. 135 (1955).

46. R. W. Powers and M. V. Doyle, Acta Met., Vol. 4, p. 233 (1956).
47. R. W. Powers and M. V. Doyle, J. Appl. Phys., Vol. 28, p. 255 (1957).
48. R. W. Powers and M. V. Doyle, J. Appl. Phys., Vol. 30, p. 514 (1959).
49. A. Ferro, J. Appl. Phys., Vol. 28, p. 895 (1957).
50. E. A. Gulbransen and K. F. Andrew, Trans. AIME, Vol. 188, p. 586 (1950).
51. C. Y. Ang, Acta Met., Vol. 1, p. 123 (1953).
52. J. W. Marx, G. S. Baker and J. M. Sivertsen, Acta. Met., Vol. 1, p. 193 (1953).
53. E. Gebhardt, H. D. Seghezzi and A. Stagherr, Z. Metallk., Vol. 48, p. 624 (1957).
54. Calculated by the author using the formula of A. Ferro, Ref. 44.
55. Preliminary data by the author.
56. R. M. Parke, Metal Progress, Vol. 60, p. 81, (1951).
57. R. L. Orr, O. D. Sherby and J. E. Dorn, Trans. ASM, Vol. 46, p. 113 (1954).
58. A. D. LeClaire, "Progress in Metal Physics", Vol. 1, p. 306, (1949).
59. N. H. Nachtrieb and G. S. Handler, Acta Met., Vol. 2, p. 797 (1954).
60. K. K. Kelley, Bull 383, Bureau of Mines (1935).
61. C. J. Smithells and C. E. Ransley, Proc. Roy. Soc. (London), Vol. 150, p. 172 (1935).
62. N. H. Nachtrieb and G. S. Handler, J. Chem. Phys., Vol. 23, p. 1187 (1955).
63. D. K. C. MacDonald, J. Chem. Phys., Vol. 21, p. 177 (1953).
64. N. H. Nachtrieb, E. Catalano, and J. A. Weil, J. Chem. Phys., Vol. 20, p. 1185 (1952).
65. H. S. Gutowsky, Phys. Rev., Vol. 83, p. 1073 (1951).
66. H. S. Gutowsky and B. R. McGarvey, J. Chem. Phys., Vol. 20, p. 1472 (1952).
67. R. E. Eckert and H. G. Drickamer, J. Chem. Phys., Vol. 20, p. 13 (1952).

68. E. S. Wajda, G. A. Shirn and H. B. Huntington, Acta Met., Vol. 3, p. 39 (1955).
69. G. A. Shirn, Acta Met., Vol. 3, p. 87 (1955).
70. P. H. Miller, Jr. and F. R. Banks, Phys. Rev., Vol. 61, p. 648 (1942).
71. G. A. Shirn, E. S. Wajda and H. B. Huntington, Acta Met., Vol. 1, p. 513 (1953).
72. F. E. Jaumot, Jr. and R. L. Smith, Trans. AIME, Vol. 206, p. 137 (1956).
73. P. G. Shewmon and F. N. Rhines, Trans. AIME, Vol. 200, p. 1021 (1954).
74. P. G. Shewmon, Inst. of Metals Div. AIME Meeting, February 1956.
75. A. S. Nowick, J. Appl. Phys., Vol. 22, p. 1182 (1951).
76. C. L. Raynor, L. Thomassen and L. J. Rouse, Trans. ASM, Vol. 30, p. 313 (1942).
77. F. Seitz and D. Lazarus, Progress Report, U. of Ill. AEC AT(11-1)-67, Project 3.
78. W. A. Johnson, Trans. AIME, Vol. 143, p. 107 (1941).
79. R. E. Hoffmann and D. Turnbull, J. Appl. Phys., Vol. 22, p. 634 (1951).
80. L. Slifkin, D. Lazarus and T. Tomizuka, J. Appl. Phys., Vol. 23, p. 1032 (1952).
81. G. C. Kuczynski, J. Appl. Phys., Vol. 21, p. 632 (1950).
82. H. A. C. McKay, Trans. Faraday Soc., Vol. 34, p. 845 (1938).
83. A. M. Sagrubsij, Bull. Acad. Sci. USSR, p. 903 (1937).
84. A. D. Kurtz, B. L. Averbach and M. Cohen, Acta Met., Vol. 3, p. 442 (1955).
85. F. C. Nix and F. E. Jaumot, Jr., Phys. Rev., Vol. 82, p. 72 (1951).
86. R. C. Ruder and C. E. Birchenall, Trans. AIME, Vol. 191, p. 142 (1951).
87. H. Burgess and R. Smoluchowski, J. Appl. Phys., Vol. 26 (1955).
88. R. E. Hoffman, F. W. Pikus and R. A. Ward, Trans. AIME, Vol. 206, p. 483 (1956).
89. C. E. Birchenall and R. F. Mehl, Trans. AIME, Vol. 188, p. 144 (1950).

90. F. S. Buffington, J. D. Bakalar and M. Cohen, Trans. AIME, Vol. 188, p. 1374 (1950).
91. P. L. Gruzin, U. V. Kornev and G. V. Kurdimov, Doklady Akad. Nauk, U.S.S.R., Vol. 80, p. 49 (1951).
92. H. W. Mead and C. E. Birchenall, Inst. of Metals Div. AIME Meeting, February 1956.
93. G. V. Kidson and R. Ross, Proc. of International Conf. on Use of Radioisotopes in Scientific Res. Vol. 1, p. 185 (Paris, 1957).
94. R. Resnick and L. S. Castleman, Trans. AIME, Vol. 218, p. 307 (1960).
95. R. Maringer and G. T. Muehlenkamp, J. Metals, Vol. 4, p. 149 (1952).
96. C. Wert and J. Marx, Acta Met., Vol. 1, p. 113 (1953).
97. E. S. Byron and V. E. Lambert, J. Electrochem. Soc., Vol. 102, p. 38 (1955).
98. M. B. Neiman and A. Ya Shinyaev, Doklady Akad. Nauk, U.S.S.R., Vol. 103, No. 1, p. 101 (1955).
99. M. B. Neiman and A. Ya Shinyaev, Doklady Akad. Nauk, U.S.S.R., Vol. 102, No. 5, p. 969 (1954).
100. G. Grube and F. Lieberwirth, Z. Anorg. Chem., Vol. 188, p. 274 (1930).
101. J. L. Ham, Trans. ASM., Vol. 35, p. 331 (1945).
102. L. S. Birks and R. E. Seebold, NRL Report No. 5461, March 1960.
103. K. Budde, Dissertation, Munster, 1954, as reported by W. Seith. "Diffusion in Metallen" Springer-Verlag Berlin, 1955.
104. R. A. Swalin, A. Martin and R. Olsen, Trans. AIME, Vol. 209, p. 936 (1957).
105. P. G. Shewmon and J. H. Bechtold, Acta Met., Vol. 3, p. 452 (1955).
106. D. Goold, J. Inst. Metals, Vol. 88, p. 444 (1960).
107. H. Nelting, Z. Physik, Vol. 115, p. 469 (1940).
108. Y. Adda and J. Philibert, Compt. Rend., Vol. 246, p. 113 (1958).
109. R. W. Powers and M. V. Doyle, Trans. AIME, Vol. 209, p. 1285 (1957).
110. W. M. Albrecht, W. D. Goode and M. W. Mallett, J. Electrochem. Soc., Vol. 106, p. 981 (1959).

111. W. M. Albrecht and W. D. Goode, Battelle Memorial Inst. Report BMI-1360 (1959).
112. R. I. Jaffee, W. D. Klopp and C. T. Sims, Trans. ASM, Vol. 51, p. 282 (1959).
113. N. V. G. Grzhimailo, Izvest. Akad. Nauk. S.S.S.R., Otdel Tekh Nauk, No. 7, p. 24 (1957).
114. M. Hansen, E. L. Kamen, H. D. Kessler and D. J. McPherson, Trans. AIME, Vol. 191, p. 881 (1951).
115. N. L. Peterson and R. E. Ogilvie, Trans. AIME, Vol. 218, p. 439 (1960).
116. W. R. Ham, J. Chem. Phys., Vol. 1, p. 476 (1933).
117. A. Bolk, Acta Met., Vol. 6, p. 59 (1958).
118. A. S. Darling, R. A. Mintern and J. C. Chaston, J. Inst. Metals, Vol. 81, p. 125 (1952).
119. W. Jost, Z. Phys. Chem., Vol. B21, p. 158 (1933).
120. A. Jedelev, Z. Electrochem., Vol. 39, p. 691 (1933).
121. C. Matano, Proc. Physical Math Soc. of Japan, Vol. 15, p. 405 (1933).
122. C. Matano, Japan J. of Physics, Vol. 9, p. 41 (1934).
123. O. Kubaschewski and H. Ebert, Z. Electrochem. Vol. 50, p. 138 (1944).
124. D. K. Deardorff and E. T. Hayes, Trans. AIME, Vol. 206, p. 509 (1956).
125. K. K. Kelley, Bur. of Mines Bull., 584 (1960).
126. J. P. Pemsler, J. Electrochem. Soc., Vol. 106, p. 1067 (1959).
127. W. W. Smeltzer and M. T. Simnad, Acta Met., Vol. 5, p. 328 (1957).
128. D. E. Thomas and E. T. Hayes, "The Metallurgy of Hafnium", USAEC Publication (1960).
129. M. W. Mallett and W. M. Albrecht, J. Electrochem. Soc., Vol. 104, p. 142 (1957).
130. C. M. Schwartz and M. W. Mallett, Trans. ASM, Vol. 41, p. 306 (1945).
131. E. A. Gulbransen and K. F. Andrew, Trans. AIME, Vol. 185, p. 515 (1949).

132. M. W. Mallett, J. Belle and B. B. Cleland, J. Electrochem. Soc., Vol. 101, p. 1 (1954).
133. M. W. Mallett, E. M. Baroody, H. R. Nelson and C. A. Papp, J. Electrochem. Soc., Vol. 100, p. 103 (1953).
134. Private Communication in Ref. 128.
135. J. P. Pemsler, J. Electrochem. Soc., Vol. 105, p. 315 (1958).
136. M. W. Mallett, W. M. Albrecht and P. R. Wilson, BMI-1154 (1957).
137. R. M. Tresco, Trans. ASM, Vol. 45, p. 872 (1953).
138. H. W. Allison and H. Samelson, J. Appl. Phys., Vol. 30, p. 1419 (1959).
139. H. E. Martens, "Titanium Symposium on Diffusion and Mechanical Behavior" held at Columbia Univ., June, 1954.
140. Y. Adda, J. Philibert and H. Faraggi, Rev. Metal., Vol. 54, p. 597 (1957).
141. T. Smith, J. Electrochem. Soc., Vol. 106, p. 1046 (1959).
142. R. W. Powers and M. V. Doyle, Acta Met., Vol. 6, p. 643 (1958).
143. R. W. Powers, Acta Met., Vol. 2, p. 604 (1954).
144. J. T. Stanley and C. A. Wert, Acta Met., Vol. 3, p. 107 (1955).
145. H. W. Paxton and E. G. Gondolf, Arch. Eisenhüttenwesen, Vol. 30, p. 55 (1959).
146. G. M. Pound, W. R. Bitler and H. W. Paxton, private communication in Ref. 149.
147. C. Zener, Acta Cryst., Vol. 3, p. 345 (1950).
148. A. D. LeClaire, "Progress in Metal Physics", Vol. 4, p. 333 (1953).
149. S. J. Rothman, L. T. Lloyd, A. L. Harkness, Trans. AIME, Vol. 218, p. 605 (1960).
150. A. Bochvar, V. Kuznetsova and V. Sergeev, Second International Conf. Peaceful Uses of Atomic Energy, A/Conf. 15/P/2306, (1958).
151. Y. Adda and A. Kirianenko, Compt. Rend., Vol. 247, p. 744 (1958).
152. J. W. Weeton, Trans. ASM, Vol. 44, p. 426 (1952).
153. P. L. Gruzin and B. M. Noskow, Problemy Metallovedeniya i Fiziki Metallov, Vol. 4, p. 509 (1955).

154. J. C. Fisher, J. Appl. Phys., Vol. 22, p. 74 (1951).
155. L. C. Hicks, Trans. AIME, Vol. 113, p. 163 (1934).
156. P. Bardenheuer and R. Muller, Kaiser-Wilhelm-Inst. Eisenforsch, Vol. 14, p. 295 (1932).
157. S. Ueda, Reports, Casting Research Lab. Waseda Univ., p. 83 (1956).
158. P. L. Gruzin, Problemy Metallovedeniya i Fiziki Metallov, Vol. 4, p. 524 (1955).
159. A. J. Mortlock and D. H. Tomlin, Physical Soc. Proc. (London), Vol. 69B, p. 248 (1956).
160. A. J. Mortlock and D. H. Tomlin, Physical Soc. Proc. (London), Vol. 69B, p. 250 (1956).
161. J. E. Reynolds, H. R. Ogden and R. I. Jaffee, BMI-TML Report No. 10.
162. J. E. Dorn, "Creep and Recovery", ASM, p. 255 (1957).
163. F. B. Cuff, Jr. and N. J. Grant, Iron Age, Vol. 170, p. 134 (1952).
164. F. C. Wagner, E. J. Bucur and M. A. Steinberg, Trans. ASM, Vol. 48, p. 742 (1956).
165. Analysis of C. Wagner as presented in W. Jost, "Diffusion in Solids, Liquids, and Gases", Academic Press, Inc., 1952, New York p. 68.
166. H. Kusamichi, Y. Yagi, T. Yukawa and T. Noda, Nippon Kinzoku Gakkaishi, Vol. 20, p. 39, (1956).
167. H. Kusamichi, Y. Yagi, T. Yukawa and T. Noda, Jap Sci. Rev. Mining Met., Vol. 1, p. 133 (1957).
168. R. J. Wasilewski and G. L. Kehl, Metallurgia, Vol. 50, p. 225 (1954).
169. W. Koster, L. Bangert and M. Evers, Z. Metallkunde, Vol. 47, p. 564 (1956).
170. R. D. Daniels, E. L. Harmon, Jr. and A. R. Troiano, WADC Tech. Rept. 57-30, ASTIA Document No. AD118136 (1957).
171. R. J. Wasilewski and G. L. Kehl, J. Inst. of Metals, Vol. 83, p. 94 (1954).
172. E. A. Gulbransen and K. F. Andrew, Trans. AIME, Vol. 185, p. 741 (1949).
173. J. N. Pratt, W. J. Bratina and B. Chalmers, Acta Met., Vol. 2, p. 203 (1954).

174. J. E. Reynolds and R. I. Jaffee, TML Rept. No. 21 (1955).
175. W. P. Roe, H. R. Palmer and W. R. Opie, Trans. ASM, Vol. 52, p. 191 (1960).
176. F. Claisse and H. P. Koenig, Acta Met., Vol. 4, p. 650 (1956).
177. D. Gupta and S. Weinig, WADA Technical Report 57-420, ASTIA Document No. AD142145 (1957).
178. S. H. Moll and R. E. Ogilvie, Trans. AIME, Vol. 215, p. 613 (1959).
179. C. Zener, J. Appl. Phys., Vol. 22, p. 372 (1951).
180. Y. Adda and J. Philibert, Compt. Rend., Vol. 247, p. 80 (1958).
181. I. I. Kornilov and A. Ya Shinyaev, Izvest. Akad. Nauk, S.S.S.R. Otdel. Tekn. Nauk, No. 9, p. 50 (1957).
182. S. Z. Bokshtein, V. A. Kazakova, S. T. Kishkin and L. M. Mirsky, Izvest. Akad. Nauk, S.S.S.R. Otdel. Tekn. Nauk, No. 12, p. 18 (1955).
183. V. I. Arkharov, K. A. Efremova, S. I. Ivanouskaya, A. K. Shtol'ts and B. A. Yunikov, Doklady Akad. Nauk, S.S.S.R., Vol. 89, p. 269 (1953).
184. V. I. Arkharov, K. A. Efremova, S. I. Ivanouskaya, A. K. Shtol'ts and B. A. Yunikov, Trudy Inst. Fiz, Metal. Akad. Uavh. S.S.S.R., Ural Filial, No. 16, p. 56, (1955).
185. M. L. Hill, Fall Meeting of AIME, October 1960, Philadelphia, Pa.
186. J. Stanley and C. A. Wert, Fall Meeting of AIME, October 1960, Philadelphia, Pa.
187. Ken-ichi Hirano, M. Cohen and B. L. Averbach, MIT Metallurgy Reports, Vol. 11, No. 6, p. 1, August 1960.
188. F. S. Buffington, Ken-ichi Hirano and M. Cohen, MIT Metallurgy Reports, Vol. 11, No. 6, p. 16, August 1960.
189. A. J. Mortlock and D. H. Tomlin, Phil. Mag., Ser. 8, Vol. 4, p. 628 (1959).
190. A. D. LeClaire, Acta Met., Vol. 1, p. 438, (1953).
191. A. Sawatzky, J. Nuclear Materials, Vol. 2, p. 62 (1960).
192. Y. Adda, C. Mairy and J. L. Andreu, Memoires Scientifiques Rev. Metallurg., Vol. 57, No. 7, p. 550 (1960).
193. M. Mosse, V. Levy and Y. Adda, Comptes. Rendus, Vol. 250, p. 3171 (1960).